GEM TN-92-195

Physics/Simulation Group Meeting - SSCL

September 23, 1992

Abstract:

Agenda, attendees and presentations of the GEM Physics/Simulation Group Meeting held at the SSC Laboratory on September 23, 1992. Agenda items are: Discussion of Physics Issues Related to Hadron Calorimeter; Critique of SDC TDR Physics Performance Section; Discussion of Topics and Responsibilities for GEM; and Plans for Simulation Tools -- e.g. FAST1+.

Tentative Agenda
Physics Performance Meeting
Sept 23 1pm ---> eve

I) Discussion of Physics Issues Related to Hadron Calorimeter Decision
  - H --> gamma+gamma (Mitselmahker et al)
  - Missing Et (F. Paige)
  - Others??

  The main issues relate to hermiticity, transition region near eta=1.5, and speed. These appear to be the main areas of performance difference between the calorimeter options. A final one I neglected above is resolution and tails.

2) Critique of SDC TDR Physics Performance Section.
  Hiro Yamamoto will lead a detailed critical discussion of the SDC Physics Section. Please read it thoroughly in advance of our meeting. It represents a good reference point for us as we develop plans for our chapter for the GEM TDR.

3) Discussion of Topics and Responsibilities for GEM TDR Physics Performance Section.

4) Plans for Simulation Tools -- eg FAST1+ (TBA)

Our plan is to have an extended Physics group meeting approximately half way between collaboration meetings, and a shorter meeting (because of conflicting meetings) during collaboration meeting weeks. We encourage all Physics/ Simulators to spend several days at SSCL around these meetings so we can interact with each other and work more as a group, rather than just interact at the formal meetings.

Sasha Vanyashin: Pointing
Peter Dingus: μ Simulation

GEM Physics/Simulation Group
Sept 23, 1992

Name	Inst.	E-mail
Barry Barish	CALTECH	SSCVX1::BARISH
F. Paige	SSC	SSCVX1::PAIGE
~~Rencheng Shang~~	~~SSC~~	~~SSCVX1::Shang~~
Ken Lane	BU	Lane @ BUPHYC
STEVE MRENNA	CALTECH	CITHEX::MRENNA
Vladimir Glebov	SSC	SSCVX1::GLEBOV
HENK Uijterwaal	SSC	SSCVX1::HENK
Shawn McKee	U of Mich	SSCVX1::MCKEE
Irwin Sheer	SSS	SSCVX1::SHEER
TORRE WENAUS	LLNL.	SSCVX1::WENAUS.
MICHI BOTLO	SSCL	botlo@sscvx1
George YOST	SSCL	SSCVX1::YOST
Henry Kasha	Yale	YALPHY::KASHA
Yuri Fisyak	SSCL	SSCVX1::FISYAK
Peter Dingus	SSCL	SSCVX1::DINGUS
Andrey Ostapchuk	SSCL	SSCVX1::OSTAPCHU
A. Vanyashin	SSCL	vanyashin@SSCVX1
Tomasz Skwarnicki	SMU	TOMASZ @ SSCVX1

Presentation by:

Yuri Kamyshkov

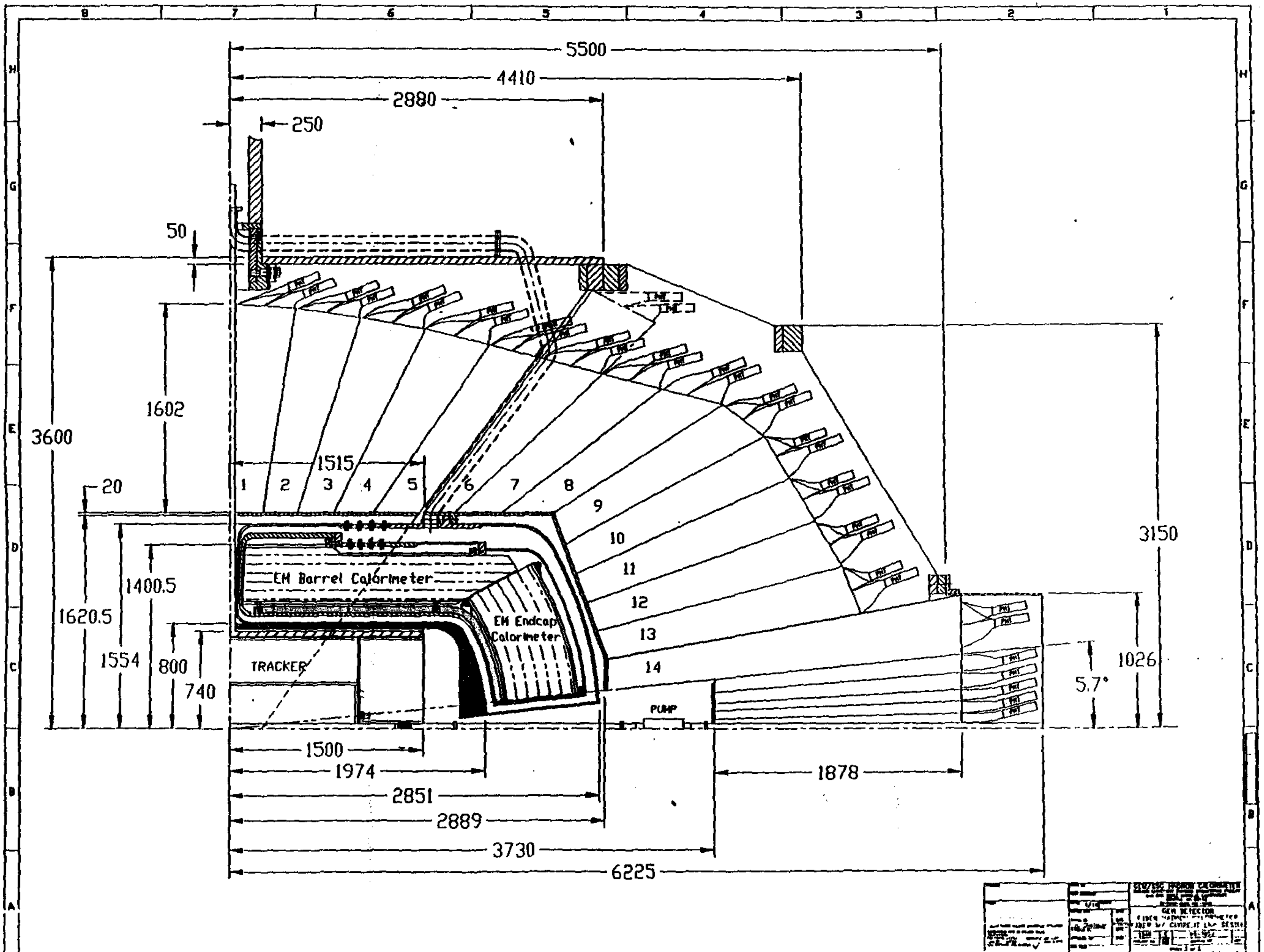
5500
4410
2880
250
50
3600
1602
1515
20
1 2 3 4 5 6 7 8 9 10 11 12 13 14
EM Barrel Calorimeter
EM Endcap Calorimeter
TRACKER
PUMP
1400.5
1620.5
1554
800
740
3150
1026
5.7°
1500
1974
2851
2889
3730
6225
1878
GEM DETECTOR

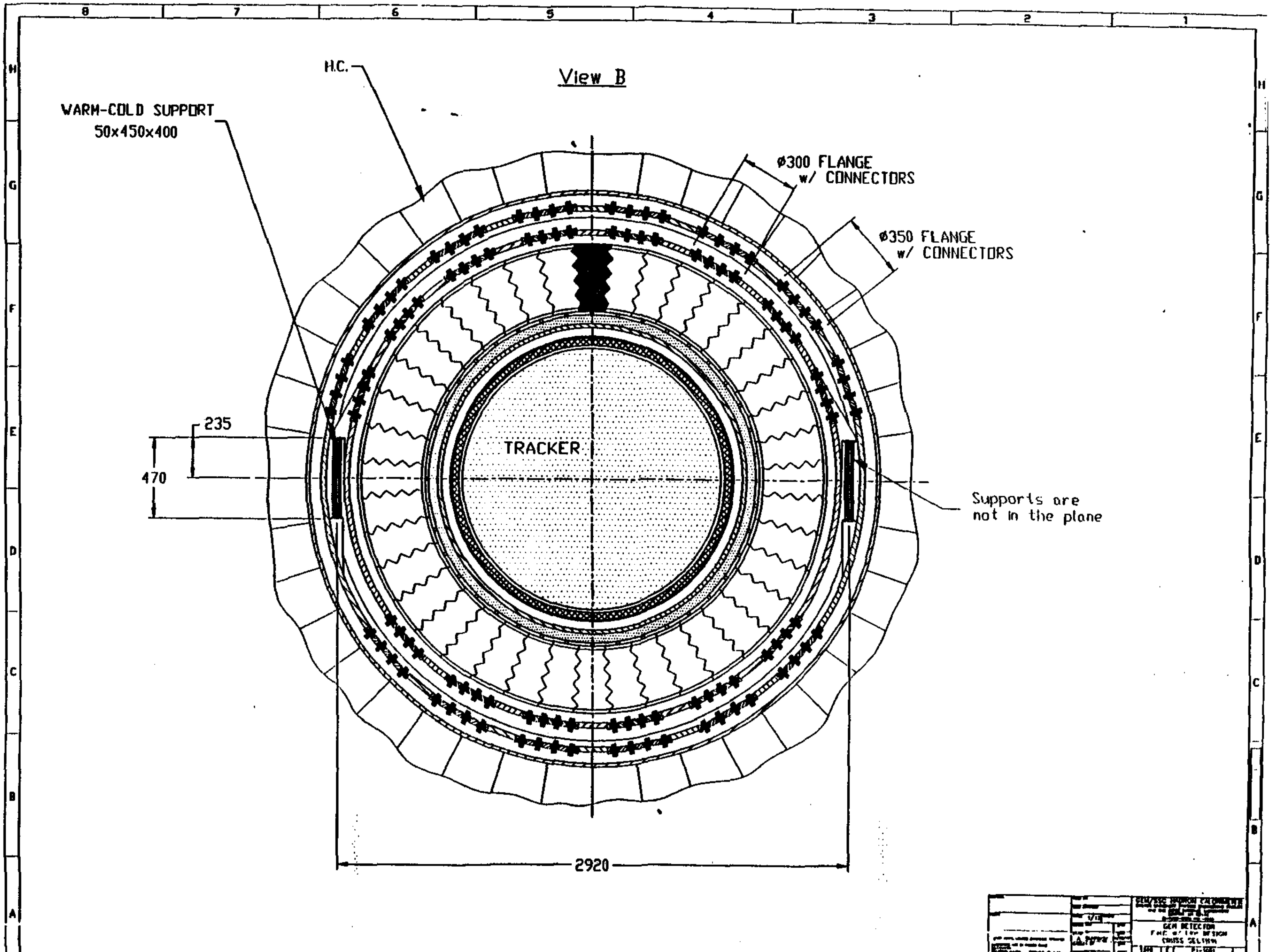
View B
H.C.
WARM-COLD SUPPORT
50x450x400
Ø300 FLANGE
w/ CONNECTORS
Ø350 FLANGE
w/ CONNECTORS
TRACKER
235
470
2920
Supports are
not in the plane
GEM DETECTOR

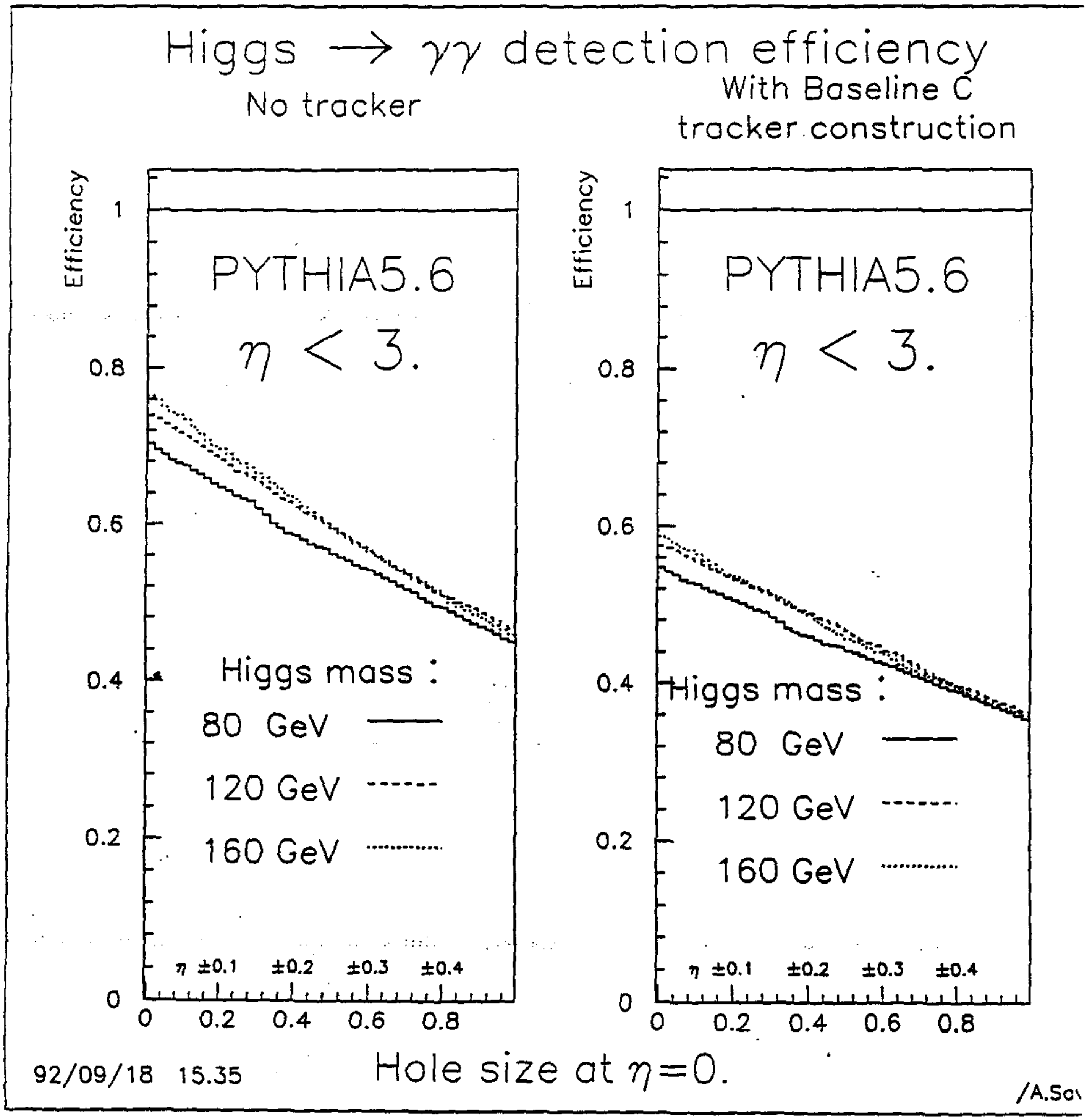

Higgs → γγ detection efficiency
No tracker
With Baseline C tracker construction
Efficiency
PYTHIA5.6
η < 3.
Higgs mass :
80 GeV
120 GeV
160 GeV
η ±0.1 ±0.2 ±0.3 ±0.4
0 0.2 0.4 0.6 0.8 1
92/09/18 15.35
Hole size at η=0.
/A.Sa

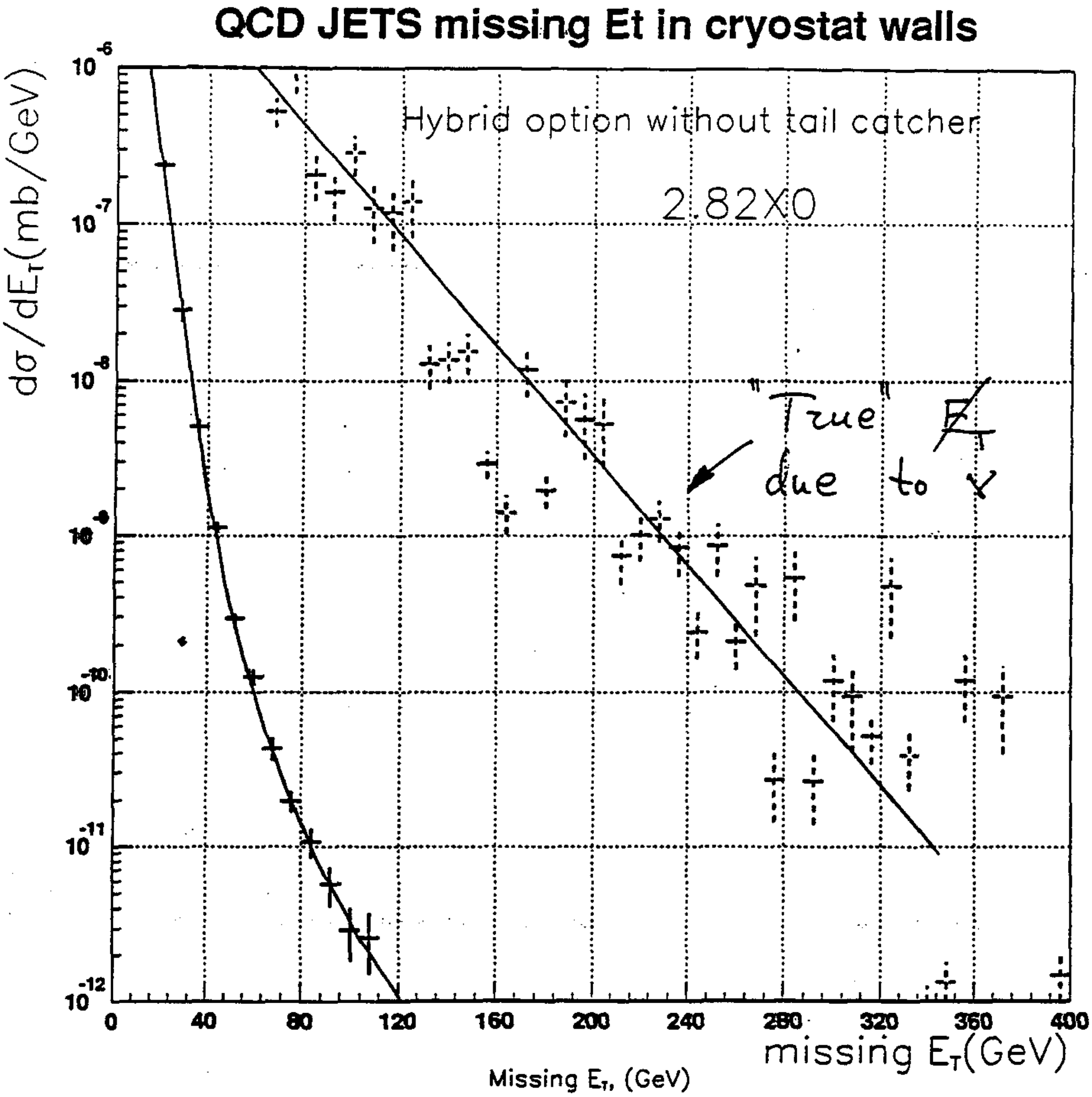
QCD JETS missing Et in cryostat walls
Hybrid option without tail catcher
2.82X0
"True" $\not{E}_T$ due to ν
dσ/dE_T(mb/GeV)
missing E_T(GeV)
Missing E_T, (GeV)
0
40
80
120
160
200
240
280
320
360
400

Fig. 12

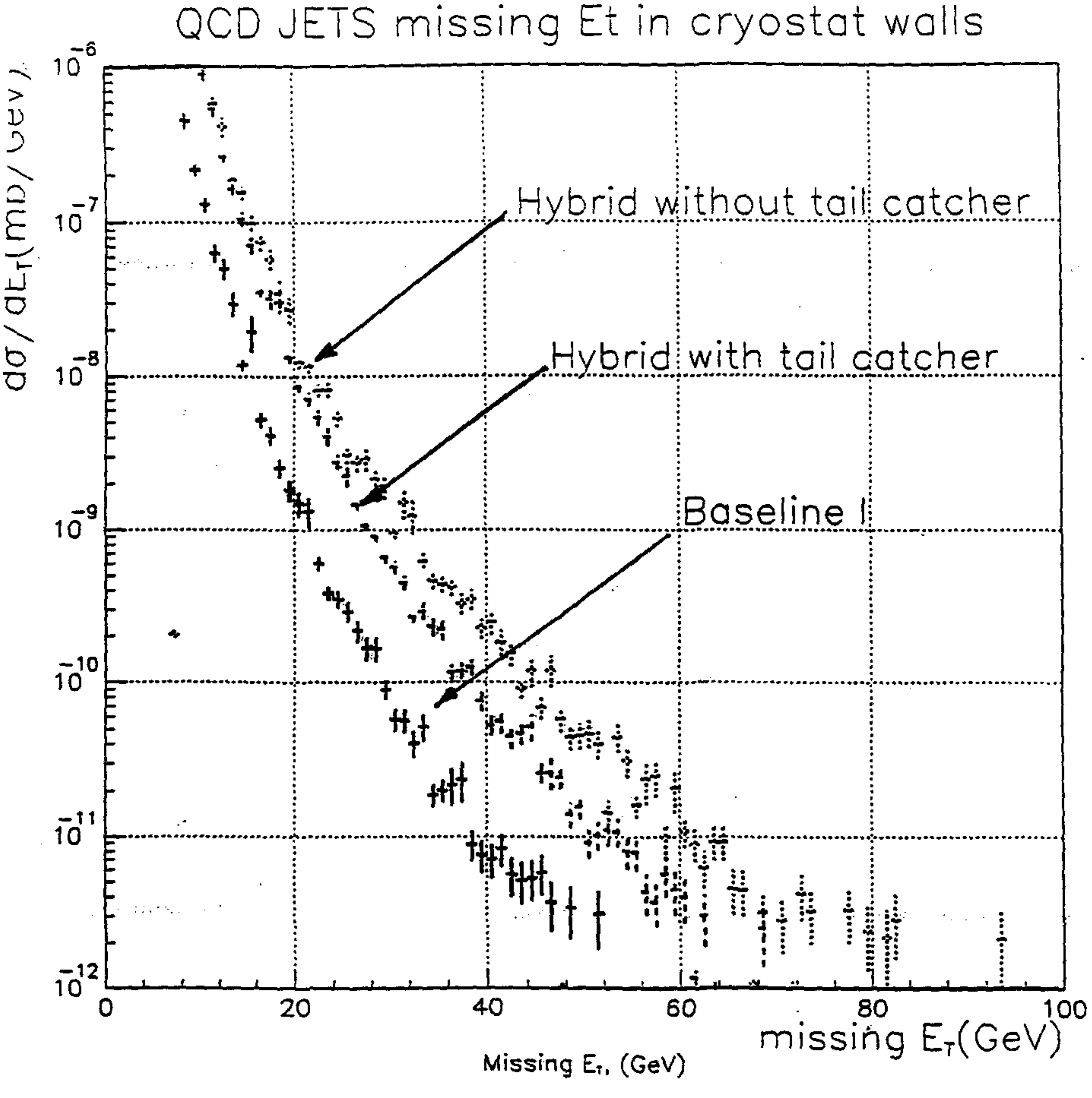
QCD JETS missing Et in cryostat walls
Hybrid without tail catcher
Hybrid with tail catcher
Baseline I
missing E_T(GeV)
Missing E_T, (GeV)

Fig. 13

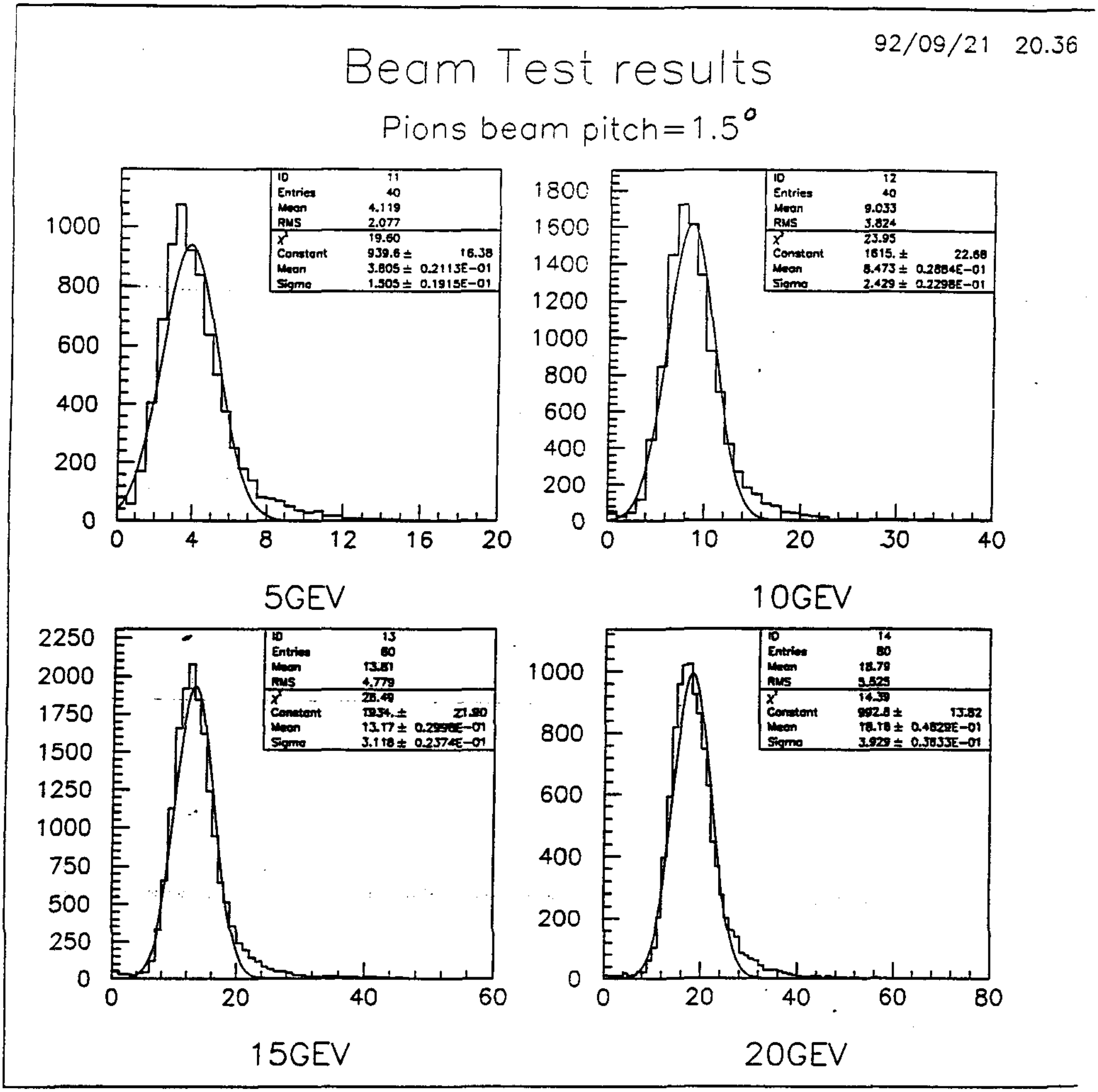

Beam Test results
92/09/21 20.36
Pions beam pitch=1.5°
ID 11
Entries 40
Mean 4.119
RMS 2.077
χ² 19.60
Constant 939.6 ± 16.38
Mean 3.805 ± 0.2113E-01
Sigma 1.505 ± 0.1915E-01
5GEV
ID 12
Entries 40
Mean 9.033
RMS 3.824
χ² 23.95
Constant 1615. ± 22.68
Mean 8.473 ± 0.2884E-01
Sigma 2.429 ± 0.2298E-01
10GEV
ID 13
Entries 60
Mean 13.81
RMS 4.779
χ² 28.49
Constant 1934. ± 21.90
Mean 13.17 ± 0.2998E-01
Sigma 3.118 ± 0.2374E-01
15GEV
ID 14
Entries 80
Mean 18.79
RMS 5.525
χ² 14.39
Constant 992.8 ± 13.82
Mean 18.18 ± 0.4829E-01
Sigma 3.929 ± 0.3833E-01
20GEV

GEANT3.15 simulation

92/09/21 20.37

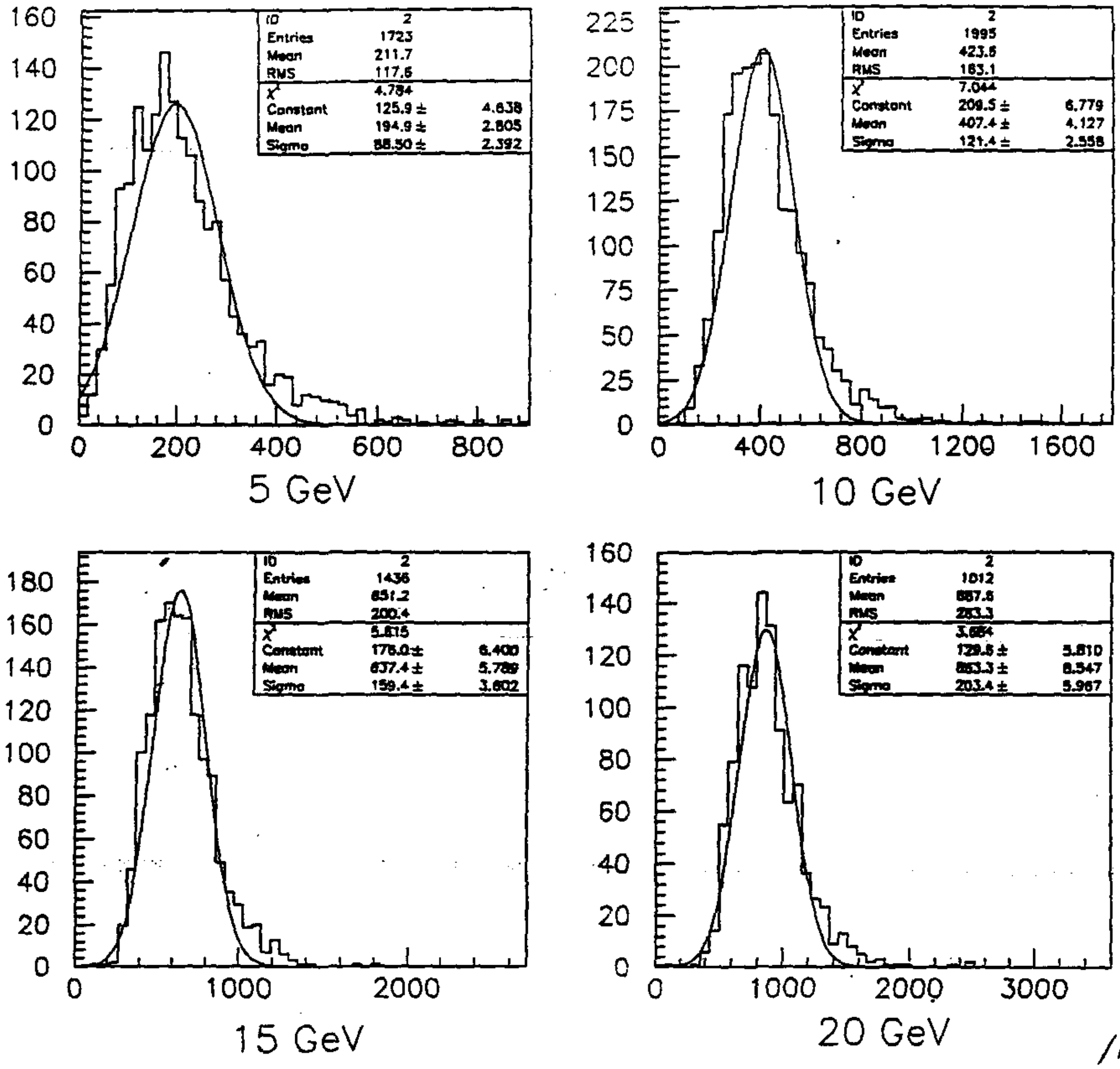

/A.Savin,

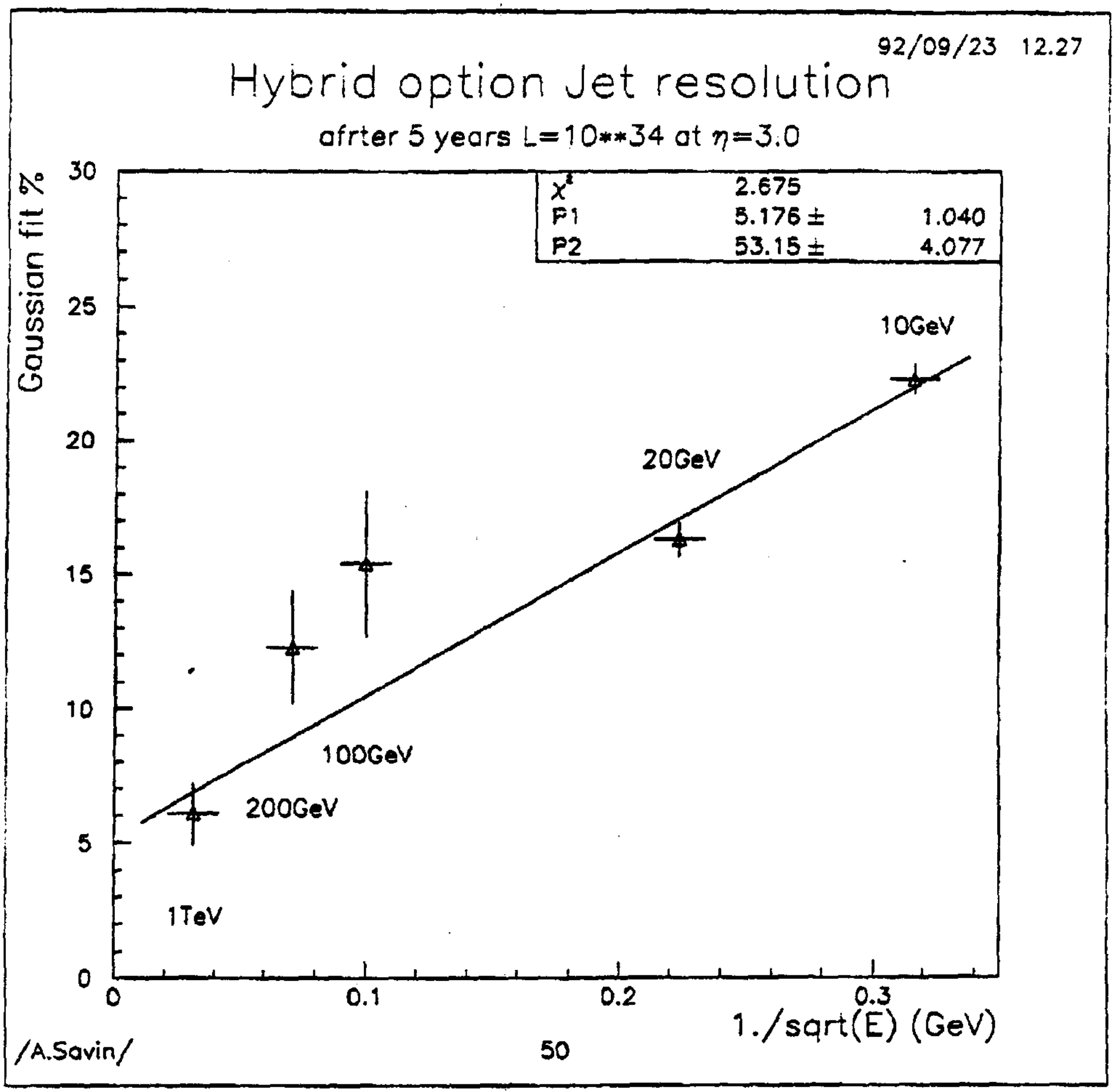
92/09/23 12.27
Hybrid option Jet resolution
afrter 5 years L=10**34 at η=3.0
χ² 2.675
P1 5.176 ± 1.040
P2 53.15 ± 4.077
Gaussian fit %
10GeV
20GeV
100GeV
200GeV
1TeV
1./sqrt(E) (GeV)
/A.Savin/
50

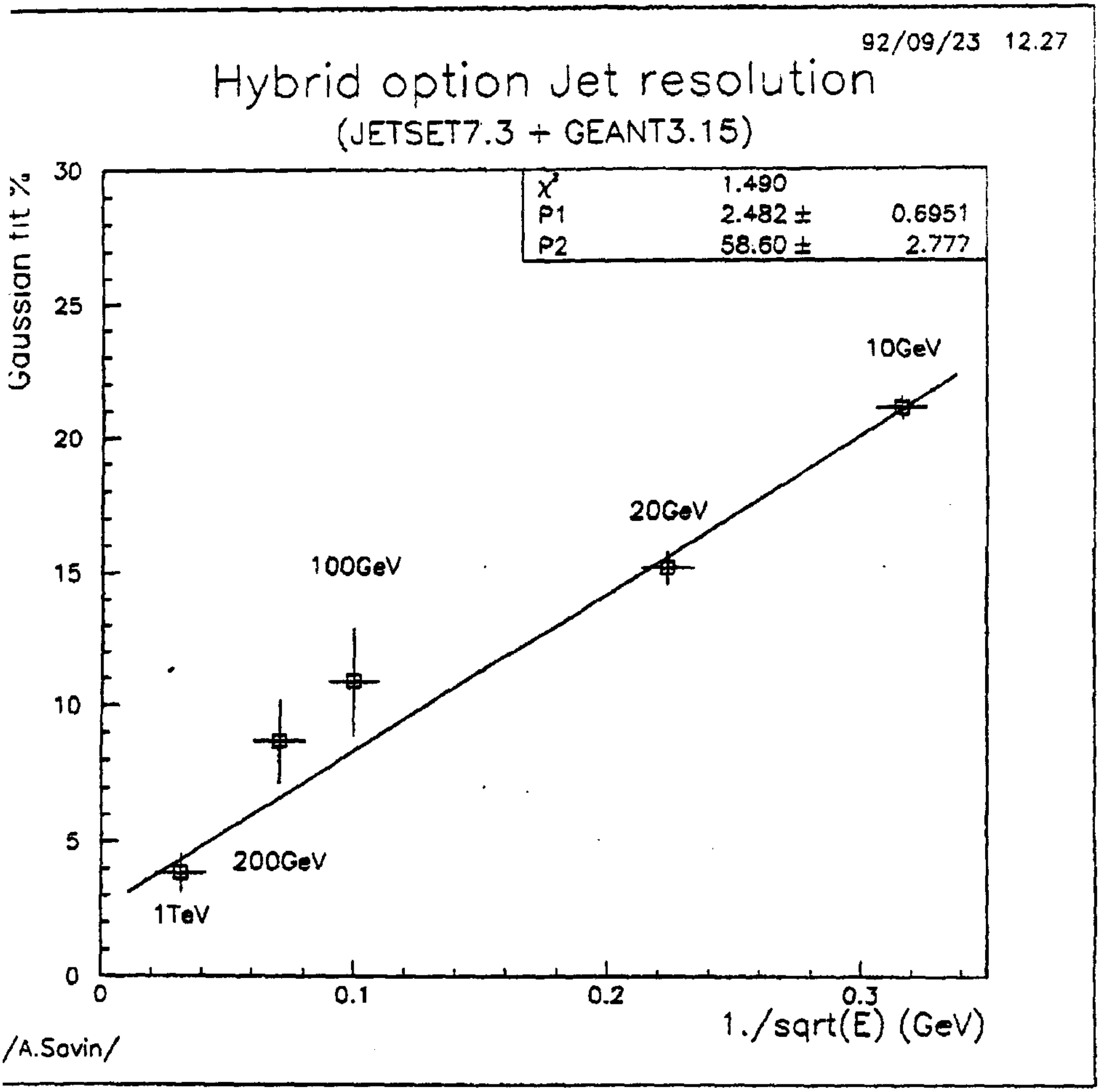
92/09/23 12.27
Hybrid option Jet resolution
(JETSET7.3 + GEANT3.15)
χ² 1.490
P1 2.482 ± 0.6951
P2 58.60 ± 2.777
10GeV
20GeV
100GeV
200GeV
1TeV
Gaussian fit %
0
5
10
15
20
25
30
0
0.1
0.2
0.3
1./sqrt(E) (GeV)
/A.Savin/

Fitting by exp(-kx) and gauss*exp(-kx)

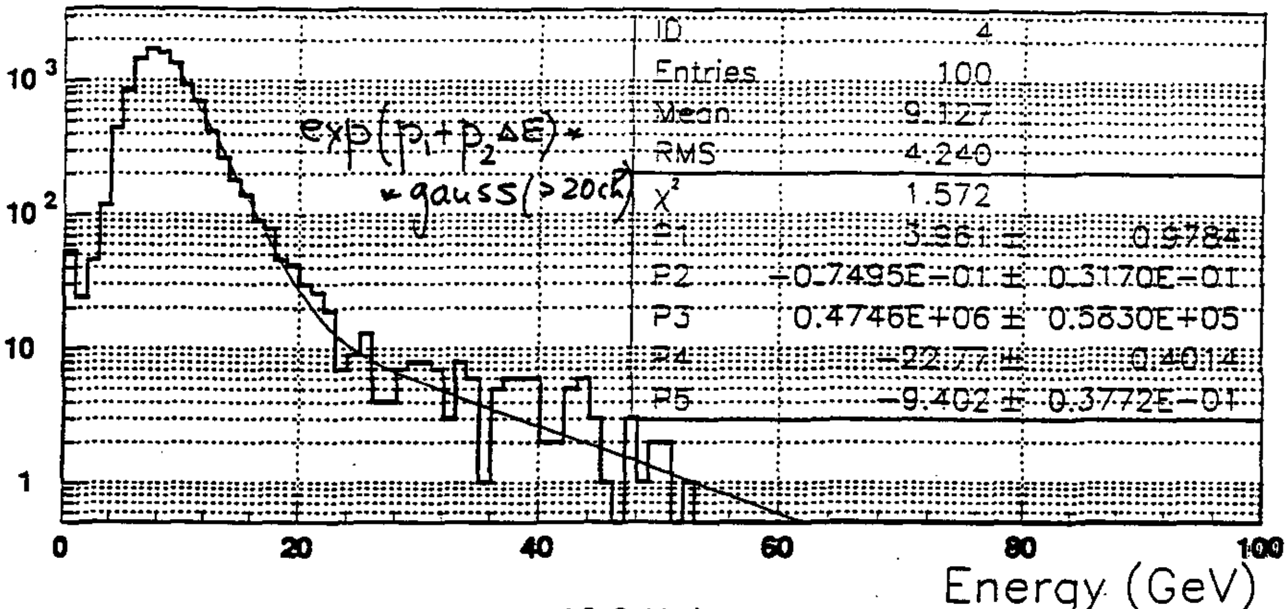

10 GeV pions

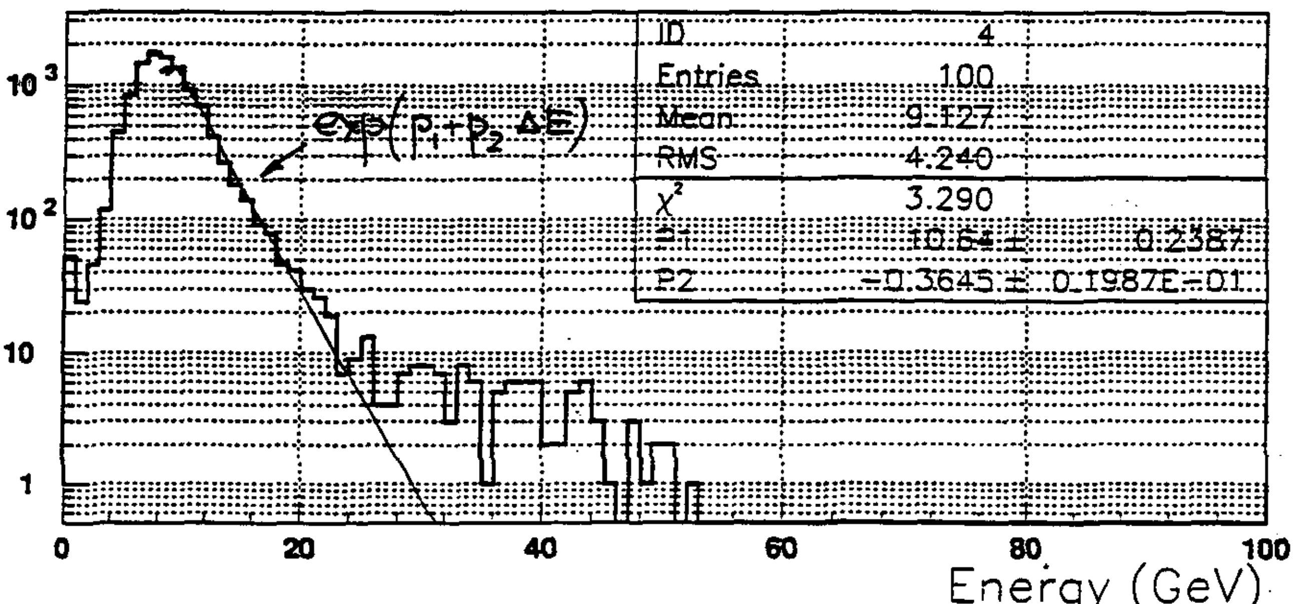

10 GeV pions

Fitting by exp(-kx) and gauss*exp(-kx)

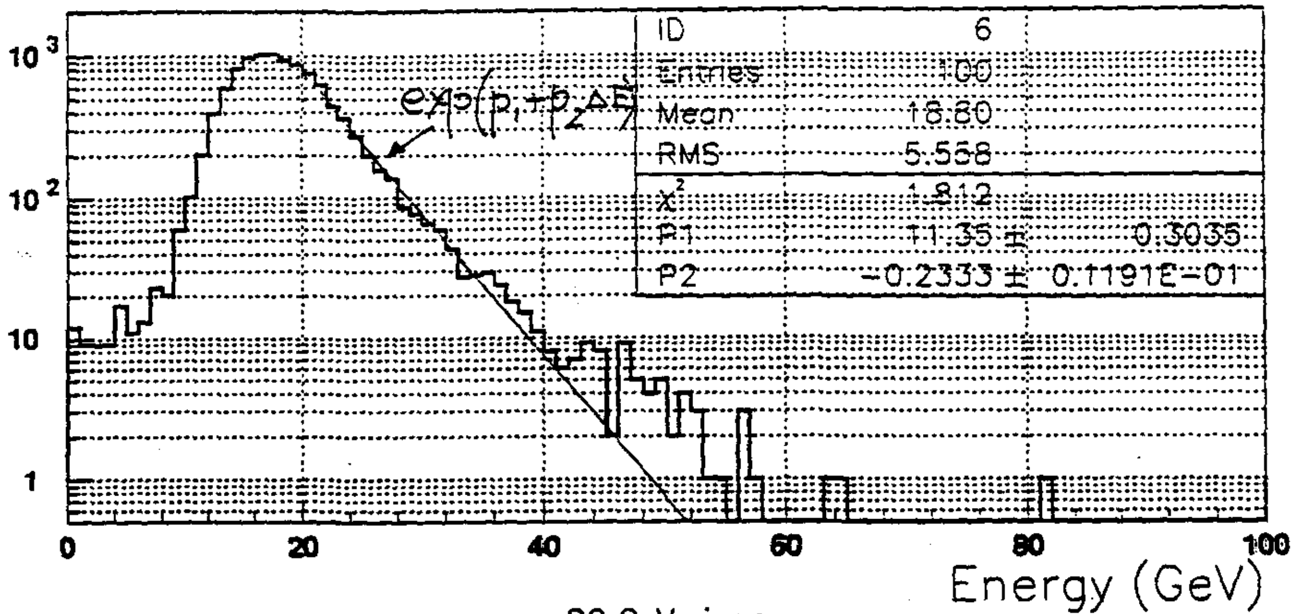

20 GeV pions

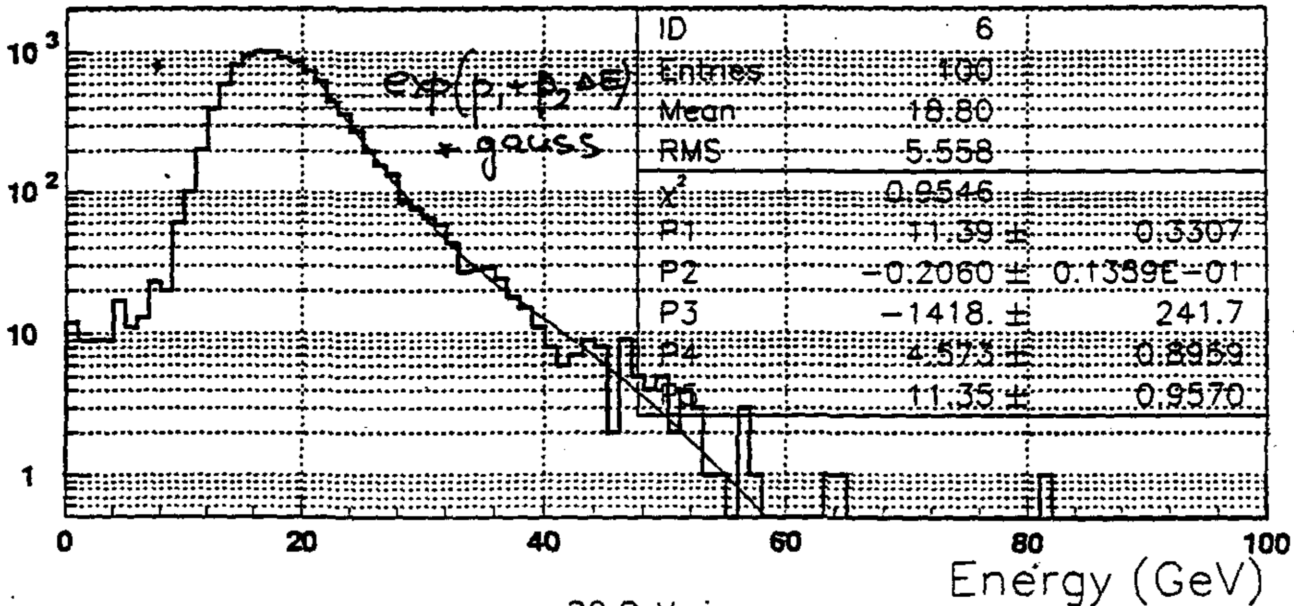

20 GeV pions

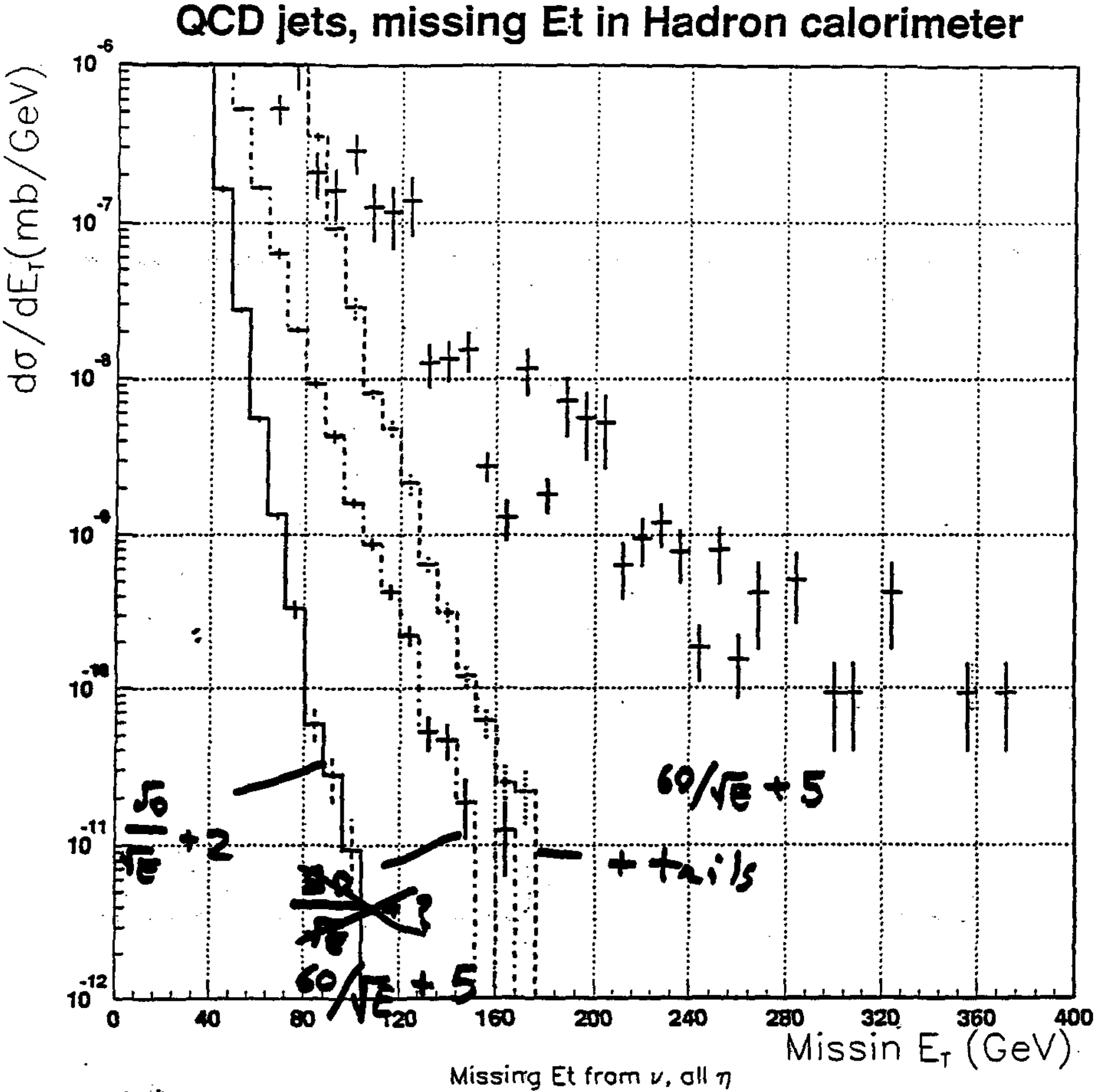
QCD jets, missing Et in Hadron calorimeter
dσ/dE_T(mb/GeV)
Missin E_T (GeV)
Missing Et from ν, all η
60/√E + 5
+ tails
60/√E + 5

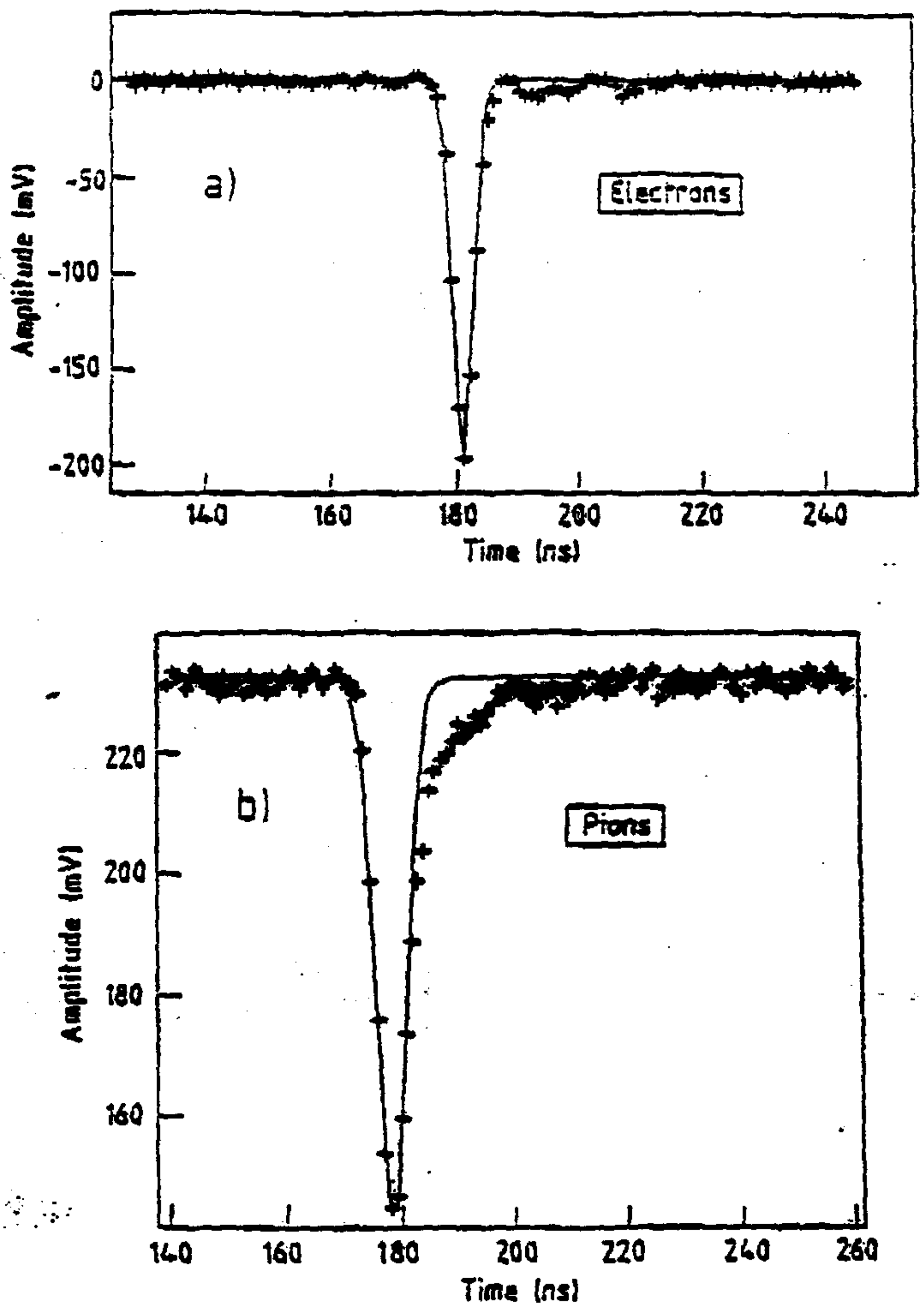

80 GeV

Figure 11

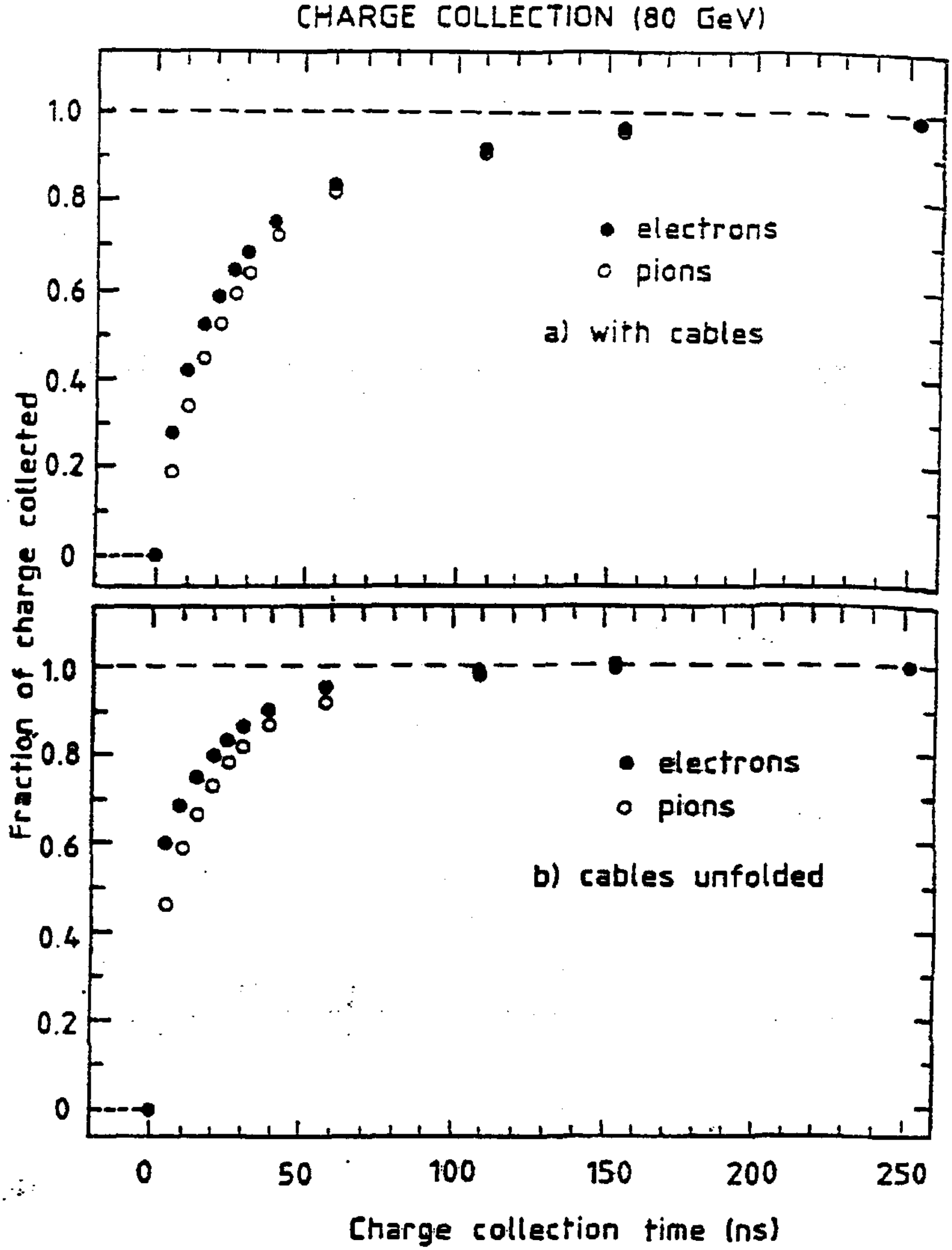
CHARGE COLLECTION (80 GeV)
Fraction of charge collected
electrons
pions
a) with cables
b) cables unfolded
Charge collection time (ns)

Figure 7

Presentation by:

F. Paige

$$\frac{dN}{d\eta} \sim 10 \qquad \langle p_T \rangle \sim .5 \qquad \Delta y = \pm 5$$

$$\langle \Sigma E_T \rangle = 50\ \mathrm{GeV}$$

$$\frac{\Delta E}{E} = \frac{\varepsilon}{\sqrt{E}}$$

$$\langle p_T \rangle = \varepsilon \sqrt{\Sigma E_T} = 5.5\ \mathrm{GeV} \times \sqrt{N}$$

$$\sigma(E_T > 100) = 5 \times 10^{-6}\ \mathrm{mb}$$

$$\sigma(p_{T\,jet} > 100) = 10^{-2}\ \mathrm{mb}$$

$$P(\text{lose jet}) = P(\eta \approx 0 \ \sim\text{to}) \times P(\text{hard frag}) \times P(\text{faulted veto}) < 10^{-4}$$

Presentation by:

A. Vanyashin

A. Vanyashin

9-23-92

Hγγ task force status report

Current activities:

1. Incorporate LKr into FASTI (Vanyashin)

2. Specifications for EM calorimeter angular resolution for a standalone mode (H → γγ) (Vanyashin)

3. γ Isolation study using HAD calorimeter (Both options) (A. Golutvin)

   Less pileup in SCINT Cal may provide important physics argument in favor of HYBRID option

Preliminary: { 3σ cut on energy deposition in HC before summing

⇓

20% difference of LAr HC from ideal calo }

A.Vanyashin
September 23 1992

$H\gamma\gamma$ task force

Specifications to Angular Resolution in EM Calorimeter

standalone mode (no vertex)

Model used:

1. 80 GeV $H^0 \rightarrow \gamma\gamma$ (PYTHIA 5.6)
2. FASTI EM Calorimeter (modified to account LKr in barrel)

$$\frac{\Delta E}{E} \simeq 5.5\% / \sqrt{E} \oplus 0.4\%$$

3. Pileup simulated explicitely (Tomasz S.)
4. Position resolution effects neglected
5. For each γ angle smeared according to

$$\Delta\Theta = \frac{a}{\sqrt{E}} \oplus b$$

6. $\Theta_{\gamma\gamma}$ corrected to account for constrained fit
7. Worsening of significance relative to a perfect angular resolution calculated and requiered to be better than 0.9

K. Shmakov

$H_0 \rightarrow \gamma\gamma$ decay:

$$\frac{\delta M_{H_0}}{M_{H_0}} = \frac{1}{2}\sqrt{\left(\frac{\delta E_1}{E_1}\right)^2 + \left(\frac{\delta E_2}{E_2}\right)^2 + \left(\frac{\delta\Theta}{\tan(\frac{\Theta}{2})}\right)^2}$$

What is requied from the EM calorimeter:

(1) Precise *energy resolution* $\sigma(E)/E$

(2) *Angular resolution* – to measure the angle Θ between 2γ. (If vertex is unknown)

Intermediate Mass Higgs Searches with GEM Detector

3.5 Effect of Position Resolution

It is also interesting to see the effect of shower position resolution. Table 7 shows the ratio of H→ $\gamma\gamma$ peak width as a function of the shower position resolution (δx) and energy resolution (a and b), for Higgs mass of 80 GeV. The numbers in the table are normalized to the case of a = 2, b = 0.5 and $\delta x = \delta y$ = 1 mm. It is clear that the shower position resolution of an order of few mm will not compromise the discovery potential of a precision EM calorimeter.

Table 7: Ratio of H→ $\gamma\gamma$ Peak Width as Function of δx, a and b.

δx (mm)		0.5	1.0	1.5	2.0	2.5	3.0
a=2	b=0.5	0.97	1.0	1.0	1.1	1.1	1.2
a=5.5	b=0.5	1.5	1.5	1.5	1.6	1.6	1.6
a=7.5	b=0.5	1.9	1.9	1.9	1.9	2.0	2.0
a=15	b=3.7	3.8	3.8	3.8	3.8	3.8	3.8

negligible

3.6 Effect of Vertex z Resolution

Table 8: Ratio of H→ $\gamma\gamma$ Peak Width as Function of δz, a and b

δz (mm)		1.0	2.0	3.0	5.0	10.	50.
a=2	b=0.5	1.0	1.0	1.1	1.1	1.5	5.4
a=5.5	b=0.5	1.5	1.5	1.6	1.6	1.9	5.5
a=7.5	b=0.5	1.9	1.9	1.9	2.0	2.2	5.6
a=15	b=1.0	3.8	3.8	3.8	3.8	3.9	6.5

?

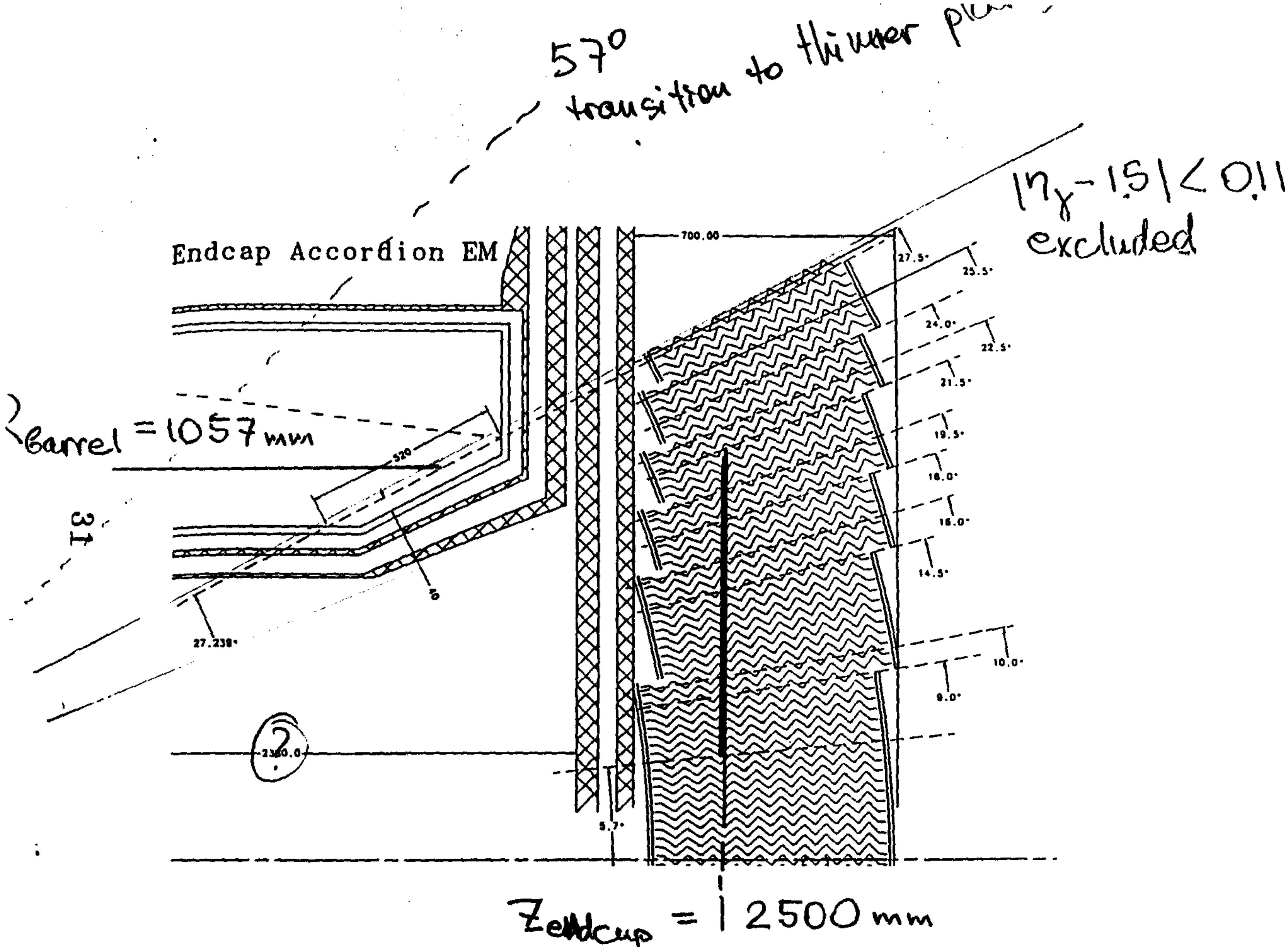
57°
transition to thinner pl...
$|\eta_\gamma - 1.5| < 0.11$
excluded
Endcap Accordion EM
700.00
27.5°
25.5°
24.0°
22.5°
21.5°
19.5°
18.0°
16.0°
14.5°
10.0°
9.0°
5.7°
520
40
27.239°
2300.0
?
Z_{endcap} = 2500 mm
Z_{barrel} = 1057 mm

92/09/23 11.26

Worsening of 80 GeV Higgs Significance Due to Angular Resolution

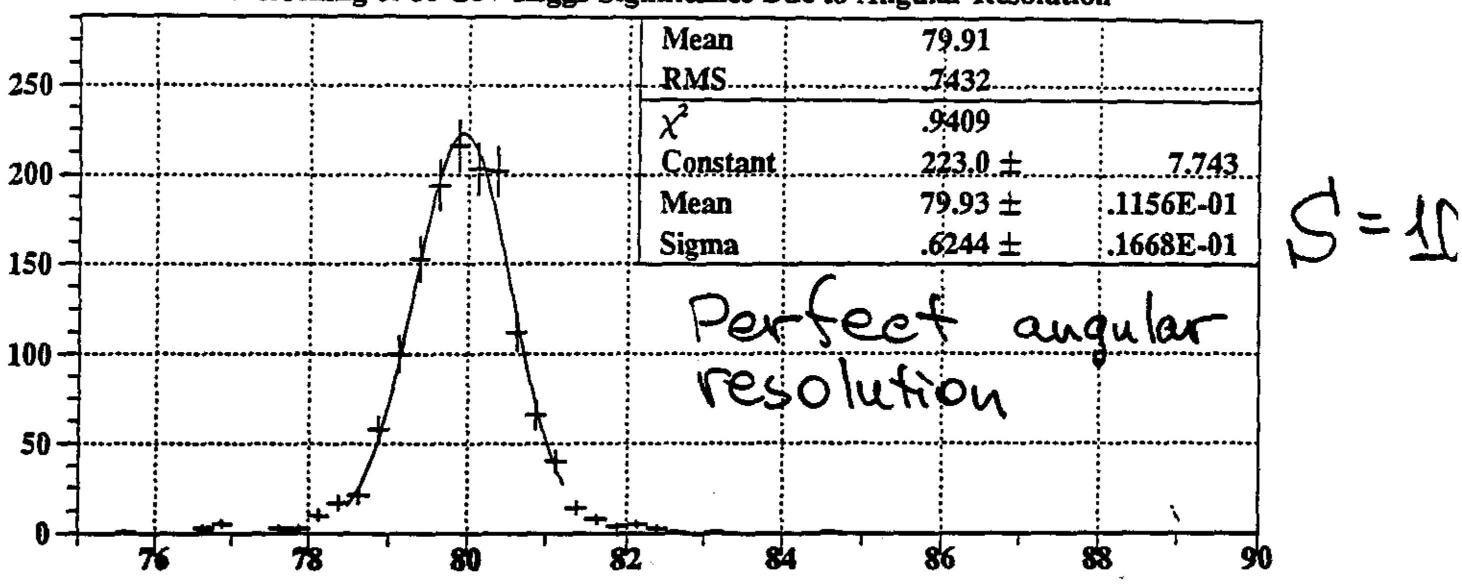

mass of GG before sm

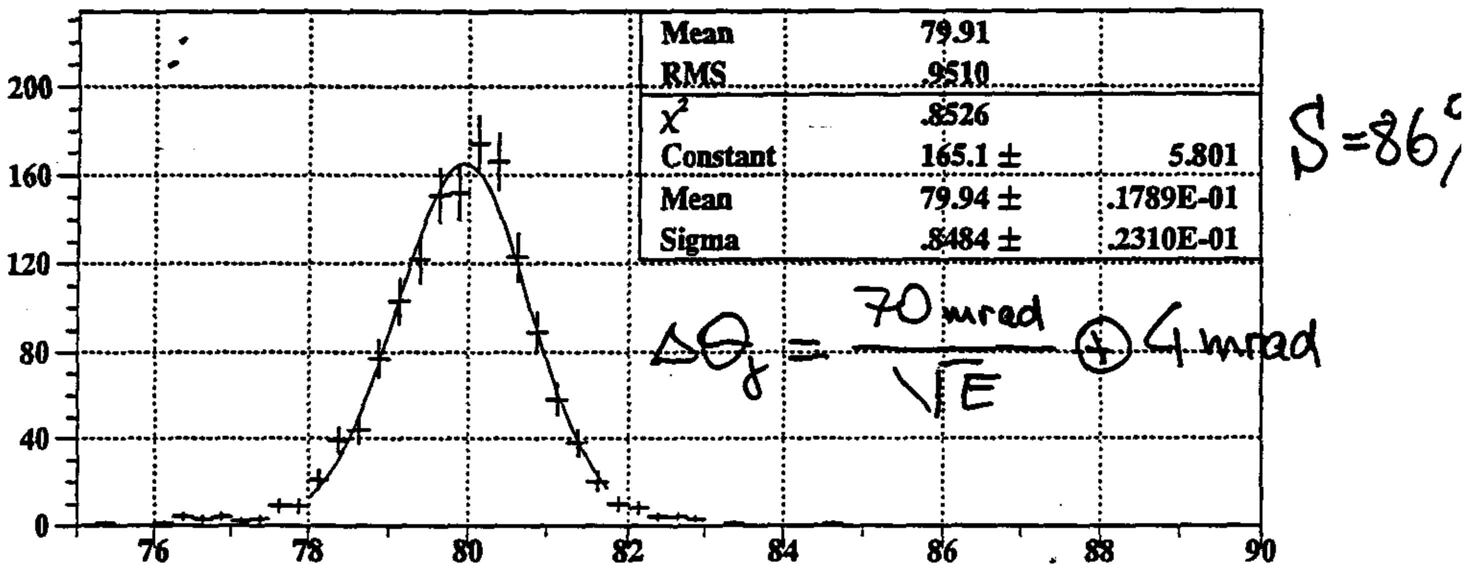

mass 70mr/sqrtE+4mr

Significance of 80 GeV Higgs
(in % of perfect resolution Significance)

a, mrad · GeV$^{1/2}$

DATE 23/09/92

a \ b (LOW-EDGE)	0	1	2	3	4	5	6	7	8	9	10	OV
OVE												
100	82.268	83.545	82.154	82.867	81.102	80.999	78.519	78.416	78.979	76.43	76.288	
90	85.512	84.292	83.891	84.132	83.332	82.474	82.014	81.673	80.445	79.364	79.192	
80	86.43	86.737	86.552	86.18	85.852	85.597	83.033	84.313	83.118	79.794	81.364	
70	89.012	87.964	88.689	87.873	86.326	86.552	85.056	82.616	84.639	82.408	81.927	
60	91.455	90.811	89.818	89.053	87.956	87.67	87.011	84.969	84.629	83.618	81.502	
50	93.355	92.504	92.039	91.948	89.055	89.504	87.047	88.393	85.288	83.641	84.679	
40				91.497	92.07	90.322	88.998	88.802	86.606	84.611	84.218	
30				95.123	93.511	91.938	89.917	88.569	87.611	86.637	84.53	
20				95.323	94.324	93.049	90.66	89.463	87.929	87.739	85.479	
10				97.035	95.45	93.239	91.571	90.958	88.455	86.484	85.229	
0				97.557	95.148	92.919	91.427	90.201	87.447	87.427	84.256	
UND												

LOW-EDGE 1.

88

acceptable parameters

b, mrad

Angular resolution parametrized as

$$\Delta\Theta_{\gamma} = \frac{a}{\sqrt{E}} \oplus b$$

92/09/23 11.19

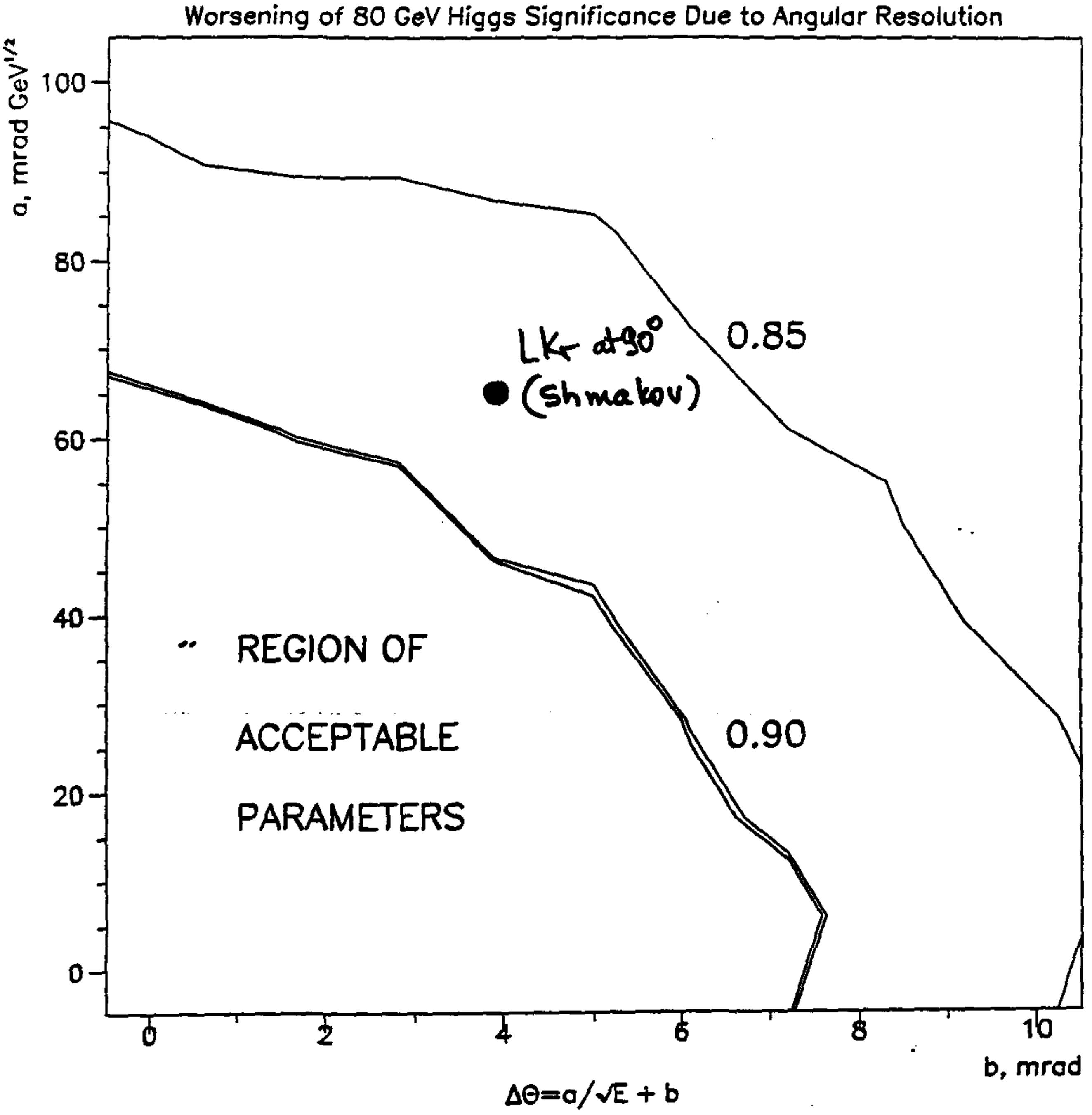
Worsening of 80 GeV Higgs Significance Due to Angular Resolution
a, mrad GeV^1/2
100
80
60
40
20
0
0
2
4
6
8
10
b, mrad
ΔΘ=a/√E + b
LKr at 90°
(Shmakov)
0.85
0.90
REGION OF
ACCEPTABLE
PARAMETERS

Conclusion

Optimized EM Calorimeter will be able to detect $H \to \gamma\gamma$ in standalone mode

Presentation by:

Yu. Fisyak

(14) $10^{12}\ n/cm^2/y \rightarrow 10^5\ n/cm^2/s$

$0.3 \div 0.5\ \%$ hit / n / 2.5 cm

$5 \cdot 10^{-3} \cdot 10^5 / 2.5$ hit/cm^3/s =

= 200 Hz / cm^3

$4 \times 4 \times 400\ cm^3 =$ ~~4.8~~ 5 $\cdot 10^3\ cm^3$

1 MHz / <u>tube</u> $0.5 \cdot 10^{-6} =$

= 50%

gem

$\gamma e \mu$

Presentation by:

P. Dingus

P. DINGUS 9/23/92

ISSUES IN PATTERN RECOGNITION

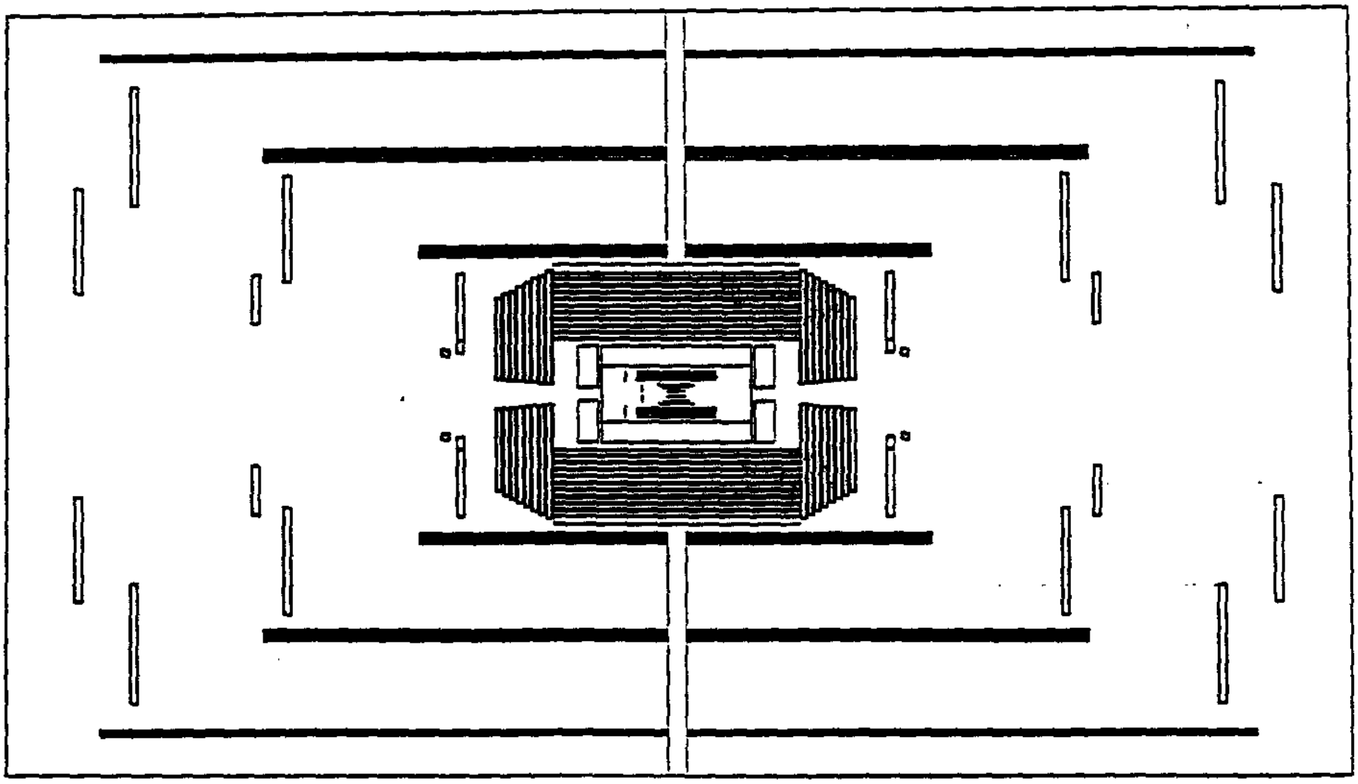

MODEL

NEWMU / CU-SIN

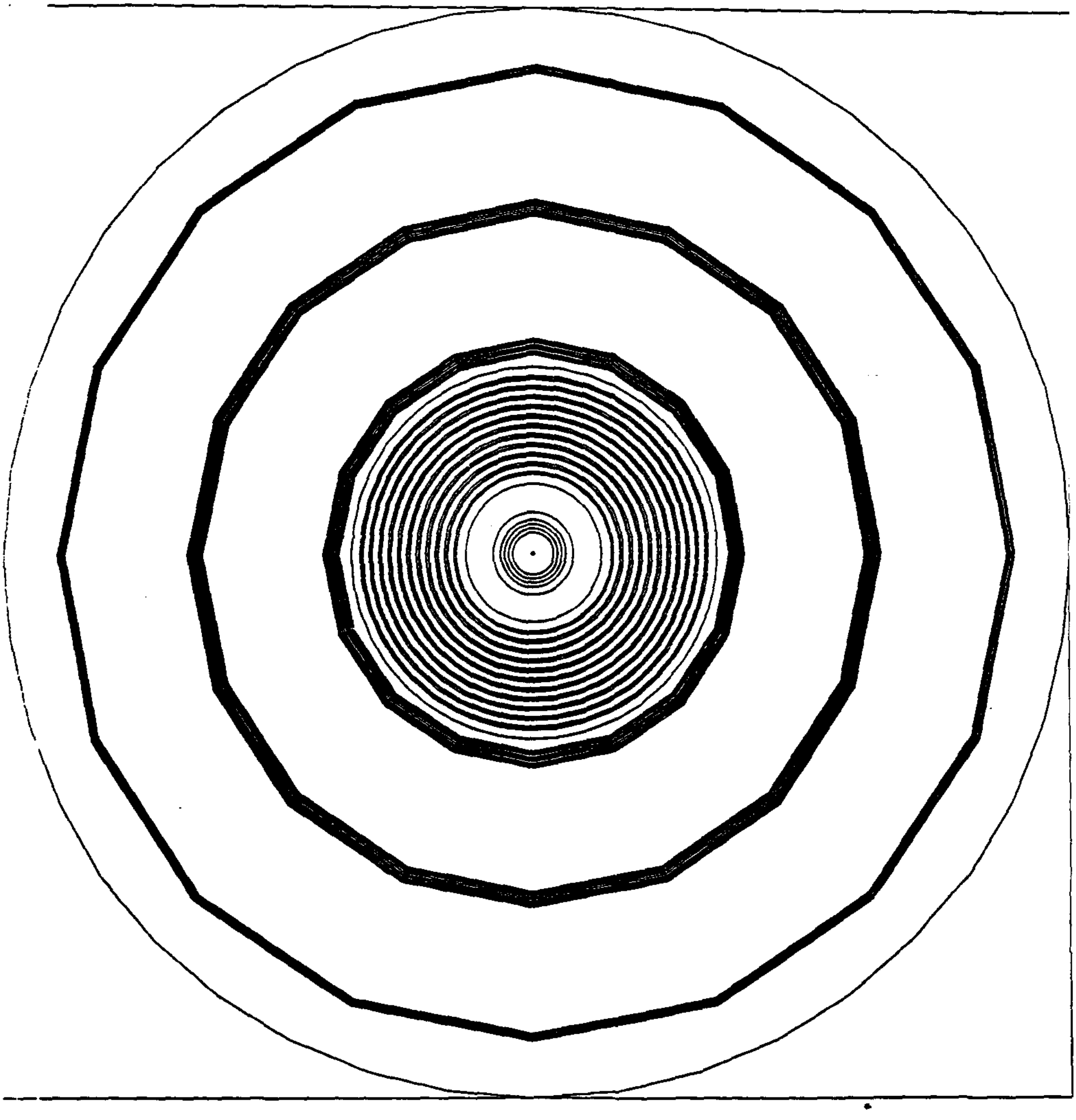

r, φ PLOT OF
μ SYSTEM 884
CONFIGURATION

BACKGROUND INDUCED
PATTERN RECOGNITION
PROBLEMS

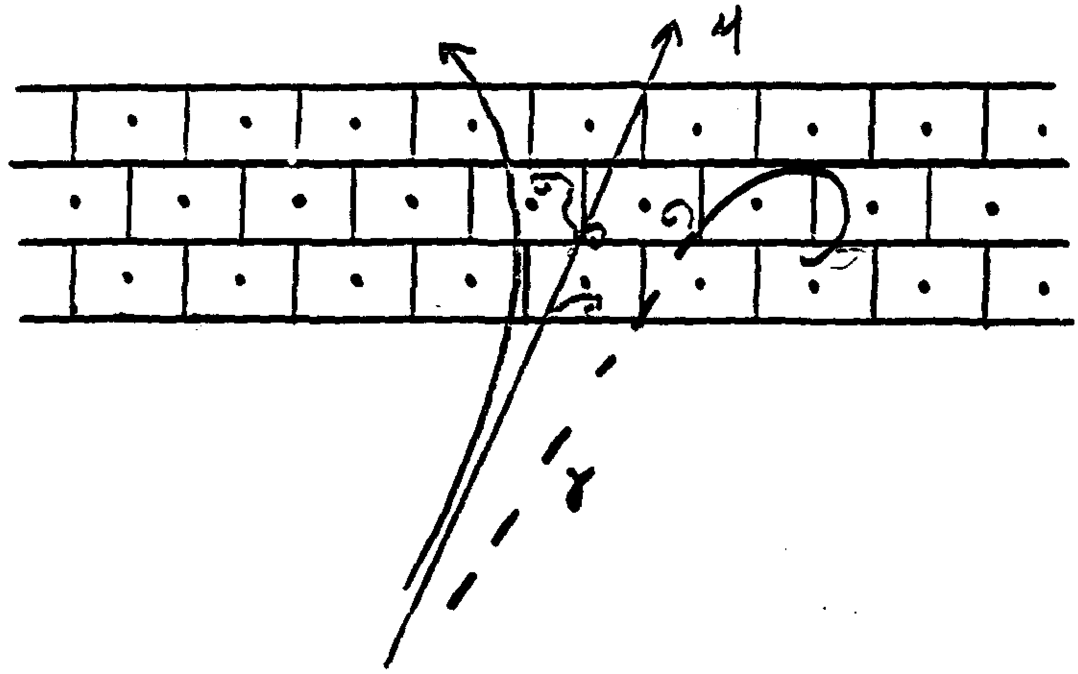

1) CHARGED PARTICLES OTHER THAN μ'S FOUND IN THE SAME CELL AS THE μ THAT COME CLOSER TO THE ANODE WIRE THAN THE μ.

2) CHARGED PARTICLES OTHER THAN THE MUON WHICH STRIKE CELLS AJACENT (± 1 CELL , ± 2 CELLS) TO THOSE WHICH THE μ HIT.

STATEMENT OF THE PROBLEM:

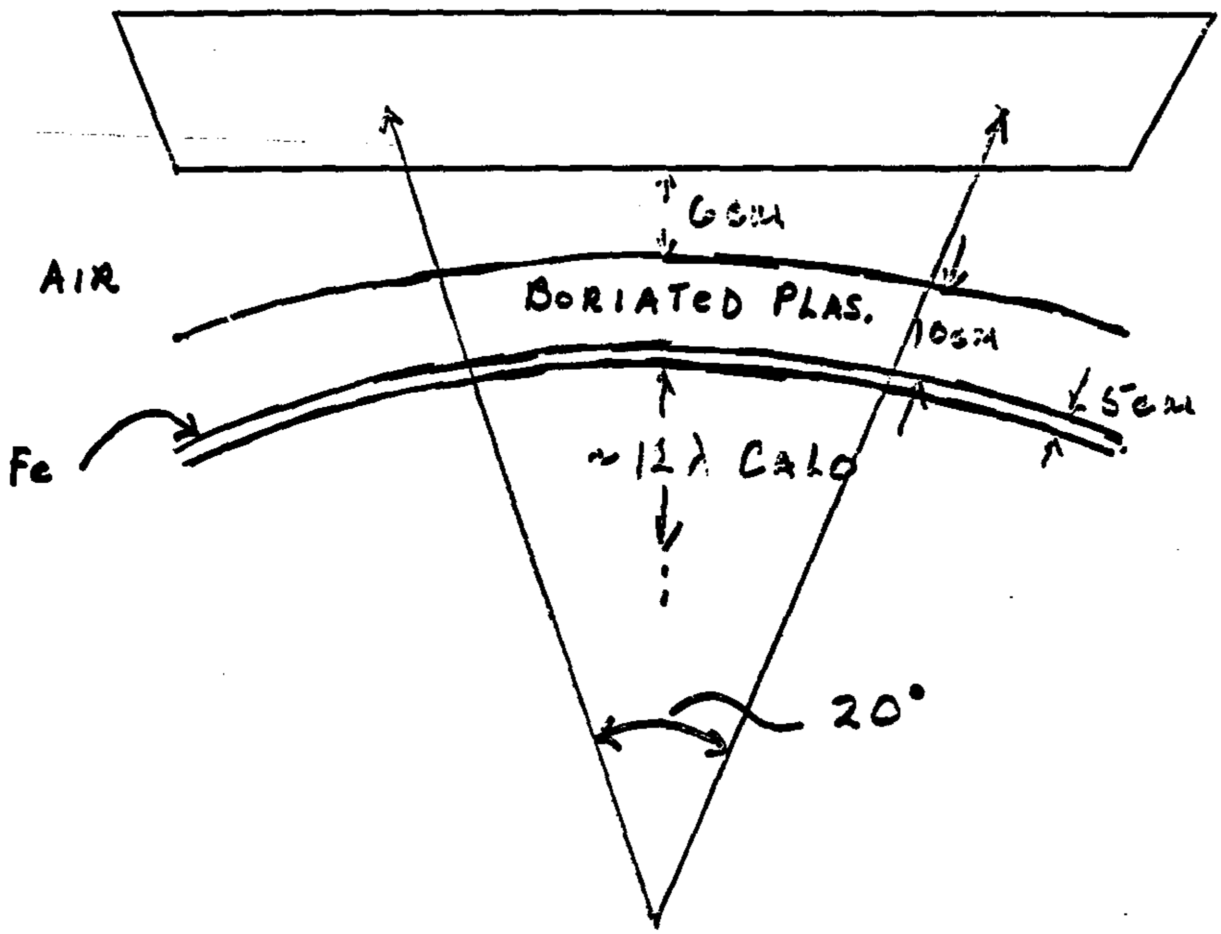

1) WANT TO DETERMINE THE NUMBER OF μ SAMPLING LAYERS LOST DUE TO μ INDUCED BACKGOUNDS; δ RAYS, CONVERSIONS, CHARGED PARTICLES COMING FROM THE TOP OF THE CALO...

2) WANT TO DETERMINE THE NUMBER OF SAMPLING LAYERS LOST IN μ SYSTEM FOR μ'S IN 'B' + 'T' JETS DUE TO BACKGROUNDS IN (1) PLUS BACKGROUNDS DUE TO CHARGED PARTICLE NOISE FROM THE JET.

3) WANT TO GET A FIRST LOOK @ THE EFFICIENCY FOR FINDING μ TRACKS IN THE BARREL IN THE PRESENCE OF CHARGED PARTICLE NOISE

4) WANT TO DETERMINE THE EFFECT ON THE RESOLUTION OF μ TRACKS DUE TO THOSE LOST MEASUREMENTS.

- FOR THIS STUDY I USED A HIT-LEVEL MC OF THE MUON SYSTEM IN THE GEM "BASELINE 1" CONFIGURATION.
- THE STUDY WAS CONDUCTED FOR μ'S IN THE BARREL SYSTEM ONLY
- THE SIMULATION USES THE MAGNETIC FIELD MAP WITH THE FLUX CONCENTRATOR AND MAGNET MEMBRANE INCLUDED.
- THE MUON SYSTEM WAS CONSTRUCTED OF "884" OR "484" LAYERS OF AL WALLS HAVING 11.8% (7.5%), 11.8%, 7.4% OF AN X_0. INSIDE THE CHAMBERS WAS THE SENSITIVE GAS Ar CO_2.
- A SCIN-Pb CALORIMETER WITH ~12 λ @ 90° WAS USED IN FRONT OF THE MUON SYSTEM.

- BEHIND THE CALO. WAS
  5cm Fe (CRYOSTAT, SINCE LAr WAS CHOOSEN THIS MAY BE AN IMPORTANT BG. CONSIDERATION)
  10 cm BORIATED Poly. AND
  A 6cm Air GAP @ $\eta = 90°$

- 1 MeV PHYSICS CUTS WERE IMPOSED EVERYWHERE ACCEPT;
  a) 20 CM INTO CALO FROM TOP - 50 keV
  b) ALL MUON SYSTEM VOLUMES - 50KeV

- WIRES AND VERTICLE CELL WALLS WERE PROVIDED IN SOFTWARE MAPS (INCREASES SPEED OF PROGRAM)

- FULL TRACKING OF SECONDARIES AND PHY. PROCESSES IMPLEMENTED.

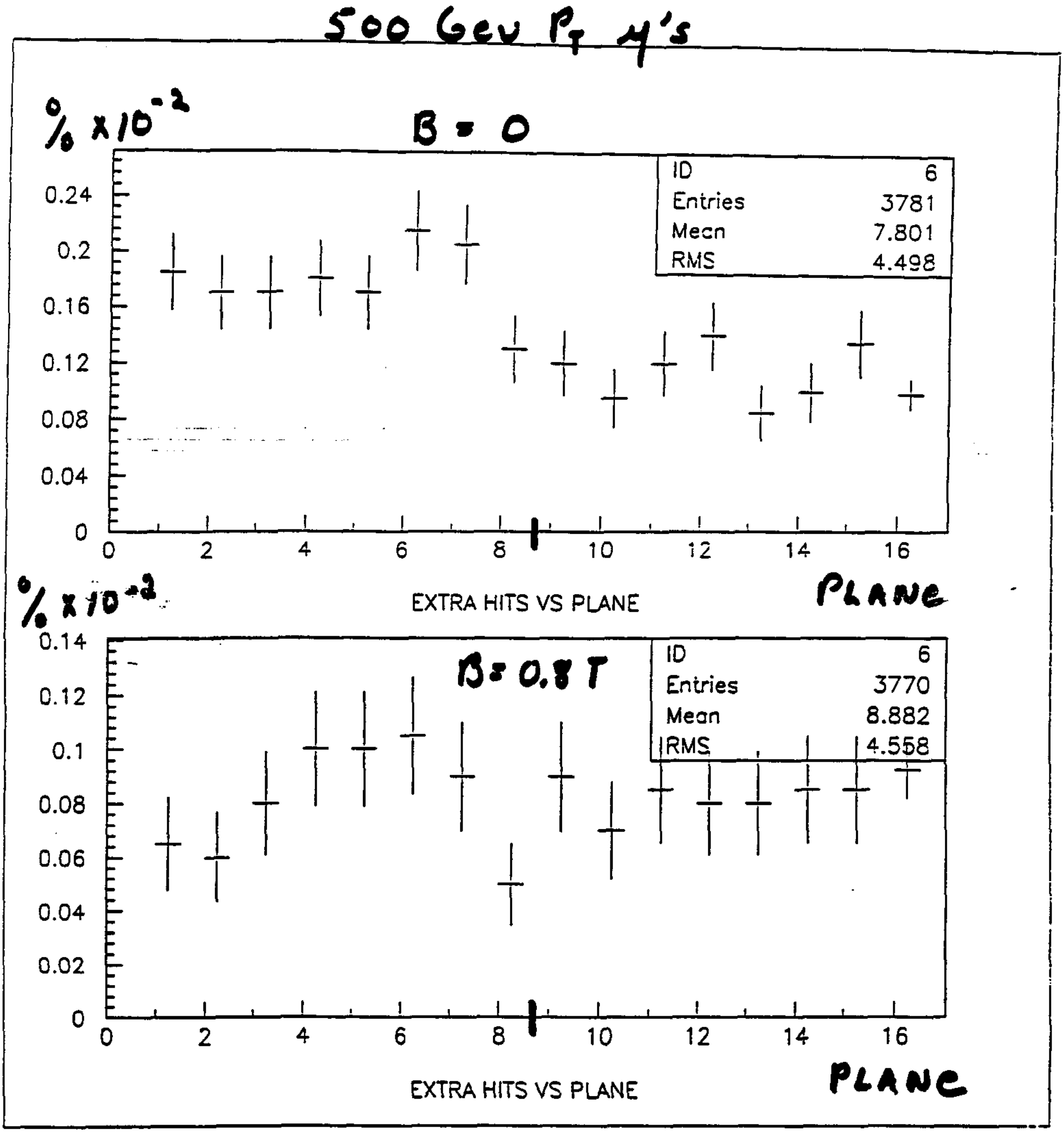

EFFECT OF TURNING FIELD ON AND OFF

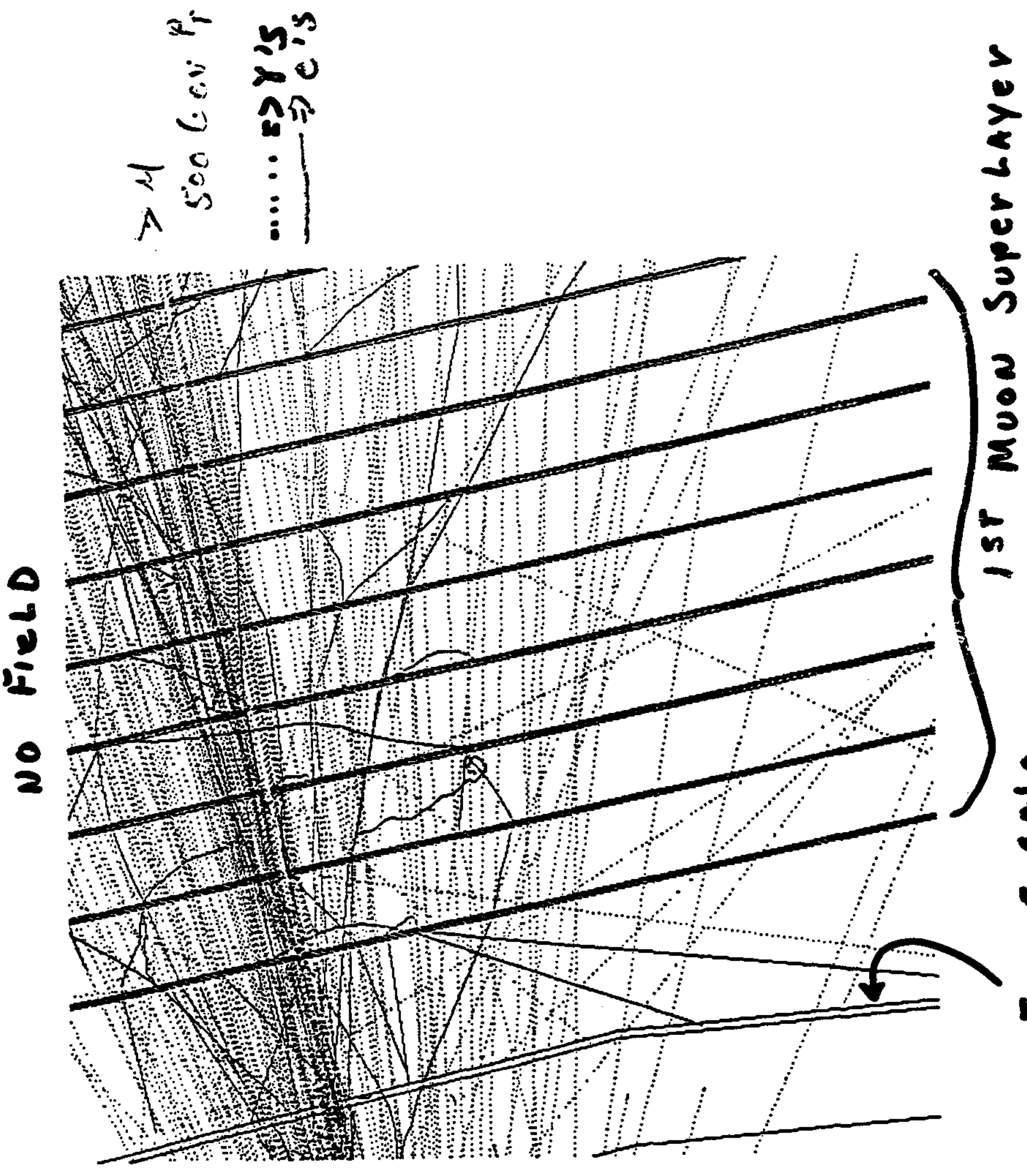
NO FIELD
> M
500 GeV PT
.... => γ's
——— => e's
1ST MUON SuperLAYer
TOP OF CALO

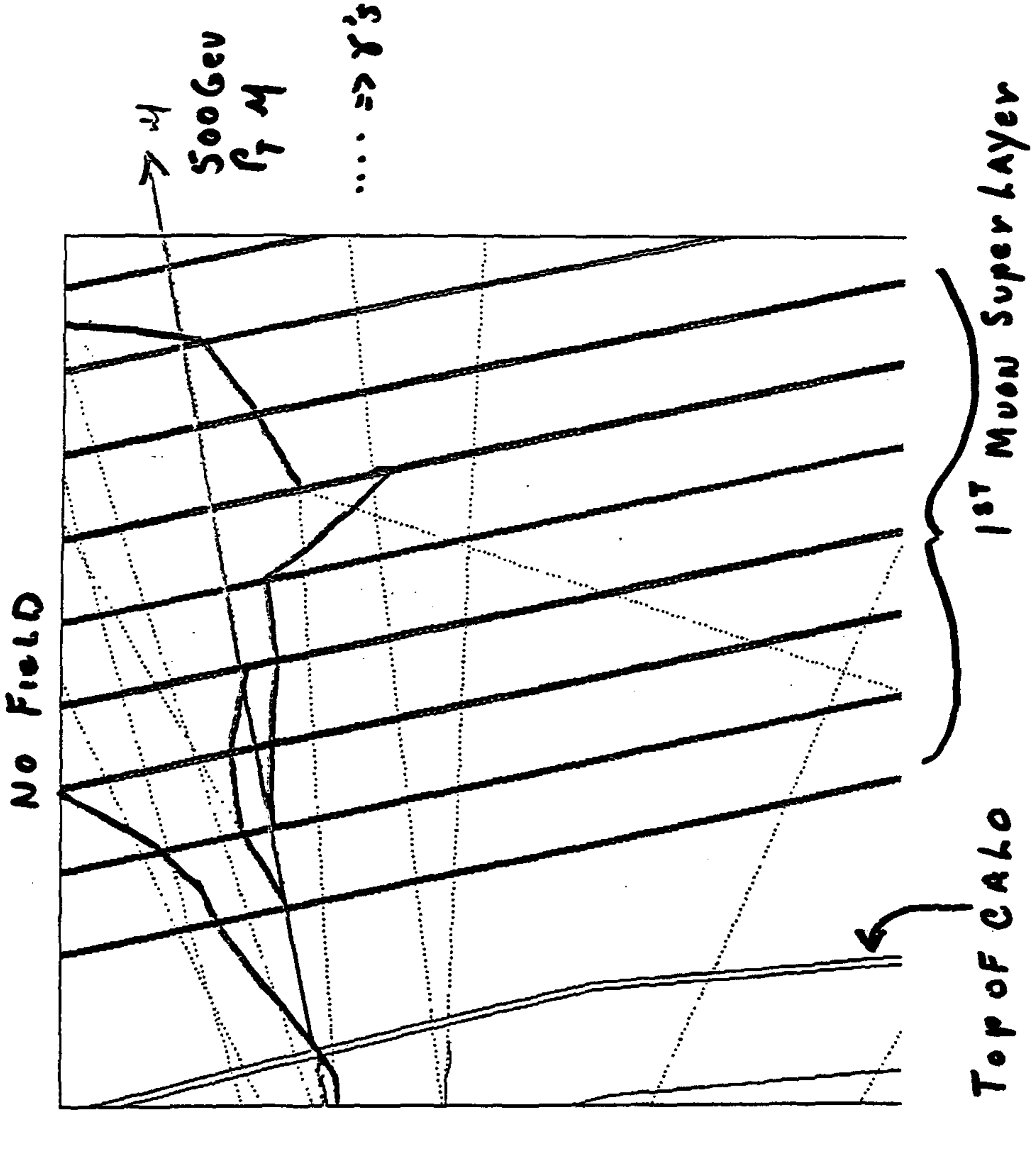
No Field
500 GeV
P_T μ
... => γ's
1st Muon Super Layer
Top of Calo

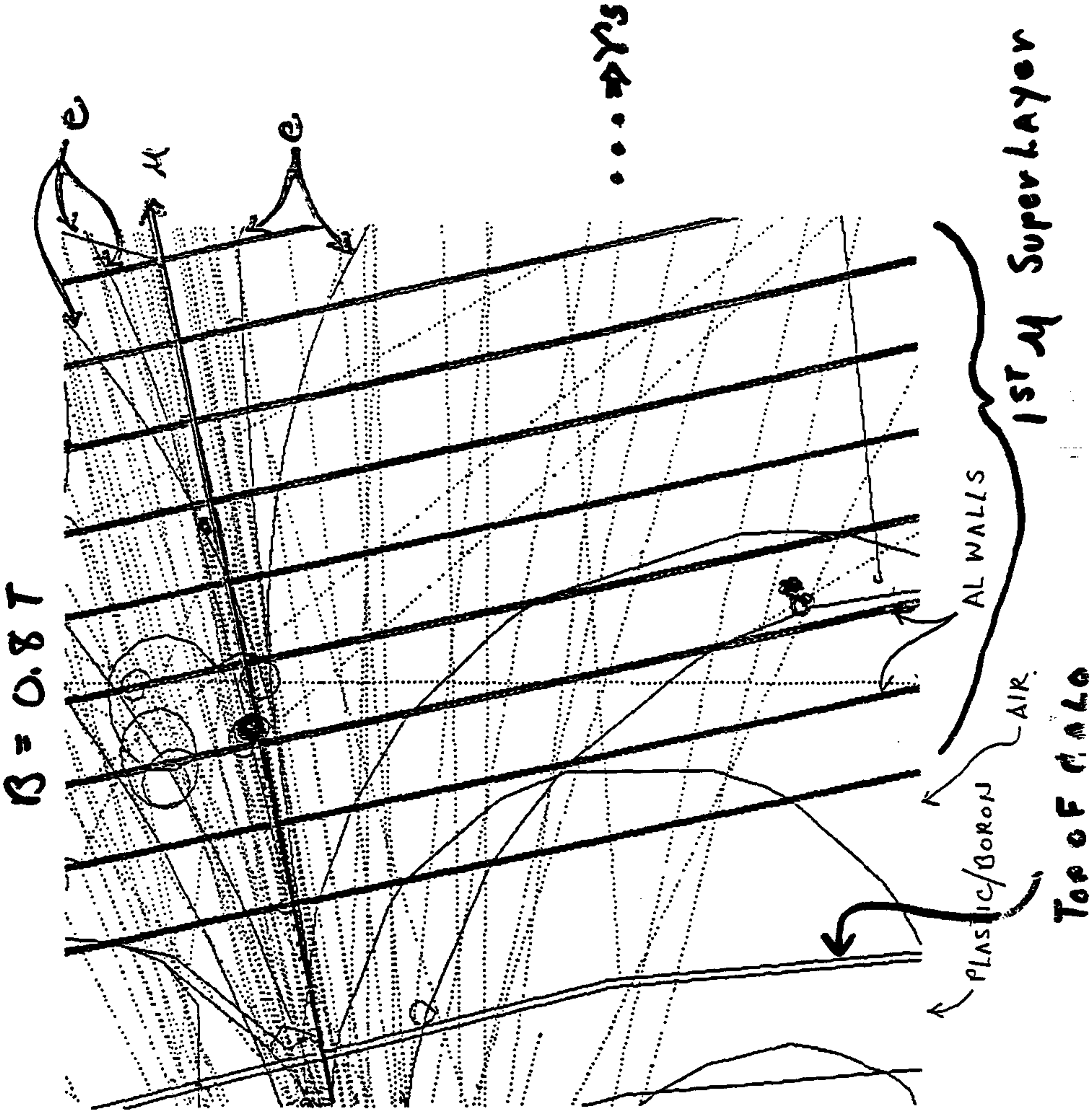
B = 0.8 T
1ST μ SuperLayer
AL WALLS
AIR
PLASTIC/BORON

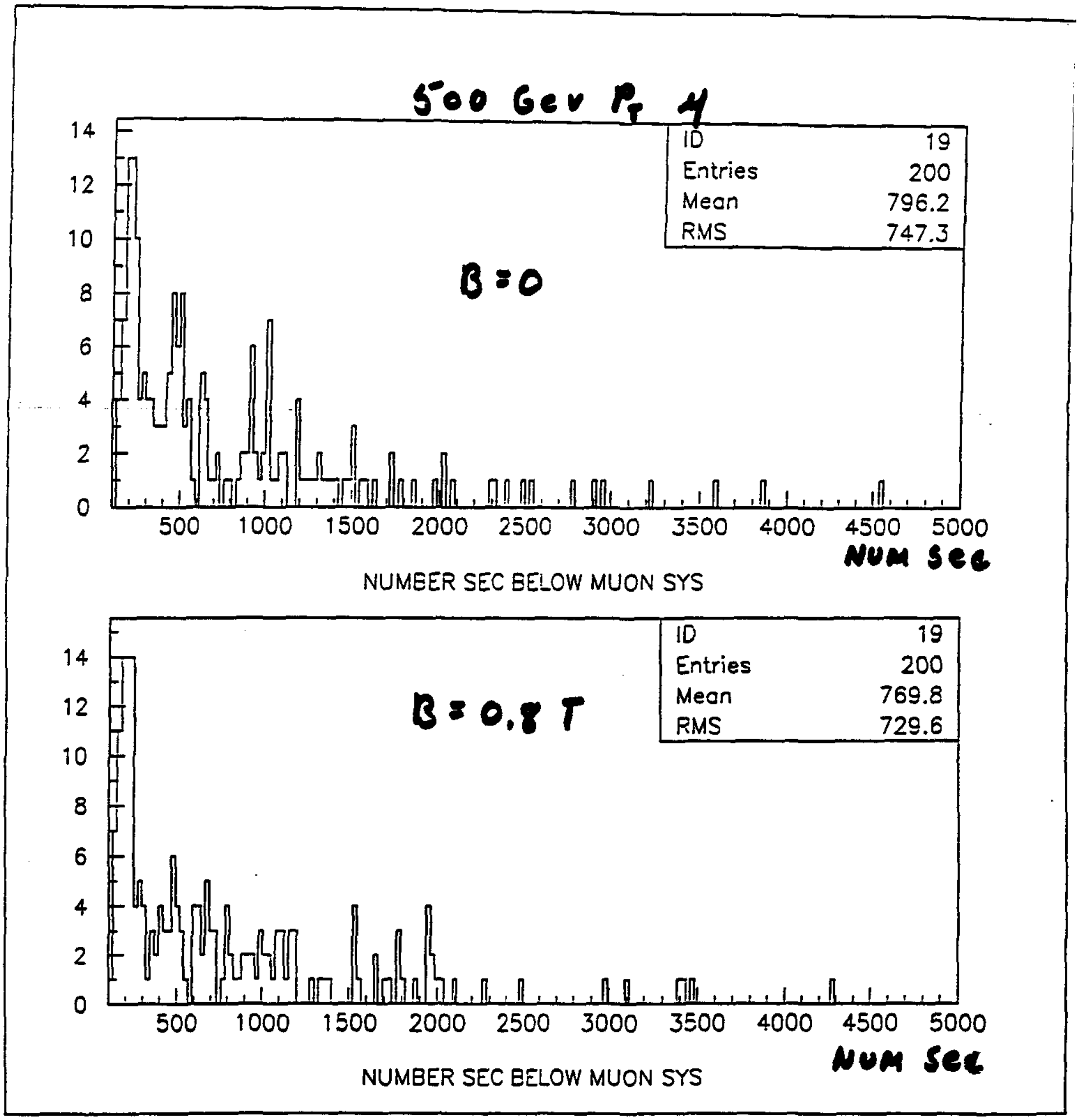

500 GeV P_T μ
ID 19
Entries 200
Mean 796.2
RMS 747.3
B = 0
NUM SEC
NUMBER SEC BELOW MUON SYS
ID 19
Entries 200
Mean 769.8
RMS 729.6
B = 0.8 T
NUM SEC
NUMBER SEC BELOW MUON SYS

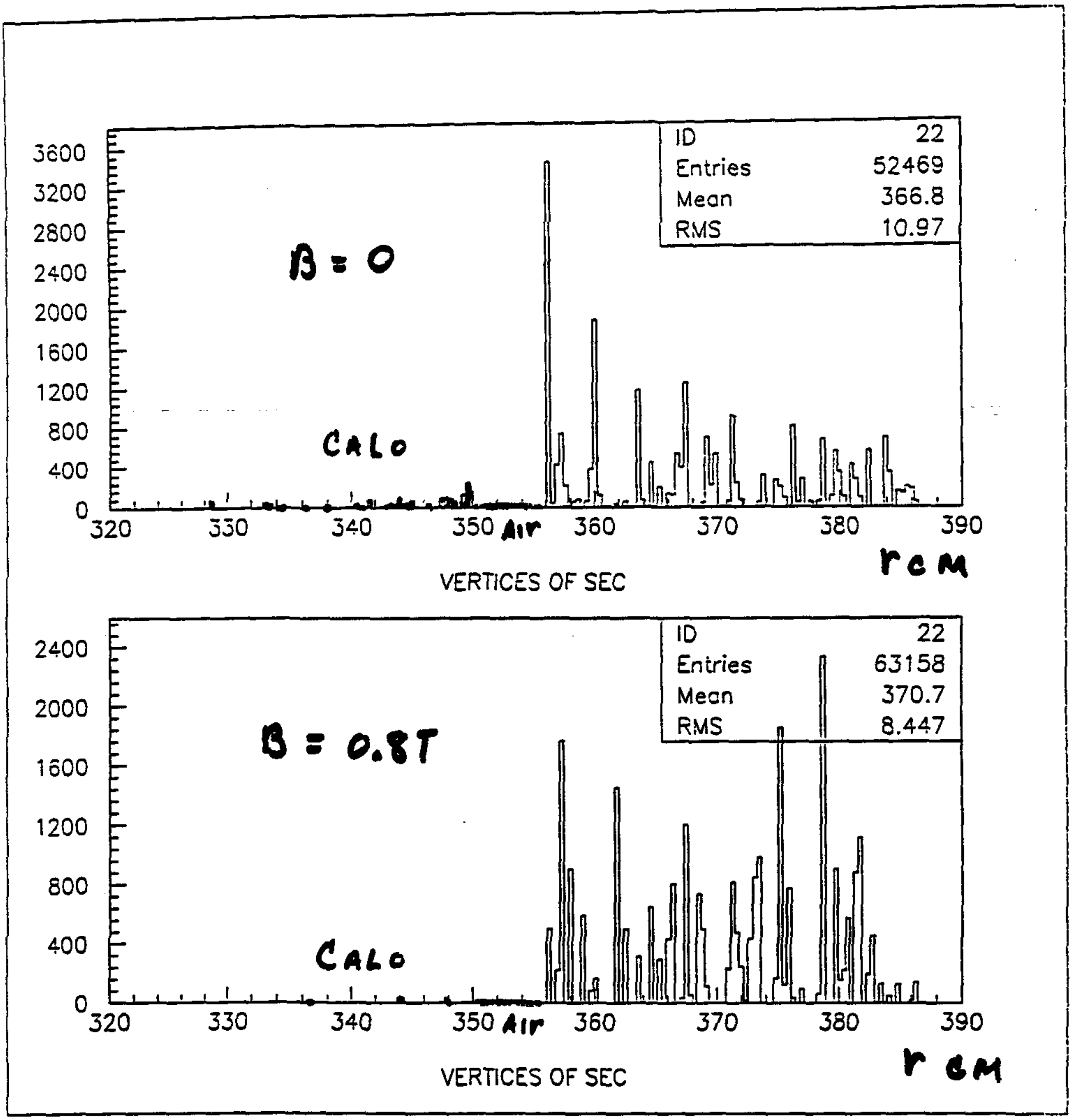

VERTICES OF ORIGIN OF SECONDARY HITS IN MUON SYSTEM SENSITIVE GAS

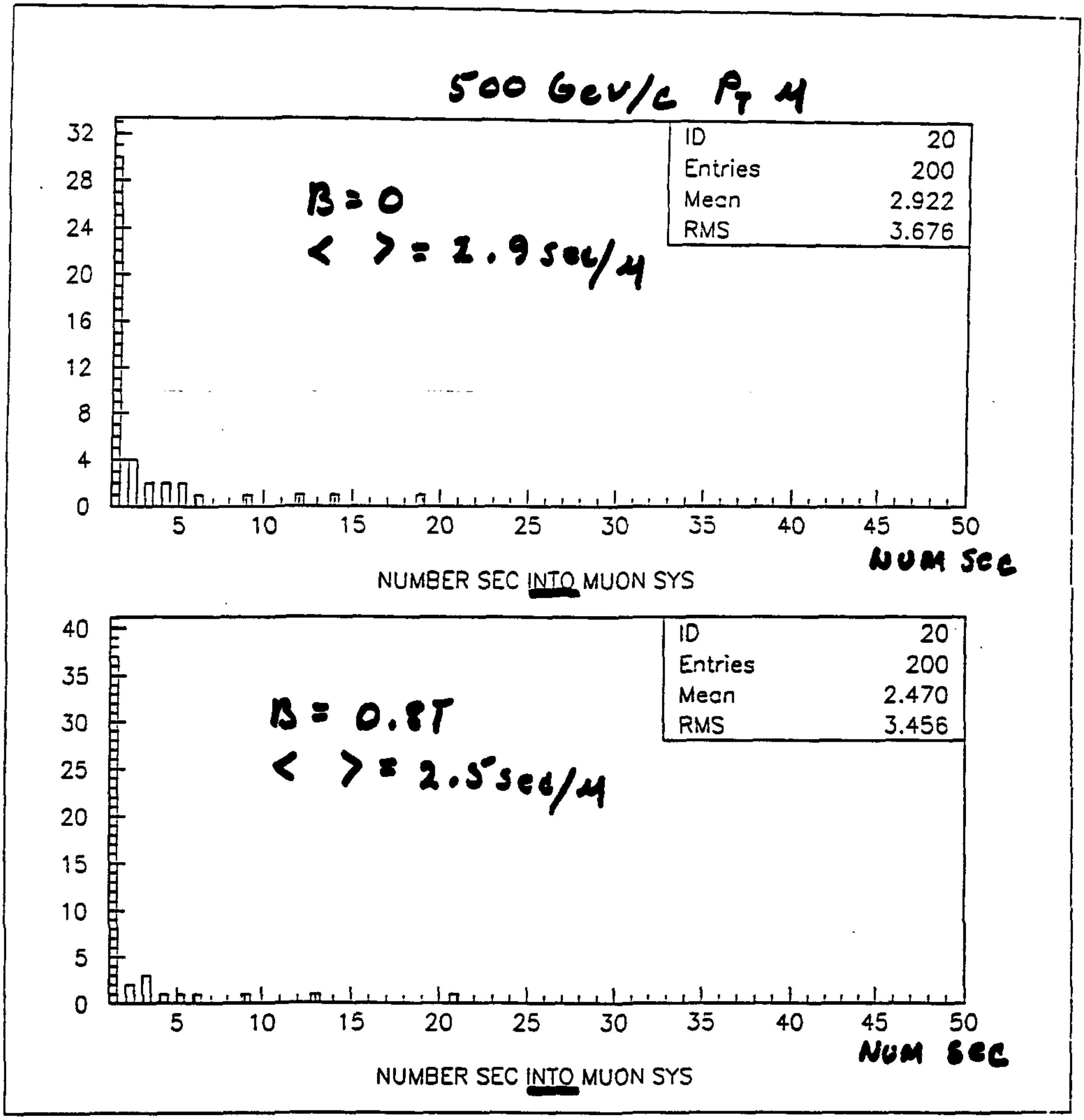
500 GeV/c P_T μ
ID 20
Entries 200
Mean 2.922
RMS 3.676
B = 0
< > = 2.9 sec/μ
NUMBER SEC INTO MUON SYS
NUM SEC
ID 20
Entries 200
Mean 2.470
RMS 3.456
B = 0.8T
< > = 2.5 sec/μ
NUMBER SEC INTO MUON SYS
NUM SEC

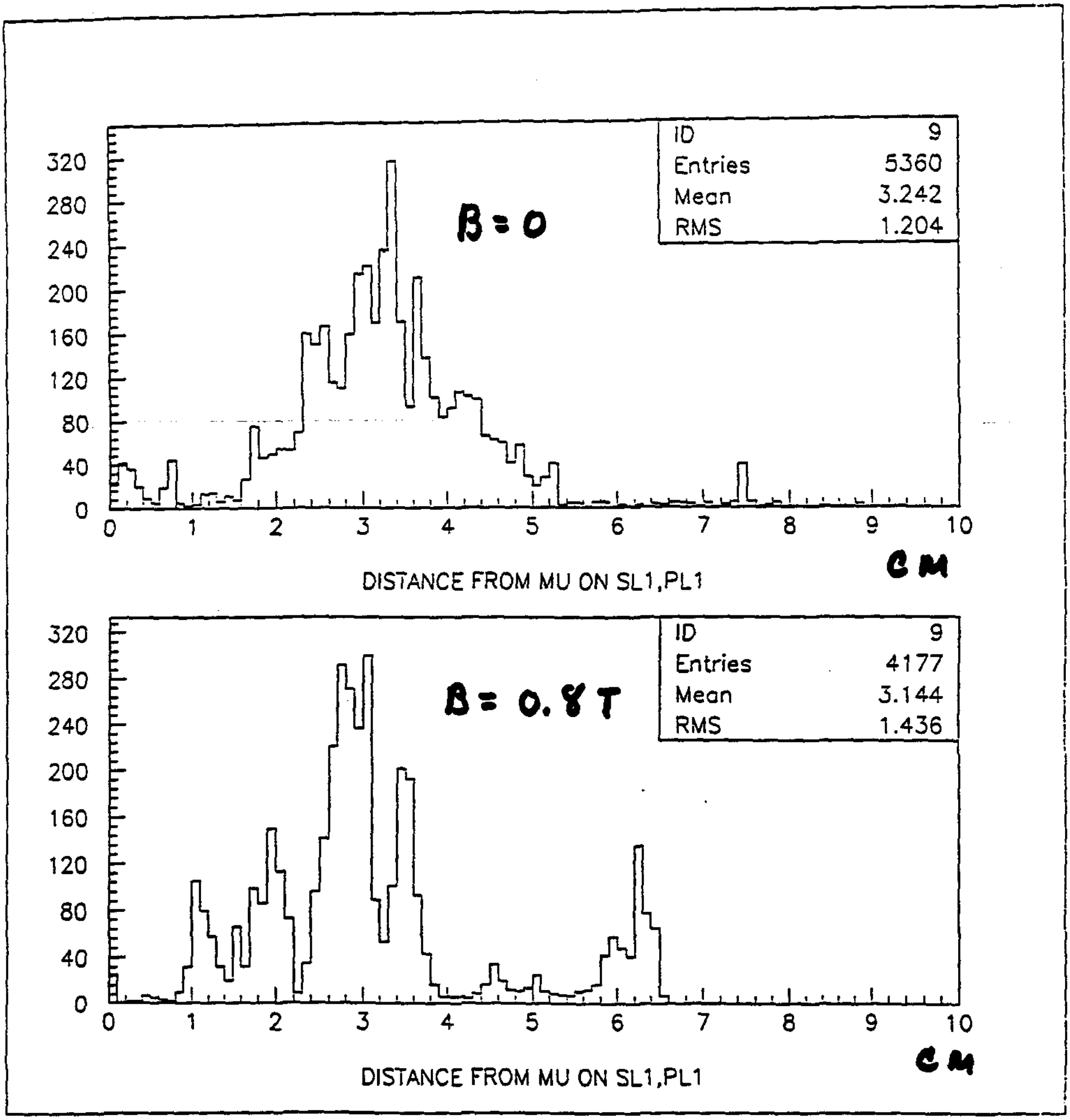

DISTANCE OF SECONDARY FROM μ CELL ON SL=1, PLN=1

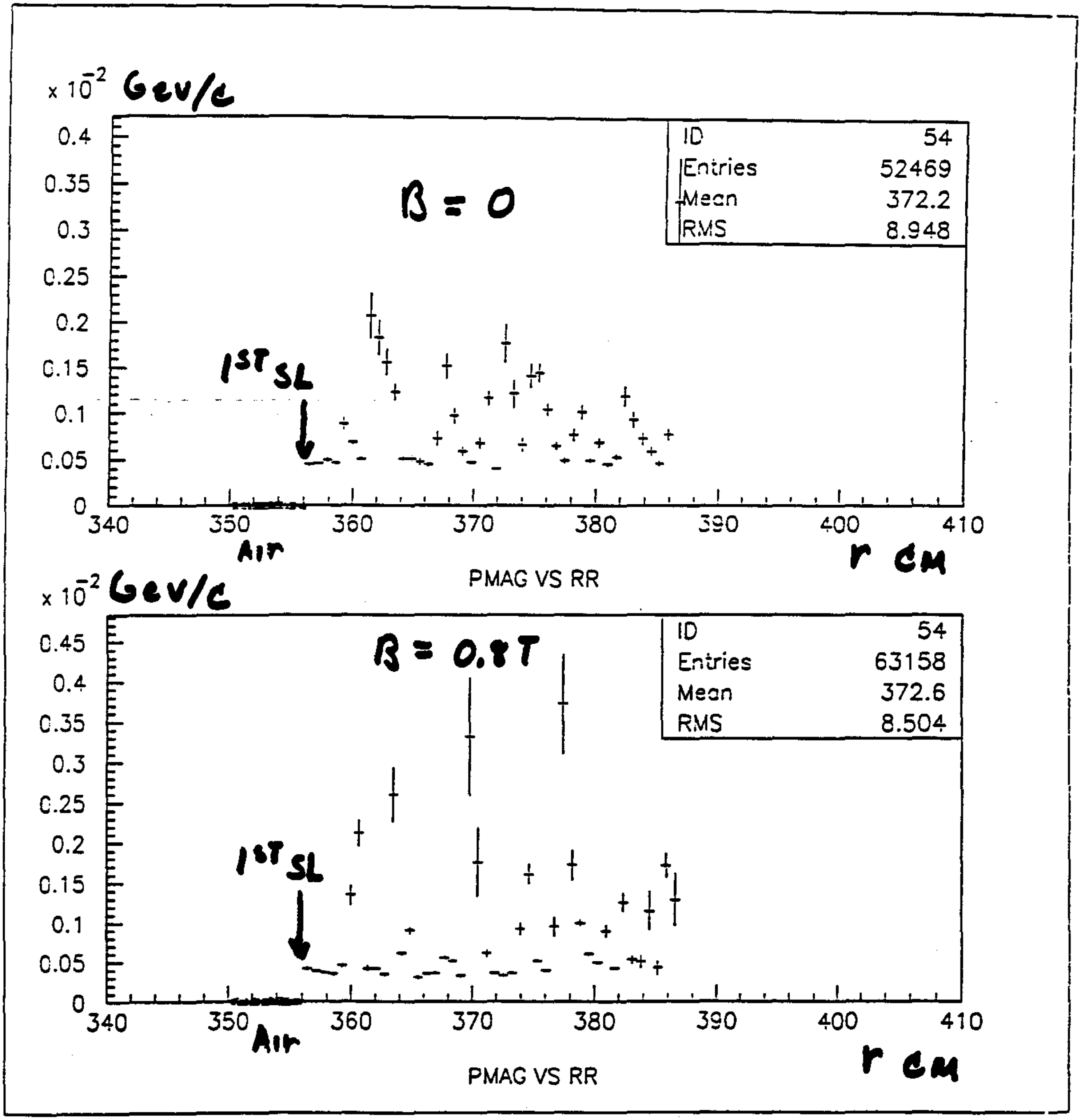
x 10^-2 Gev/c
B = 0
ID 54
Entries 52469
Mean 372.2
RMS 8.948
1ST SL
Air
r cm
PMAG VS RR
x 10^-2 Gev/c
B = 0.8T
ID 54
Entries 63158
Mean 372.6
RMS 8.504
1ST SL
Air
r cm
PMAG VS RR

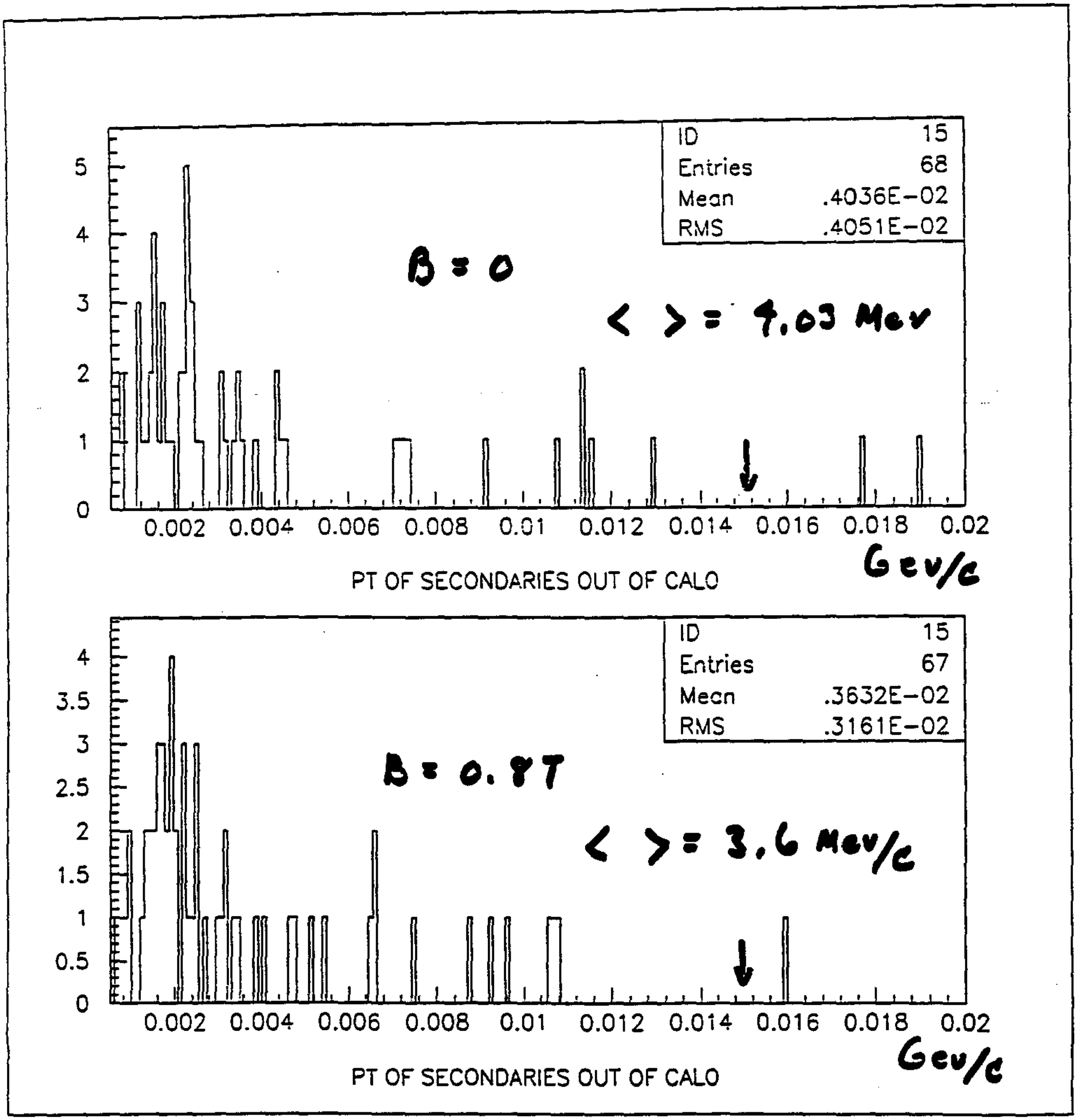

~ 15 Mev/c Required To
get To CALO, 6 cm AWAY @
Center of SL with B = 0.8T
~ 2% on Average

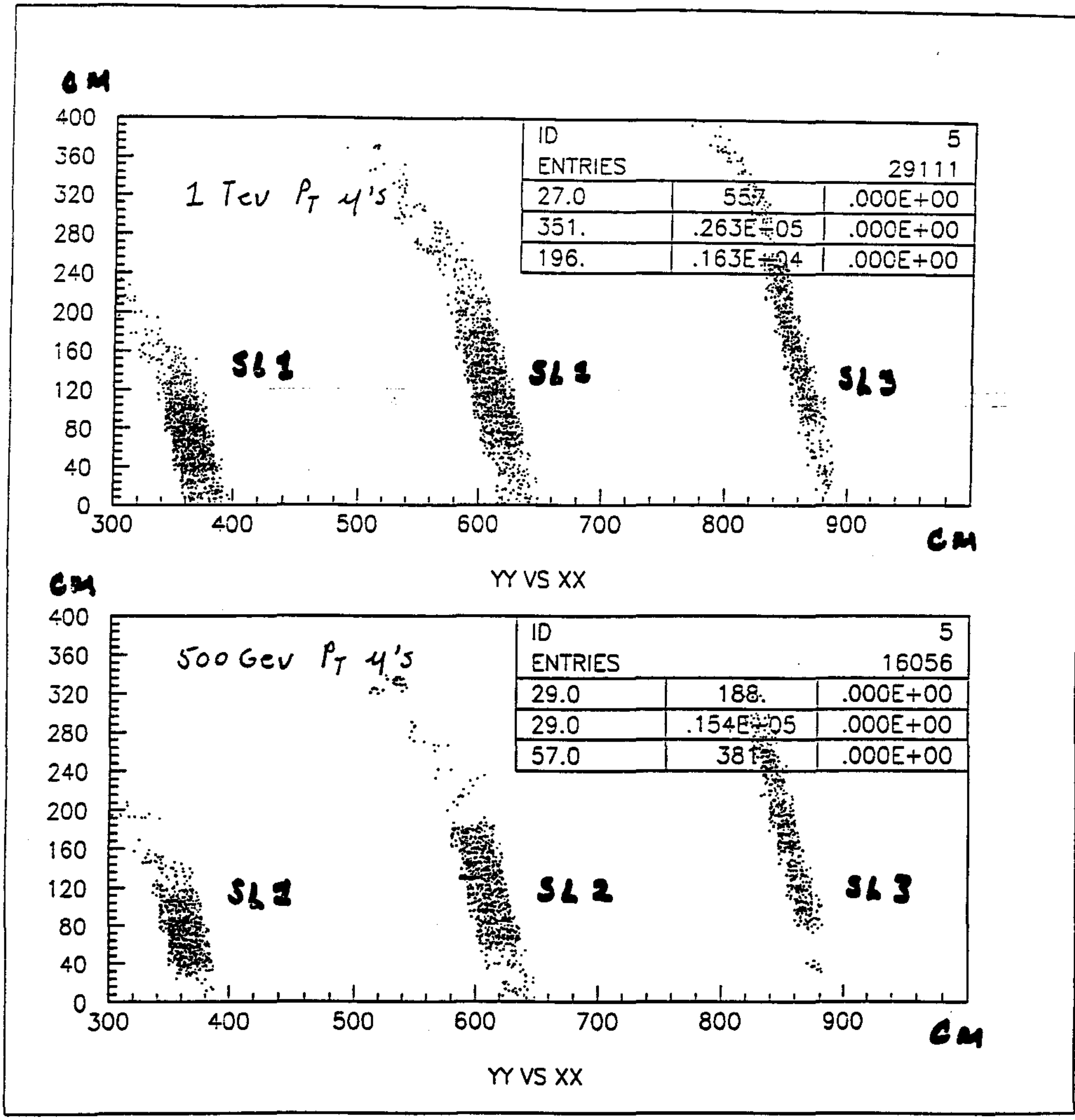

r, φ PLOT OF HITS

1 TeV P_T μ

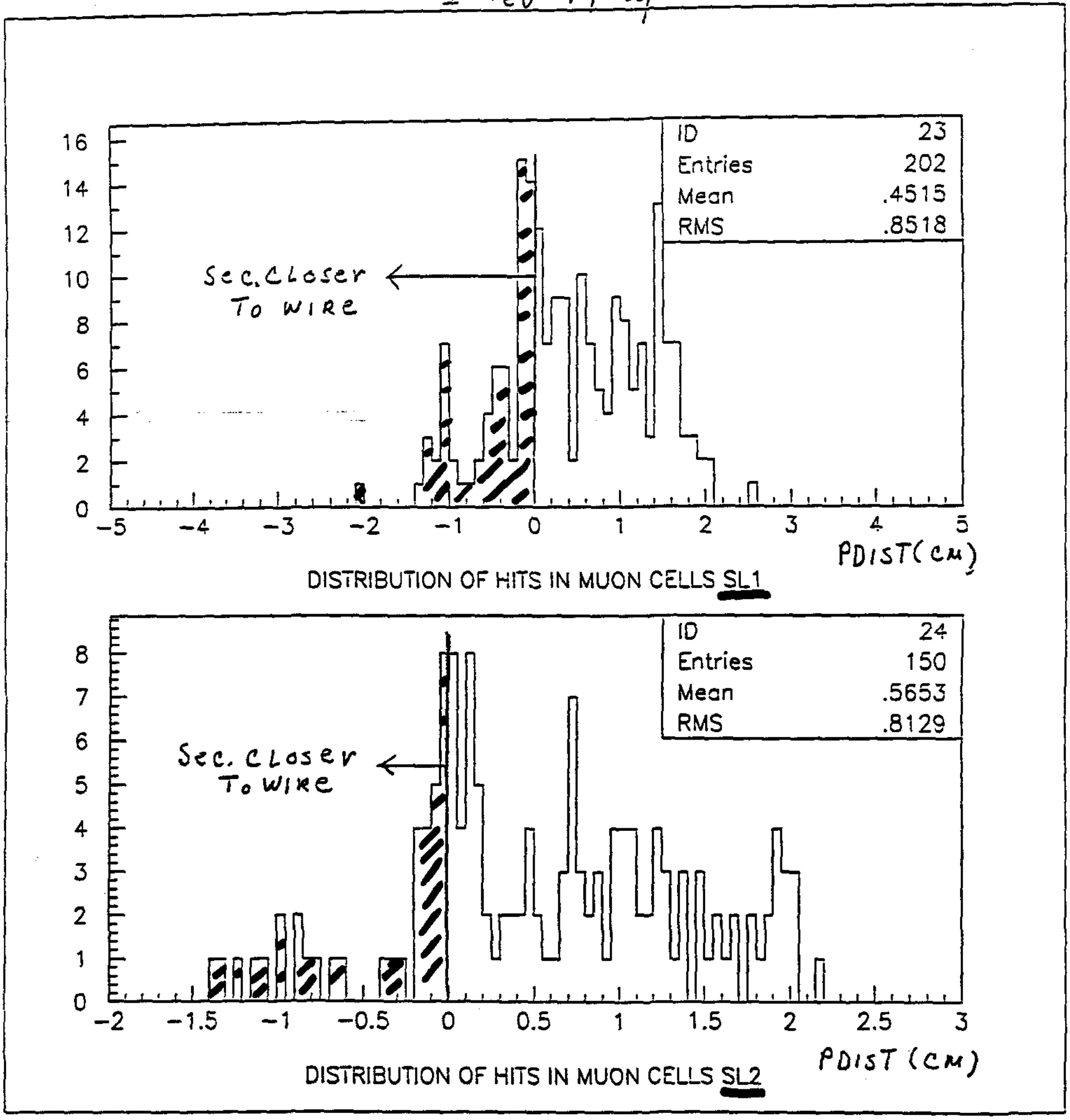

$PDIST \equiv P_{sec} - P_{\mu}$ (in cm)

IF SECONDARY IS CLOSER TO THE WIRE THAN μ PDIST → (−)

<NUM SEC CLOSER> ~ 28%

1 Tev P_T μ

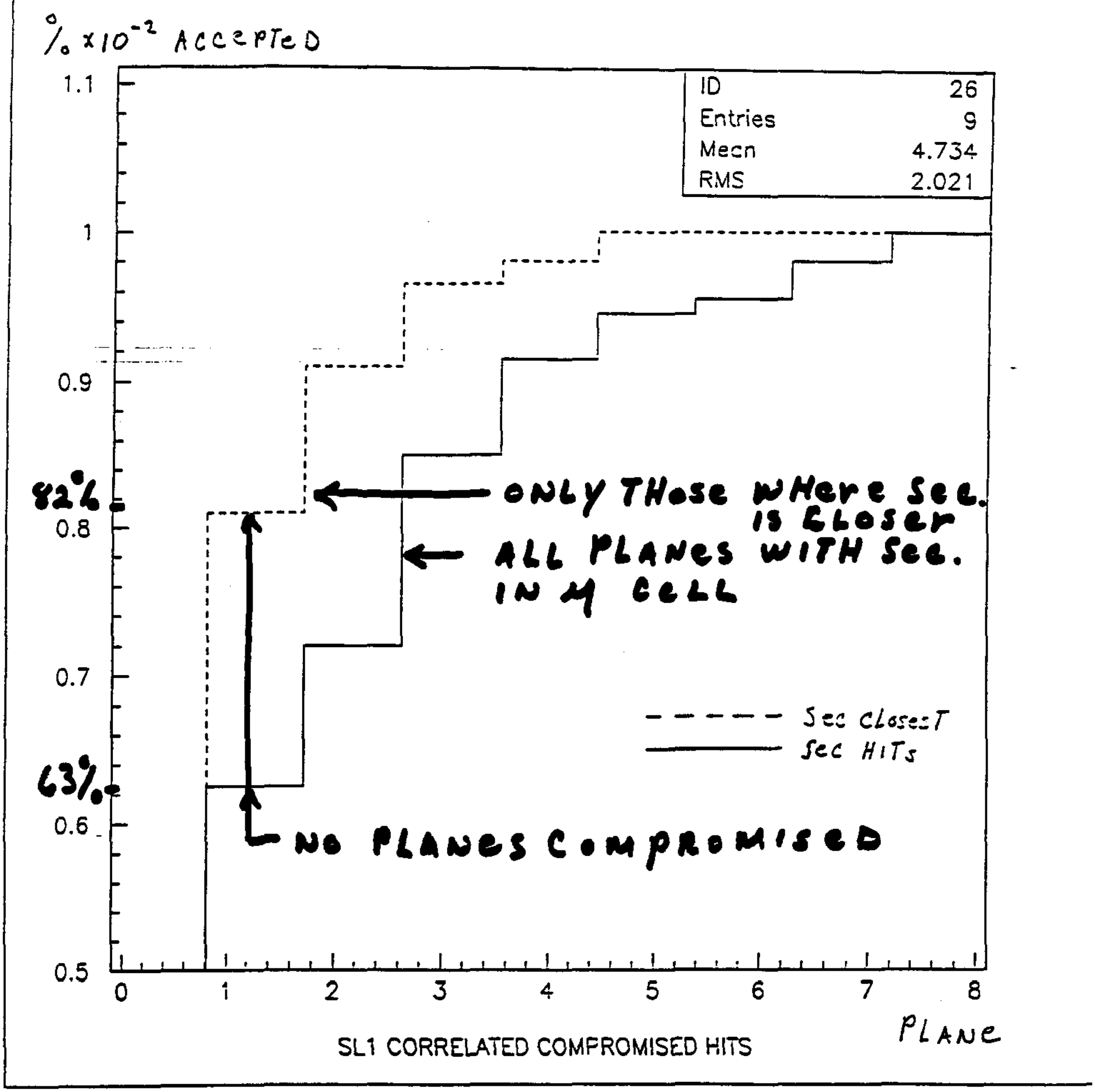

$$\frac{(82-63)}{63} = 30\%$$

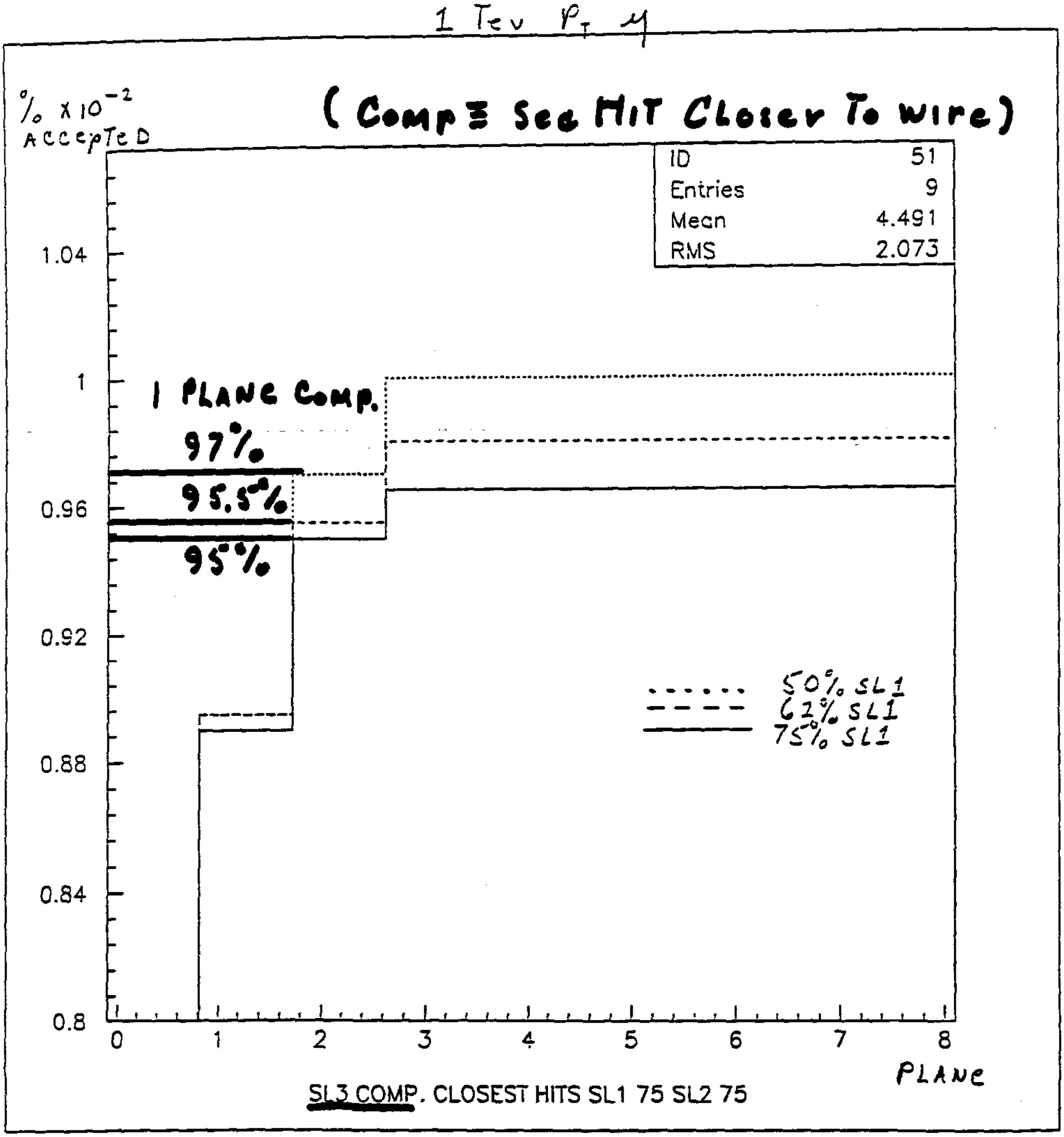

PLANES COMPROMISED ON SL3 GIVEN ≥75% PLANES ON SL1 AND SL2 UNCOMPROMISED (— SOLID LINE)

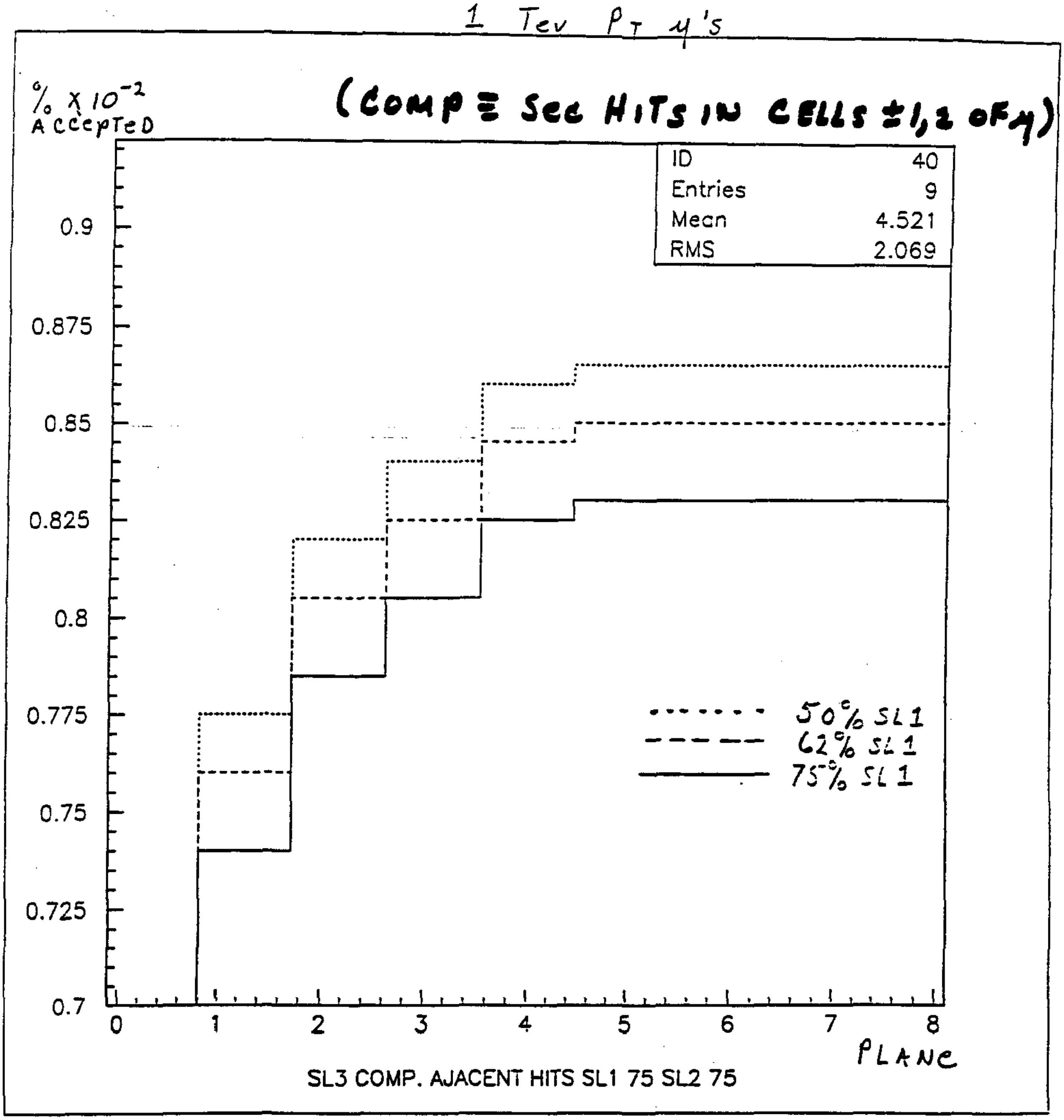

PLANES COMPROMISED ON SL3
GIVEN ≥ 75% OF PLANES ON
SL1 AND SL2 UNCOMPROMISED (— SOLID)

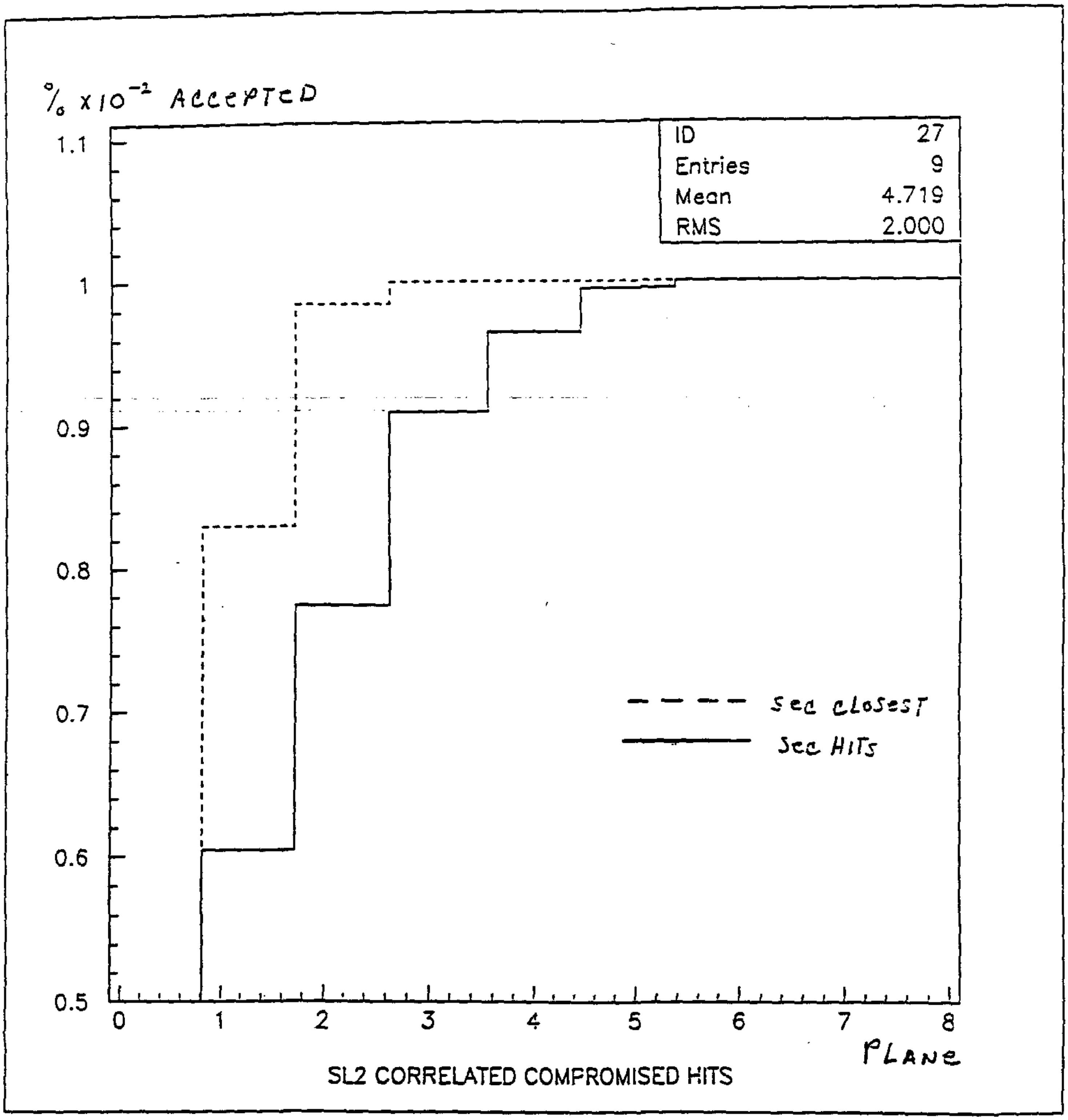

% x10⁻² ACCEPTED
ID 27
Entries 9
Mean 4.719
RMS 2.000
1.1
1
0.9
0.8
0.7
0.6
0.5
0 1 2 3 4 5 6 7 8
SEC CLOSEST
SEC HITS
PLANE
SL2 CORRELATED COMPROMISED HITS

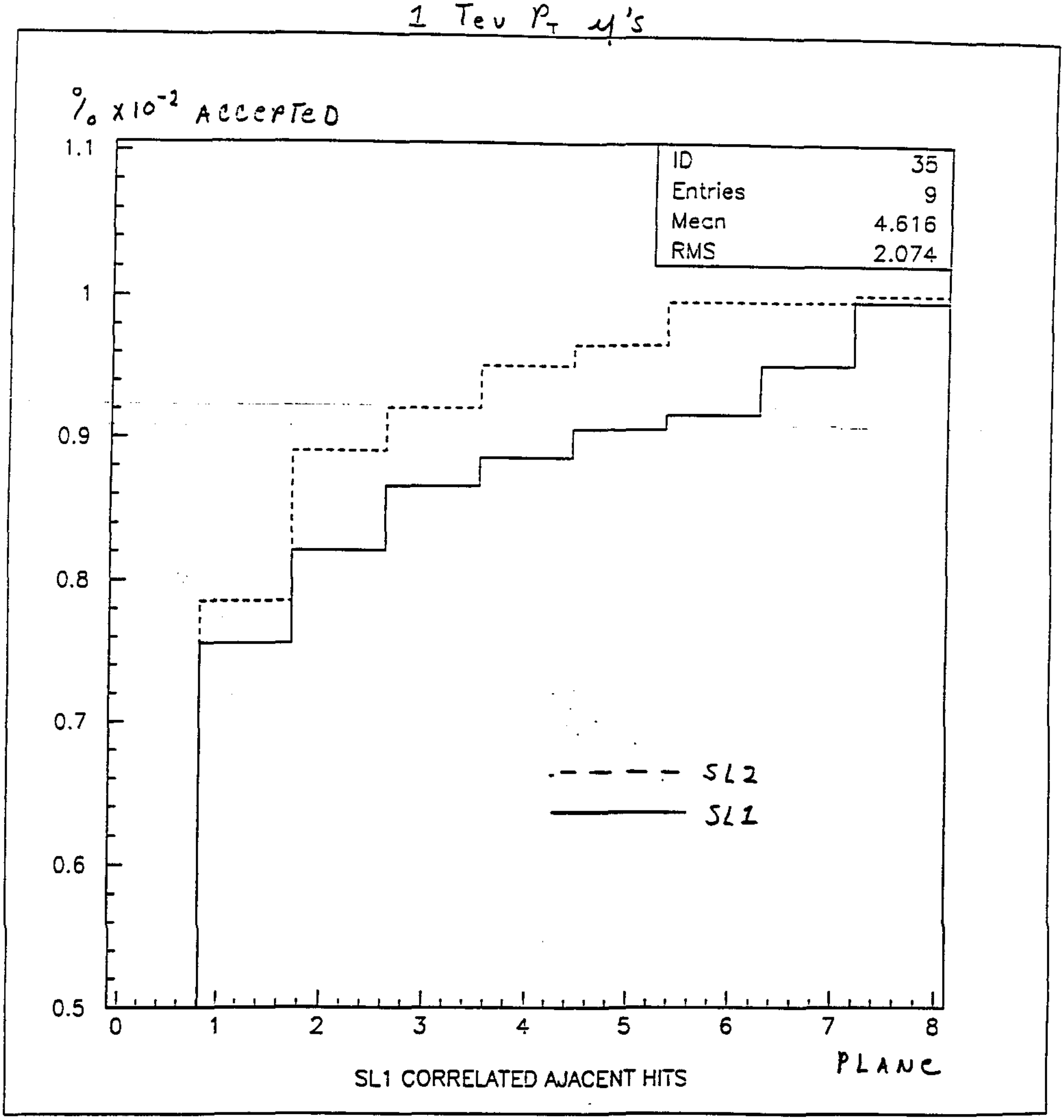

1 Tev P_T μ's
% x10^-2 ACCEPTED
ID 35
Entries 9
Mean 4.616
RMS 2.074
SL2
SL1
SL1 CORRELATED AJACENT HITS
PLANE

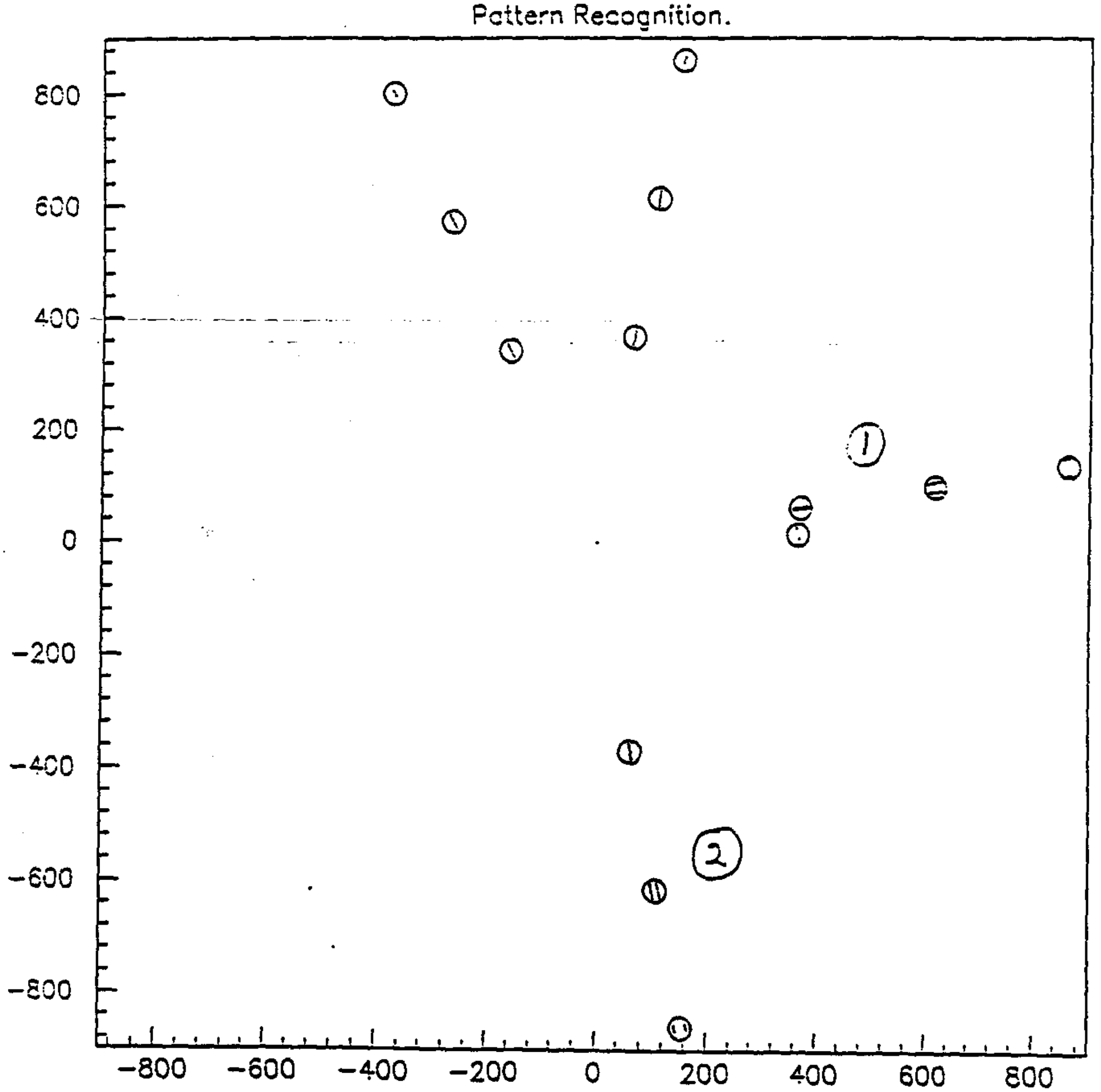

ATTempT To
CLUSTer TRACKS IN
μ SYSTem (JCWU)

1 TeV P_T μ

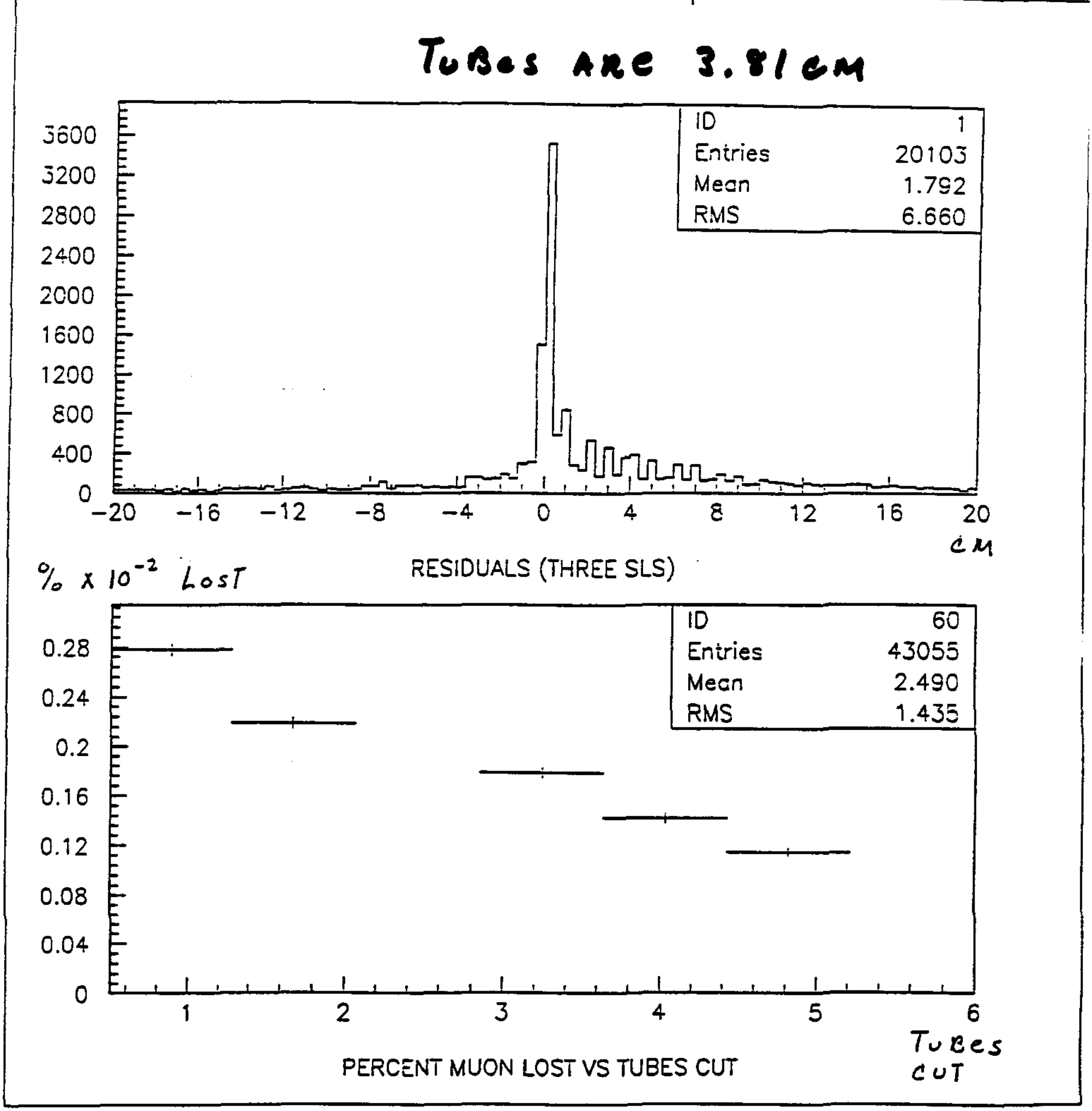

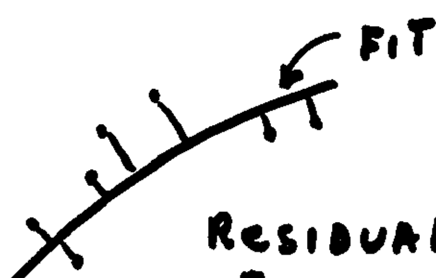

RESIDUALS OF HITS FROM FIT

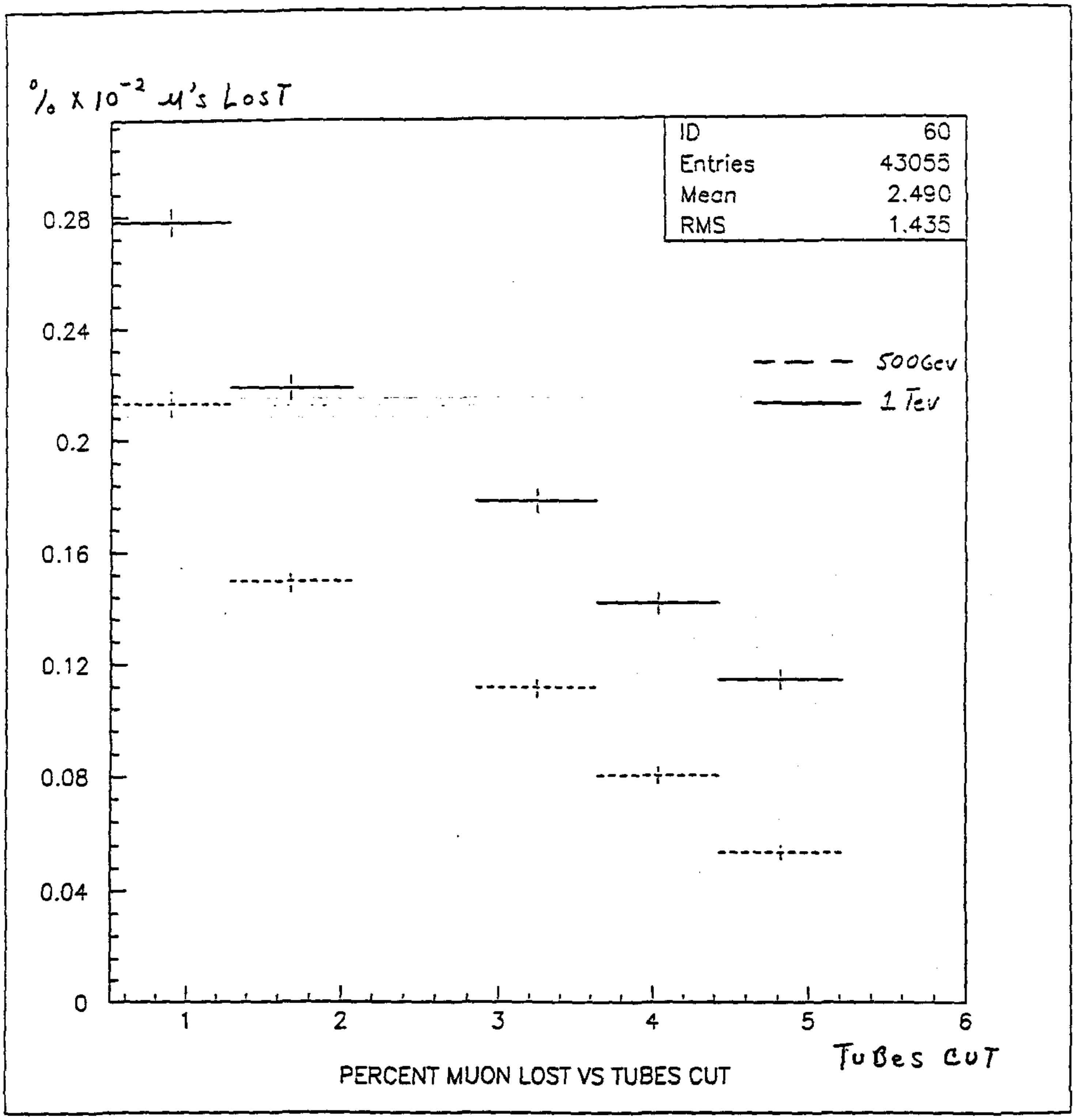
% x 10⁻² μ's LosT
ID 60
Entries 43055
Mean 2.490
RMS 1.435
0.28
0.24
0.2
0.16
0.12
0.08
0.04
0
1
2
3
4
5
6
500Gev
1 Tev
TuBes cuT
PERCENT MUON LOST VS TUBES CUT

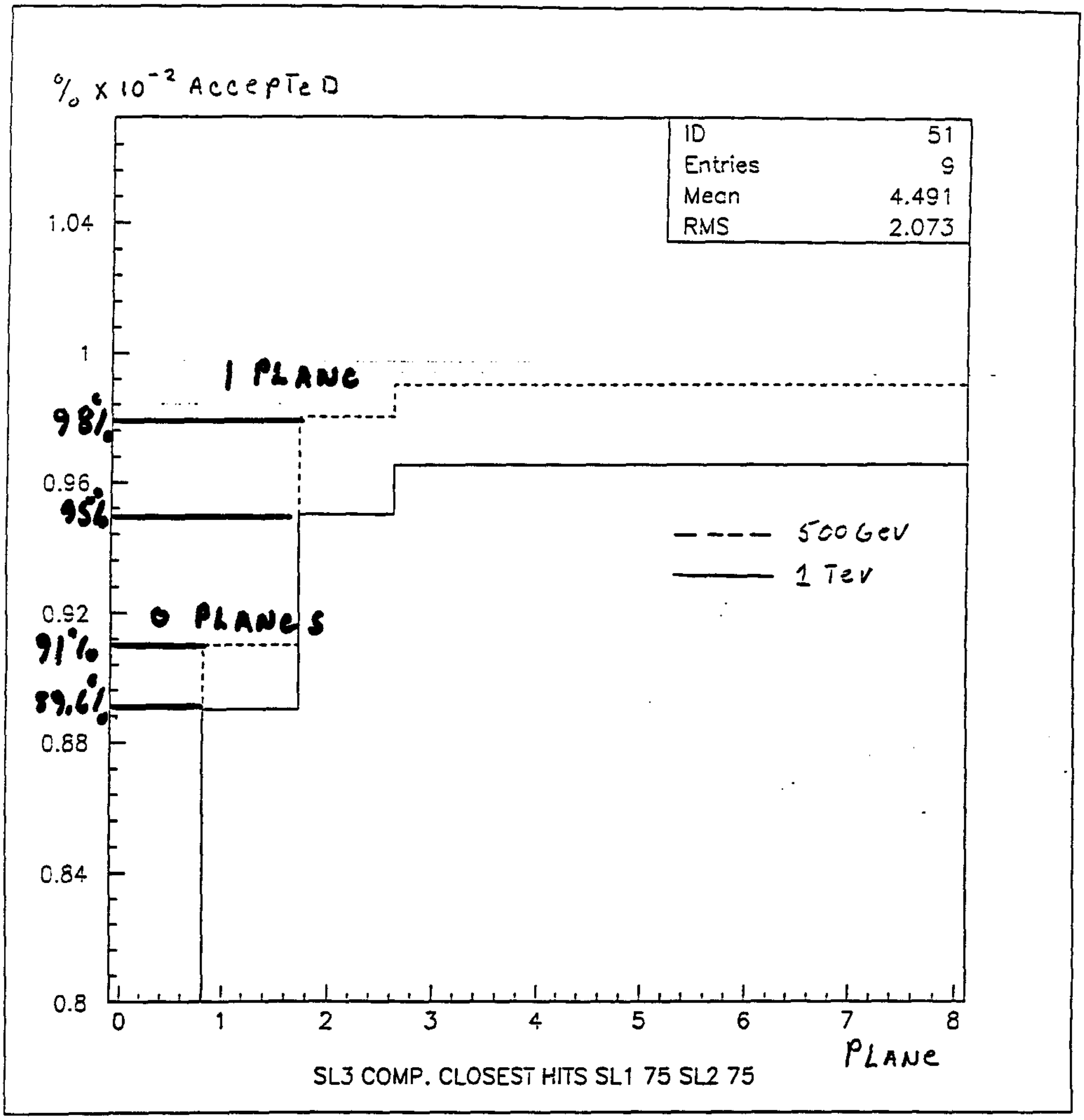

% x 10^-2 AccepTeD
ID 51
Entries 9
Mean 4.491
RMS 2.073
1.04
1
0.96
0.92
0.88
0.84
0.8
1 PLANE
0 PLANES
98%
95%
91%
89.6%
500 GeV
1 TeV
0 1 2 3 4 5 6 7 8
PLANE
SL3 COMP. CLOSEST HITS SL1 75 SL2 75

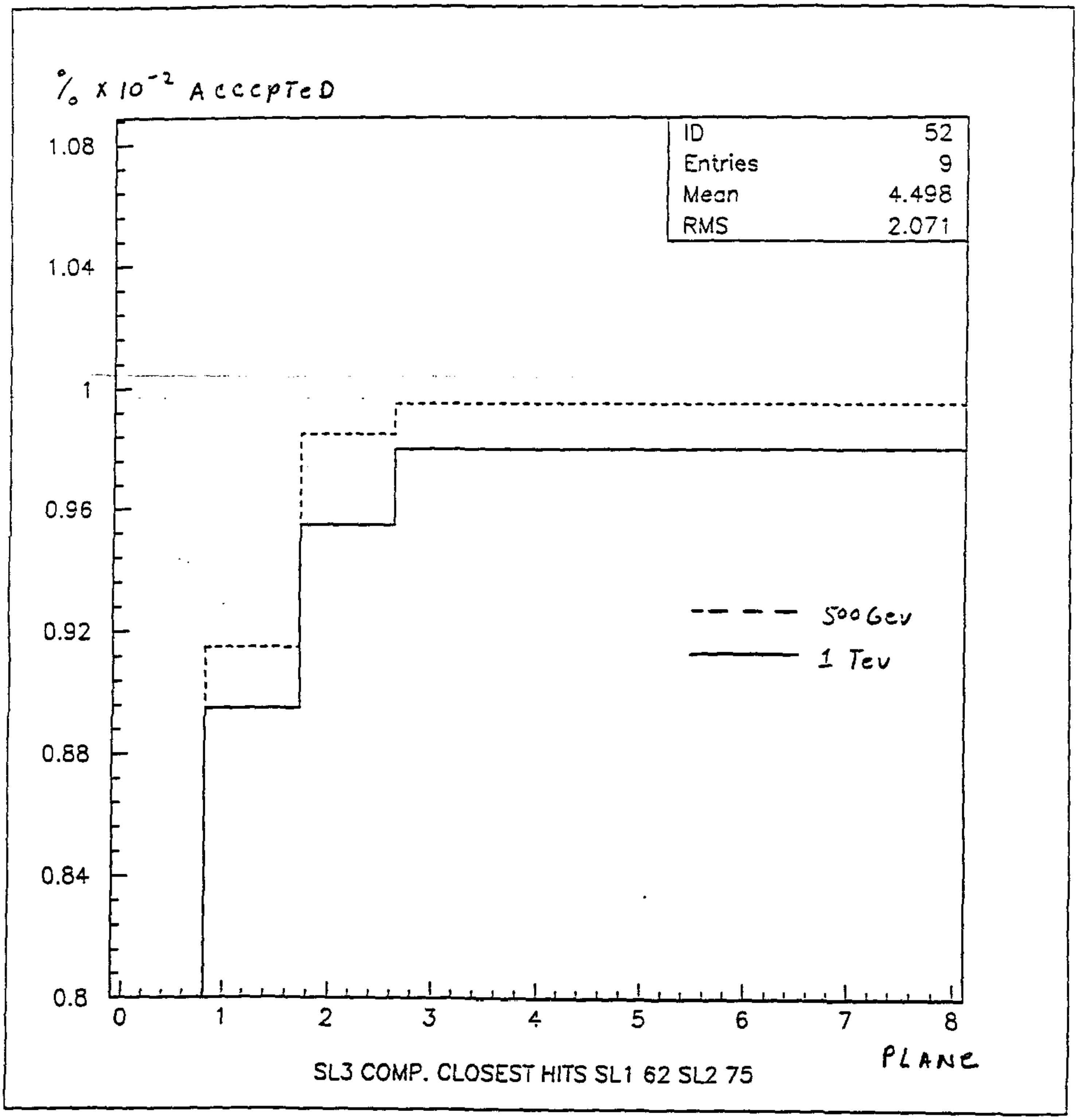

% x 10⁻² ACCEPTED
ID 52
Entries 9
Mean 4.498
RMS 2.071
1.08
1.04
1
0.96
0.92
0.88
0.84
0.8
500 GeV
1 TeV
0
1
2
3
4
5
6
7
8
PLANE
SL3 COMP. CLOSEST HITS SL1 62 SL2 75

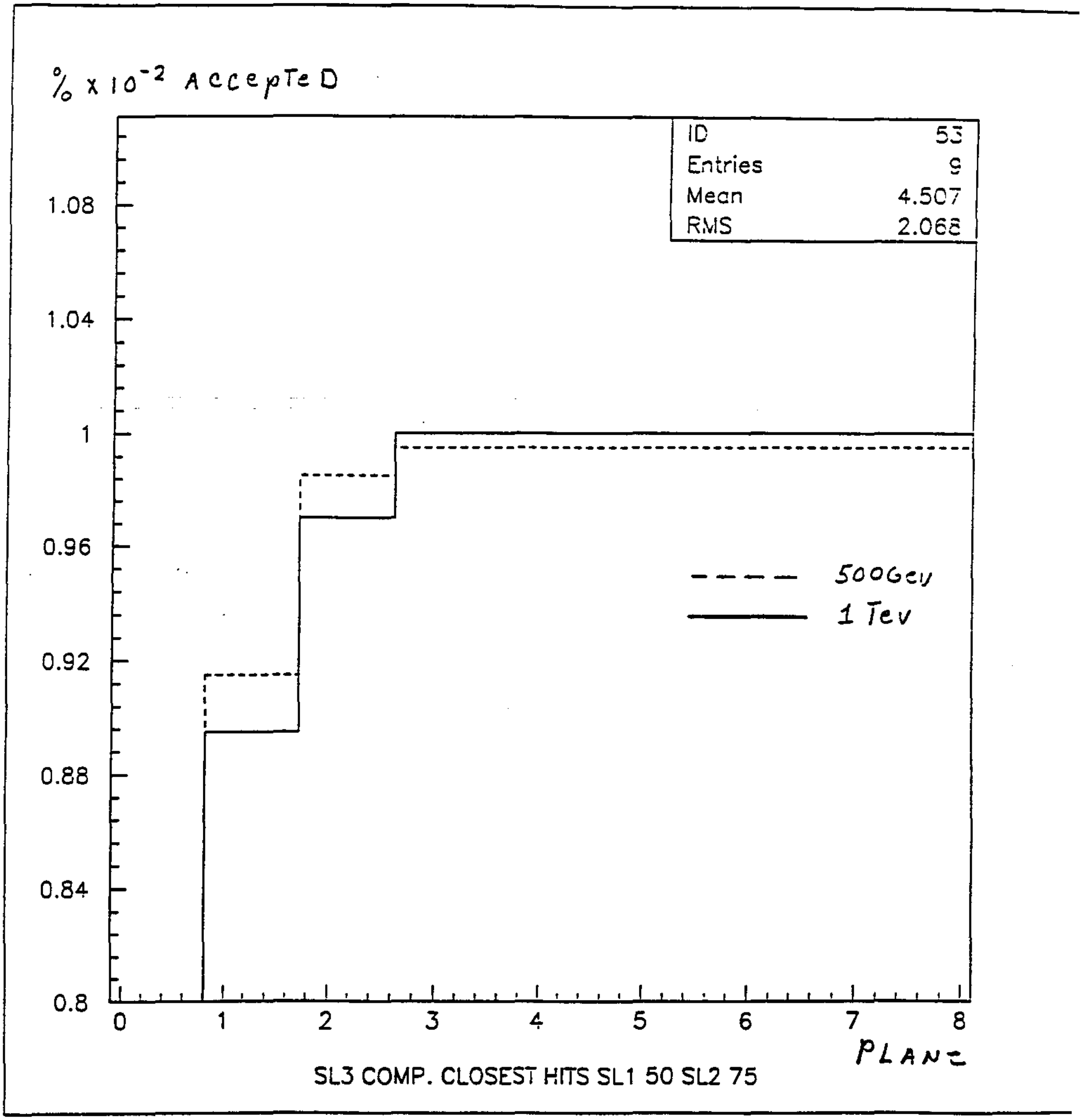
% x 10^{-2} AccepTeD
ID 53
Entries 9
Mean 4.507
RMS 2.068
1.08
1.04
1
0.96
0.92
0.88
0.84
0.8
0
1
2
3
4
5
6
7
8
500GeV
1 Tev
PLANE
SL3 COMP. CLOSEST HITS SL1 50 SL2 75

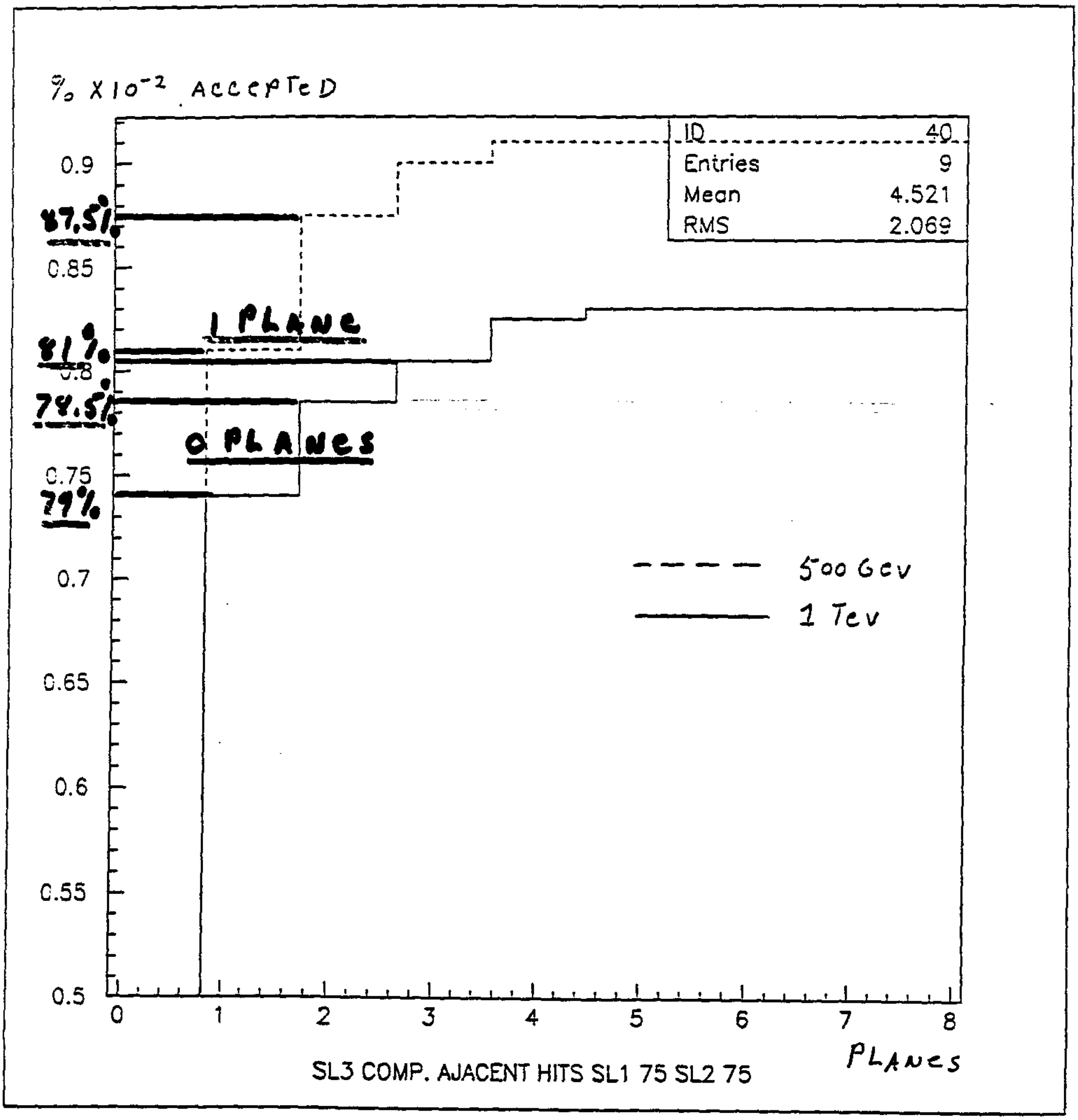

% X10⁻² ACCEPTED
ID 40
Entries 9
Mean 4.521
RMS 2.069
0.9
87.5%
0.85
1 PLANE
81%
0.8
78.5%
0 PLANES
0.75
74%
0.7
0.65
0.6
0.55
0.5
500 GeV
1 TeV
0 1 2 3 4 5 6 7 8
PLANES
SL3 COMP. AJACENT HITS SL1 75 SL2 75

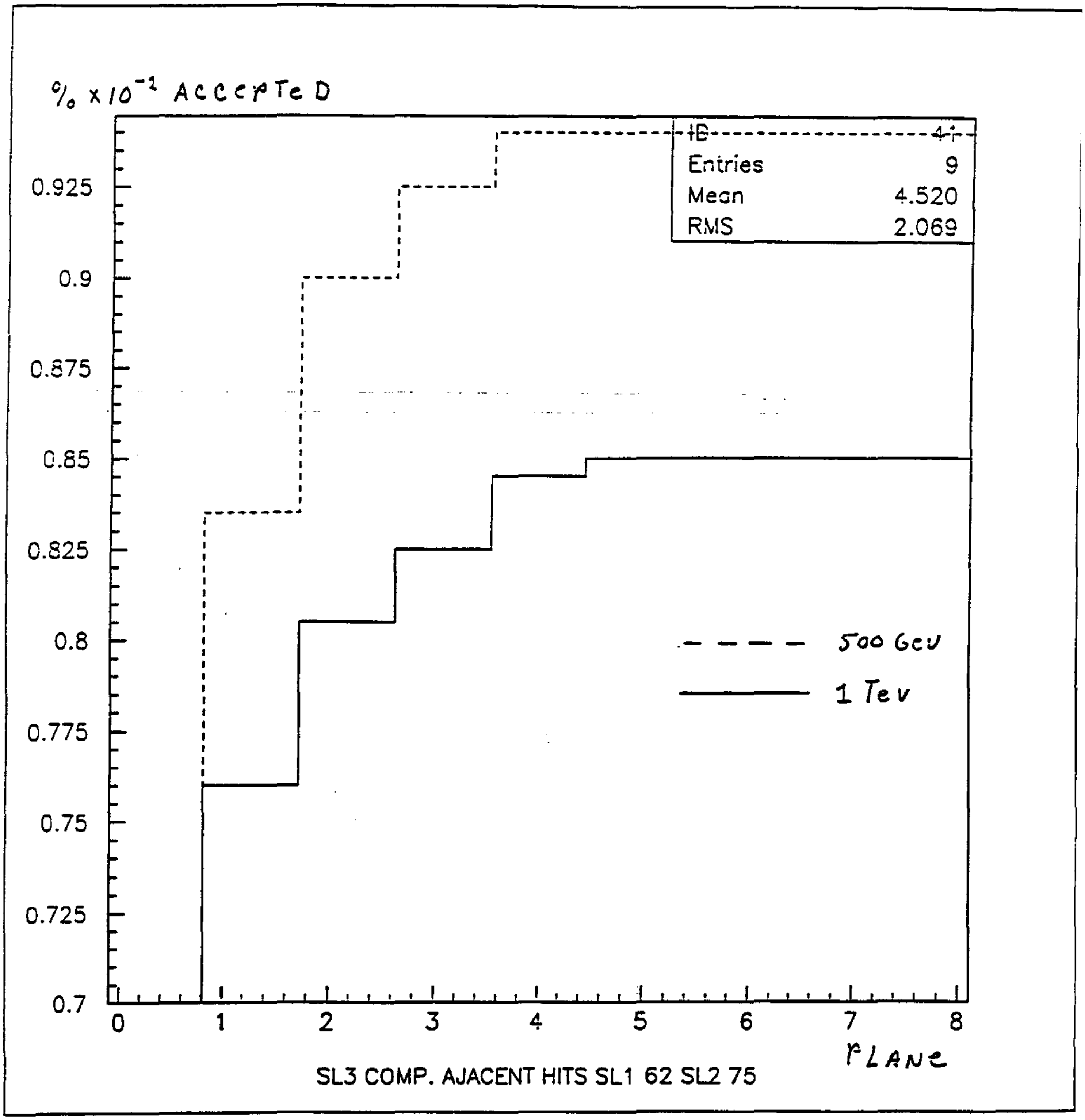

% x 10^-1 ACCEPTED
ID 41
Entries 9
Mean 4.520
RMS 2.069
0.925
0.9
0.875
0.85
0.825
0.8
0.775
0.75
0.725
0.7
0 1 2 3 4 5 6 7 8
500 GeV
1 TeV
PLANE
SL3 COMP. AJACENT HITS SL1 62 SL2 75

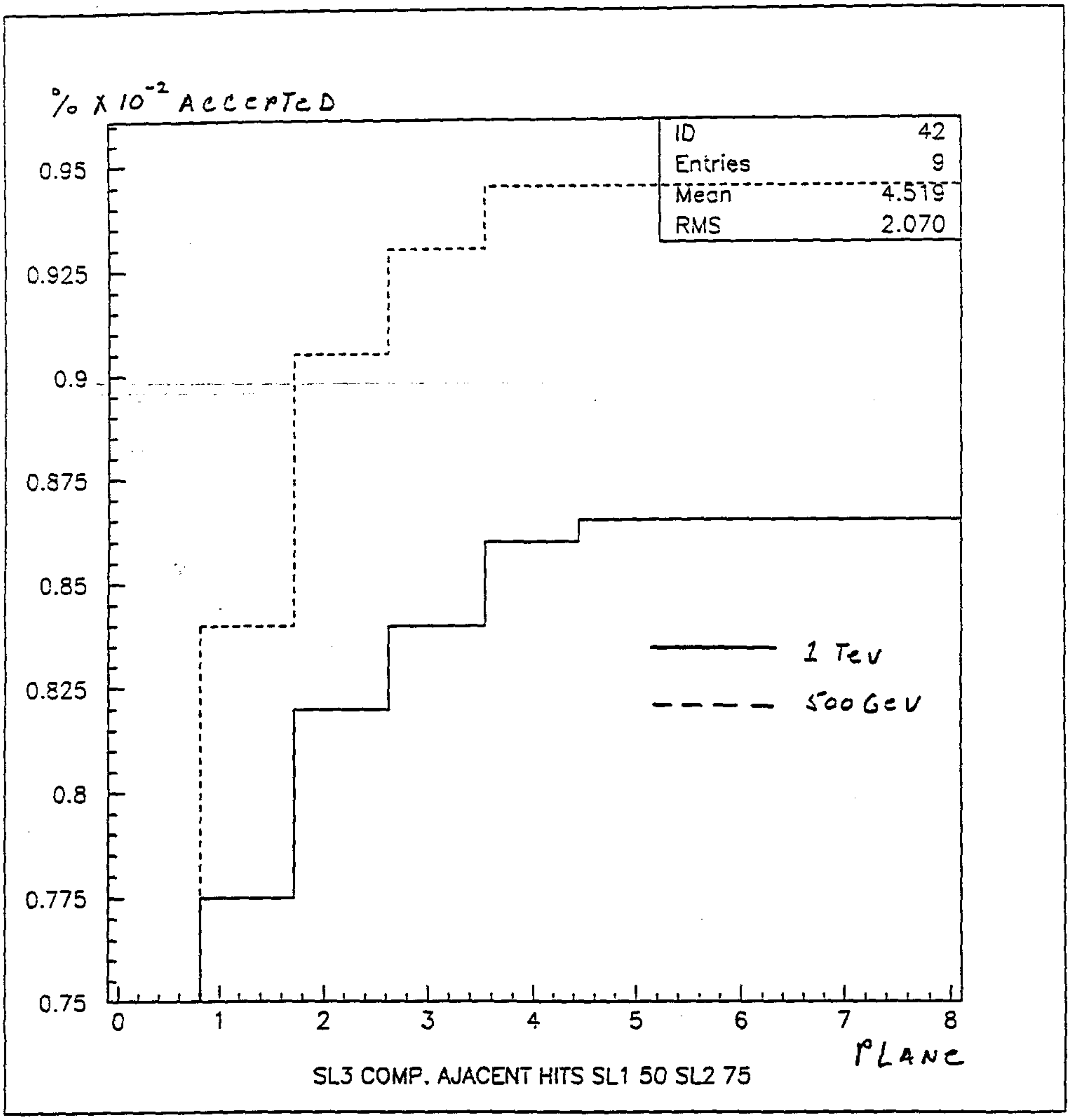

% X 10^-2 ACCEPTED
ID 42
Entries 9
Mean 4.519
RMS 2.070
0.95
0.925
0.9
0.875
0.85
0.825
0.8
0.775
0.75
0 1 2 3 4 5 6 7 8
1 TeV
500 GeV
PLANE
SL3 COMP. AJACENT HITS SL1 50 SL2 75

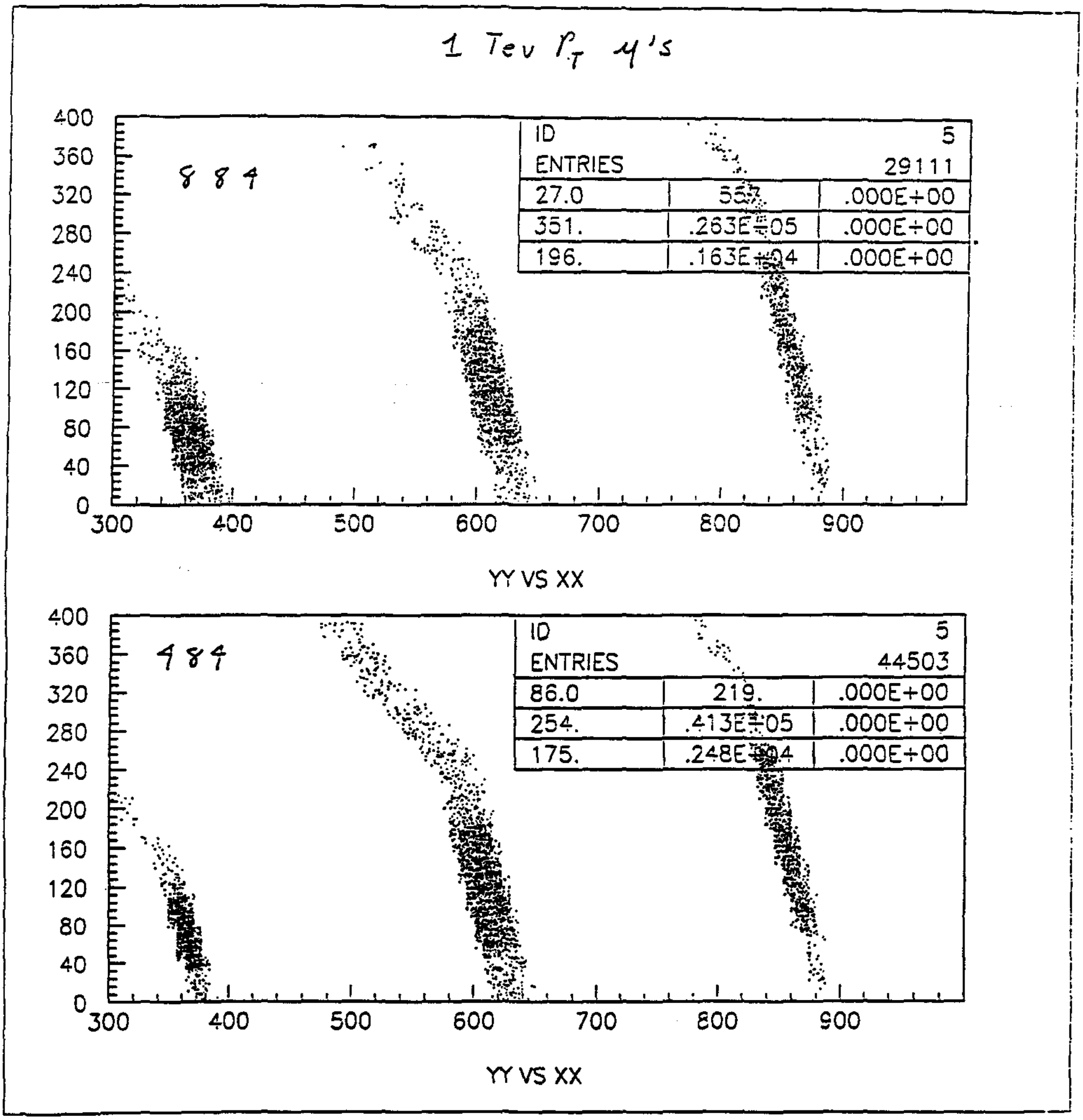

r, φ PLOT OF HITS

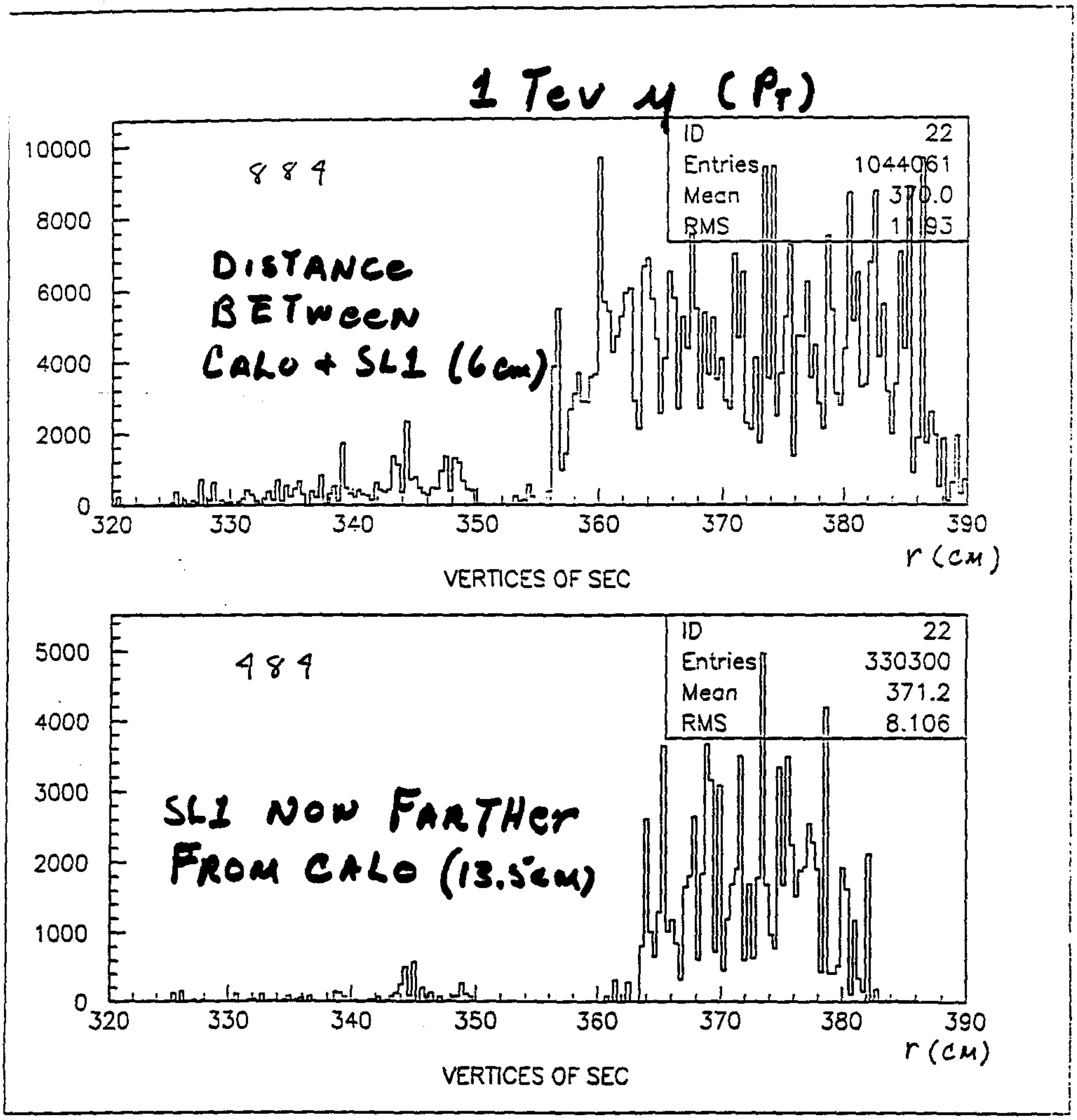

COMPARISON OF
SL1 884/484

1 TeV P_T μ's

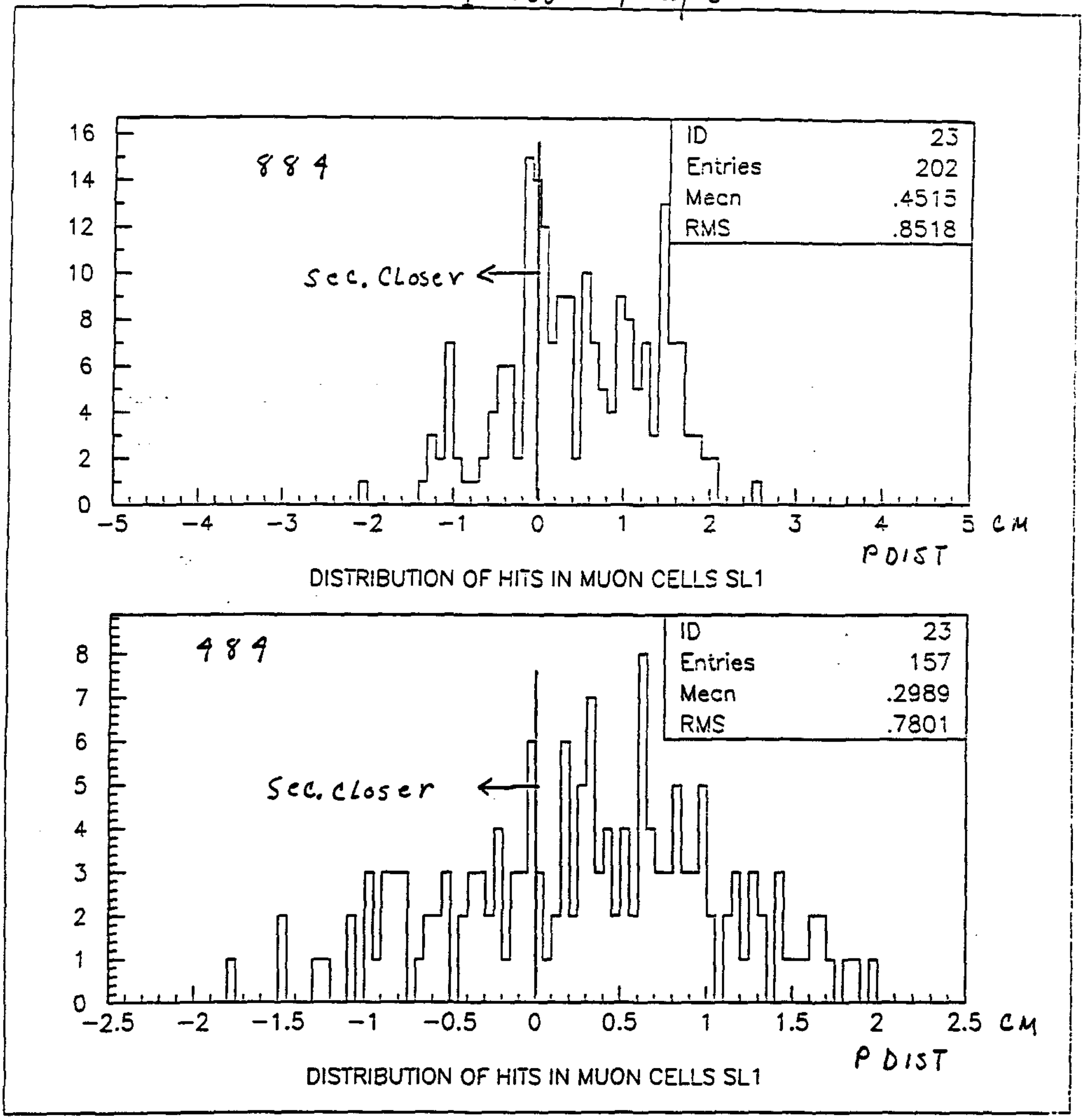

PDIST = $P_{sec} - P_{\mu}$ (IN CM FROM WIRE)

<NUM OF Sec's CLOSER> ~ 28%

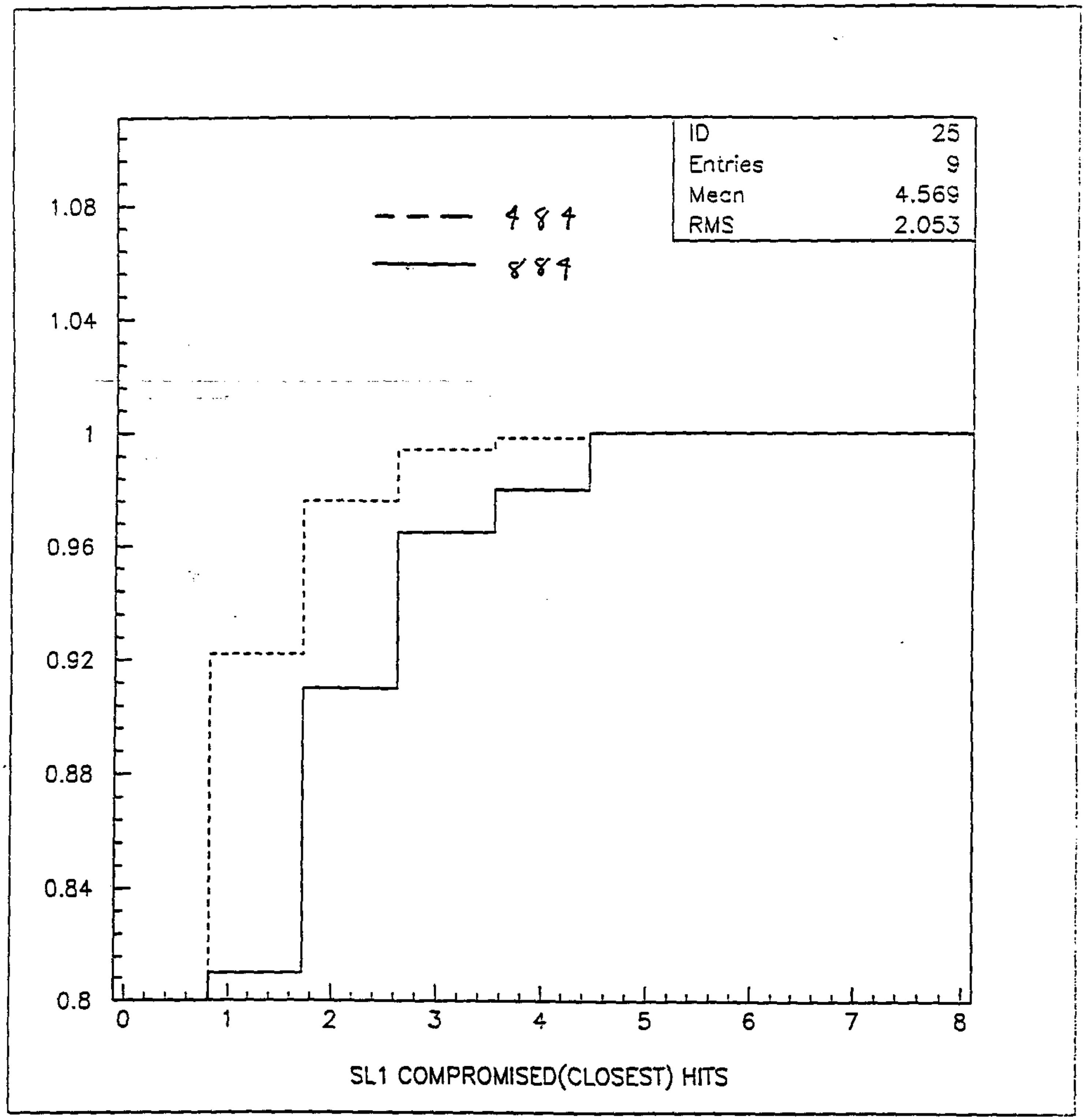
ID 25
Entries 9
Mean 4.569
RMS 2.053
484
884
1.08
1.04
1
0.96
0.92
0.88
0.84
0.8
0
1
2
3
4
5
6
7
8
SL1 COMPROMISED(CLOSEST) HITS

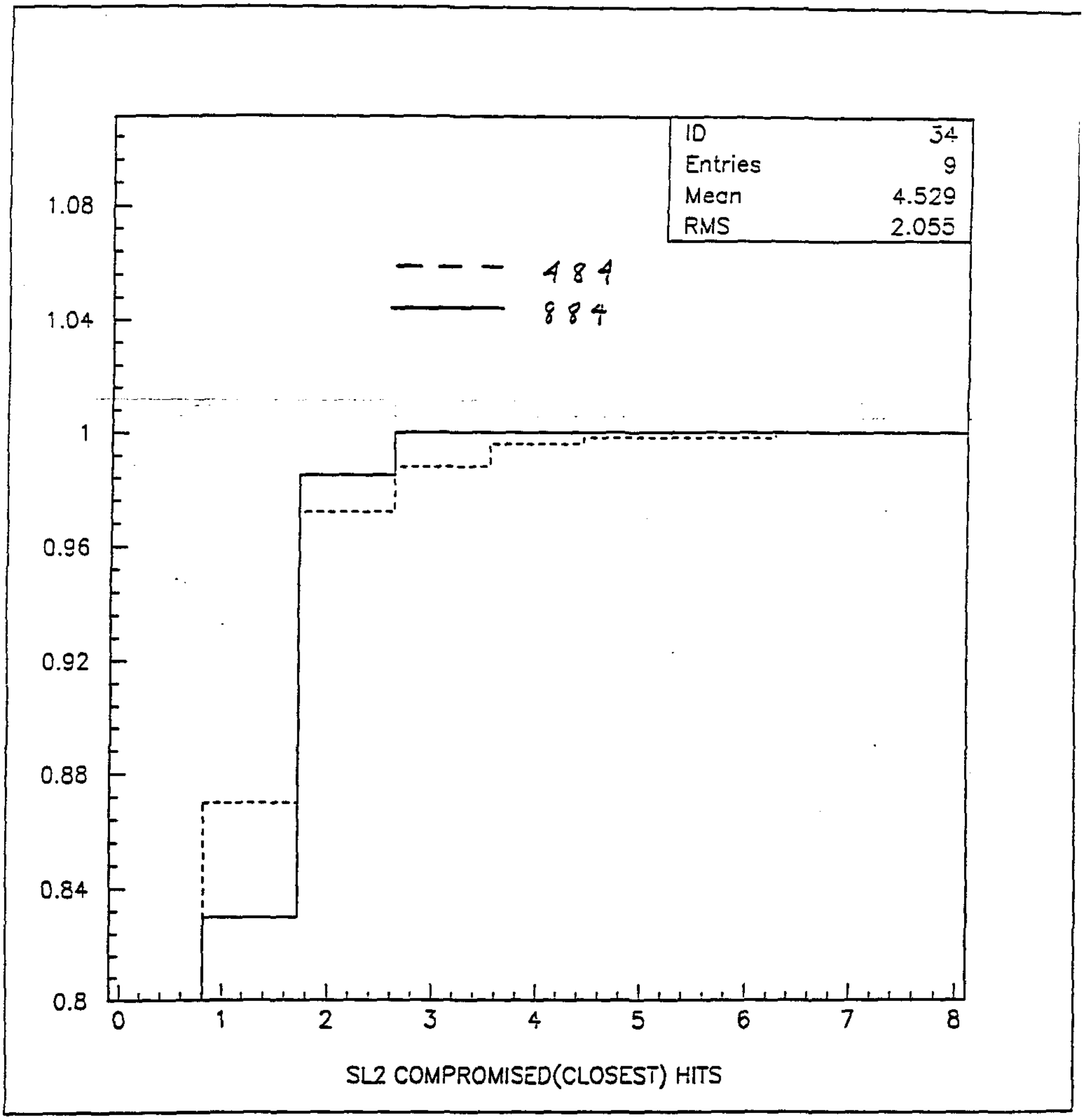
ID 34
Entries 9
Mean 4.529
RMS 2.055
484
884
1.08
1.04
1
0.96
0.92
0.88
0.84
0.8
0
1
2
3
4
5
6
7
8
SL2 COMPROMISED(CLOSEST) HITS

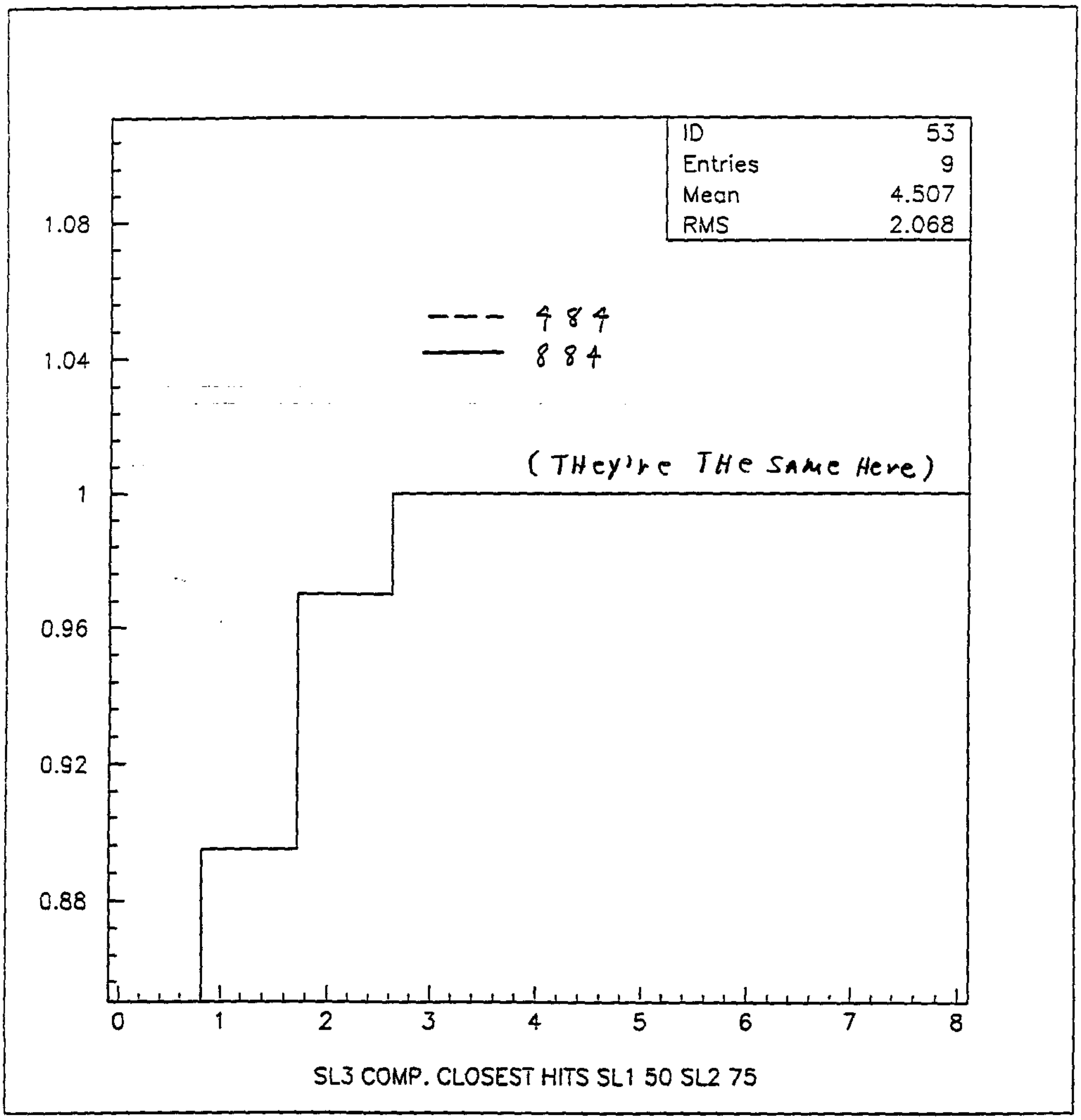

ID 53
Entries 9
Mean 4.507
RMS 2.068
1.08
1.04
1
0.96
0.92
0.88
--- 484
— 884
(They're The same Here)
0
1
2
3
4
5
6
7
8
SL3 COMP. CLOSEST HITS SL1 50 SL2 75

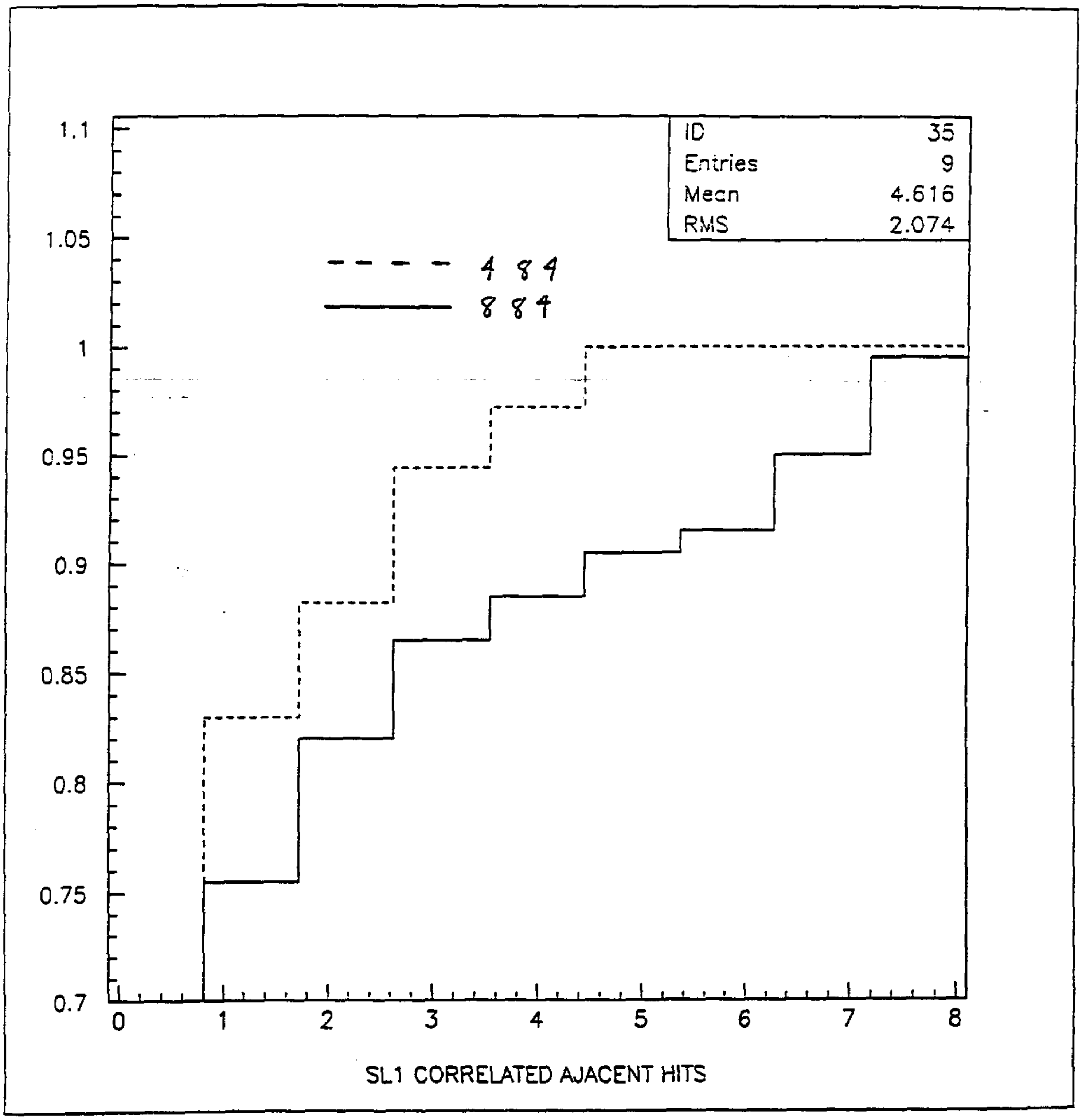
ID 35
Entries 9
Mean 4.616
RMS 2.074
4 8 4
8 8 4
SL1 CORRELATED AJACENT HITS

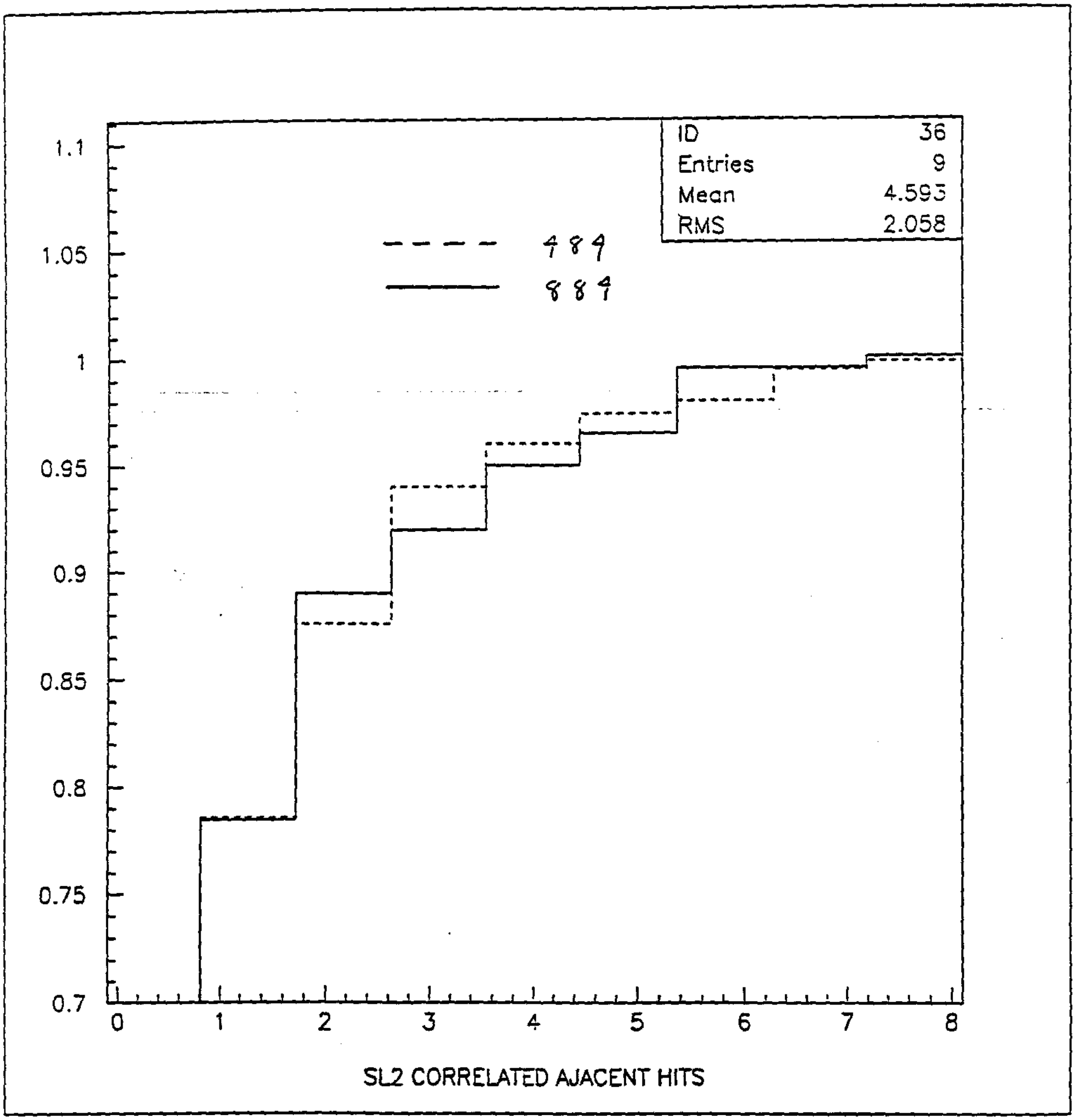

ID 36
Entries 9
Mean 4.593
RMS 2.058
484
884
1.1
1.05
1
0.95
0.9
0.85
0.8
0.75
0.7
0
1
2
3
4
5
6
7
8
SL2 CORRELATED AJACENT HITS

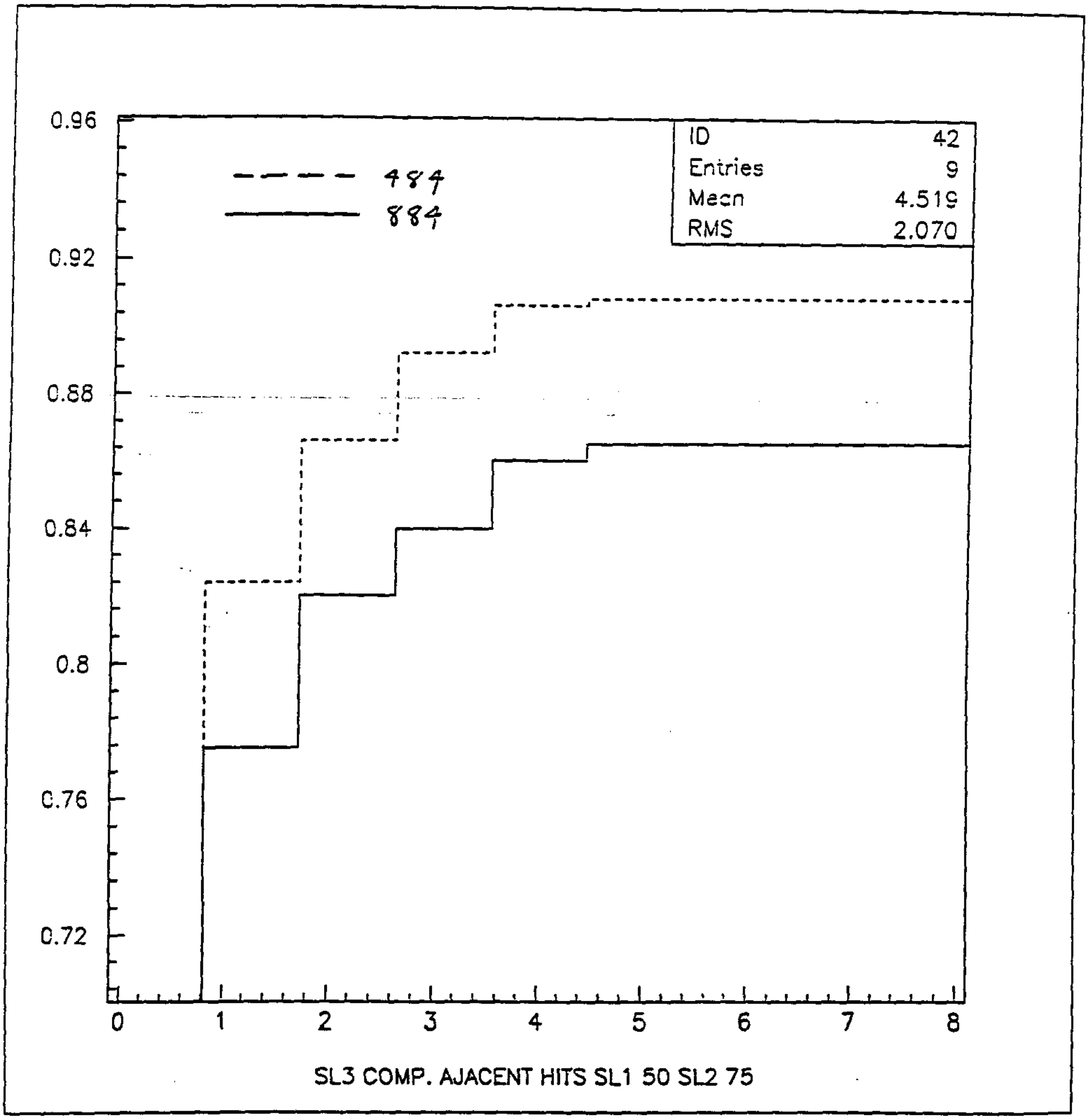

0.96
0.92
0.88
0.84
0.8
0.76
0.72
484
884
ID 42
Entries 9
Mean 4.519
RMS 2.070
0
1
2
3
4
5
6
7
8
SL3 COMP. AJACENT HITS SL1 50 SL2 75

1 Tev P_T μ's

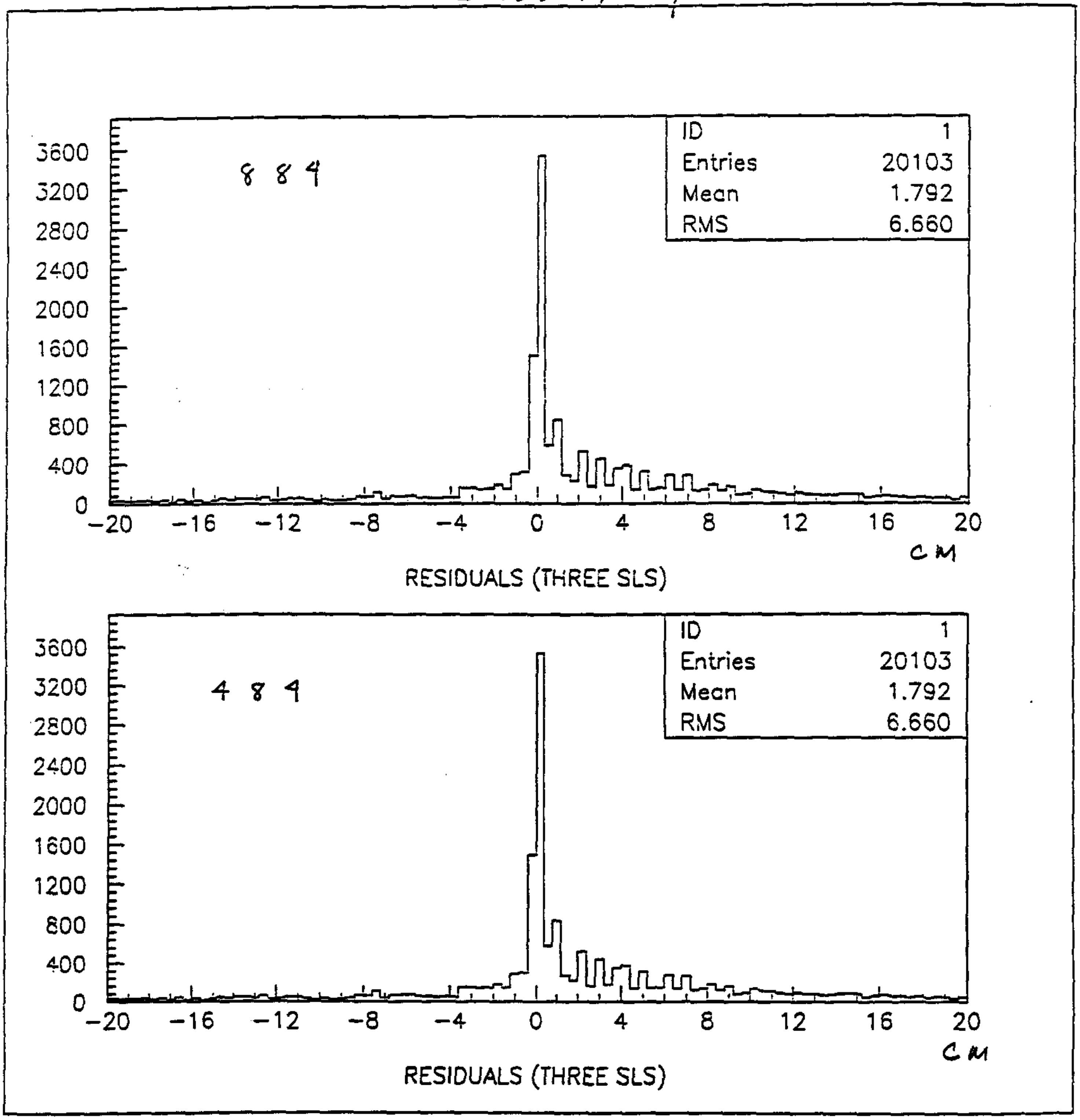
8 8 4
ID 1
Entries 20103
Mean 1.792
RMS 6.660
3600
3200
2800
2400
2000
1600
1200
800
400
0
−20 −16 −12 −8 −4 0 4 8 12 16 20
CM
RESIDUALS (THREE SLS)
4 8 4
ID 1
Entries 20103
Mean 1.792
RMS 6.660
3600
3200
2800
2400
2000
1600
1200
800
400
0
−20 −16 −12 −8 −4 0 4 8 12 16 20
CM
RESIDUALS (THREE SLS)

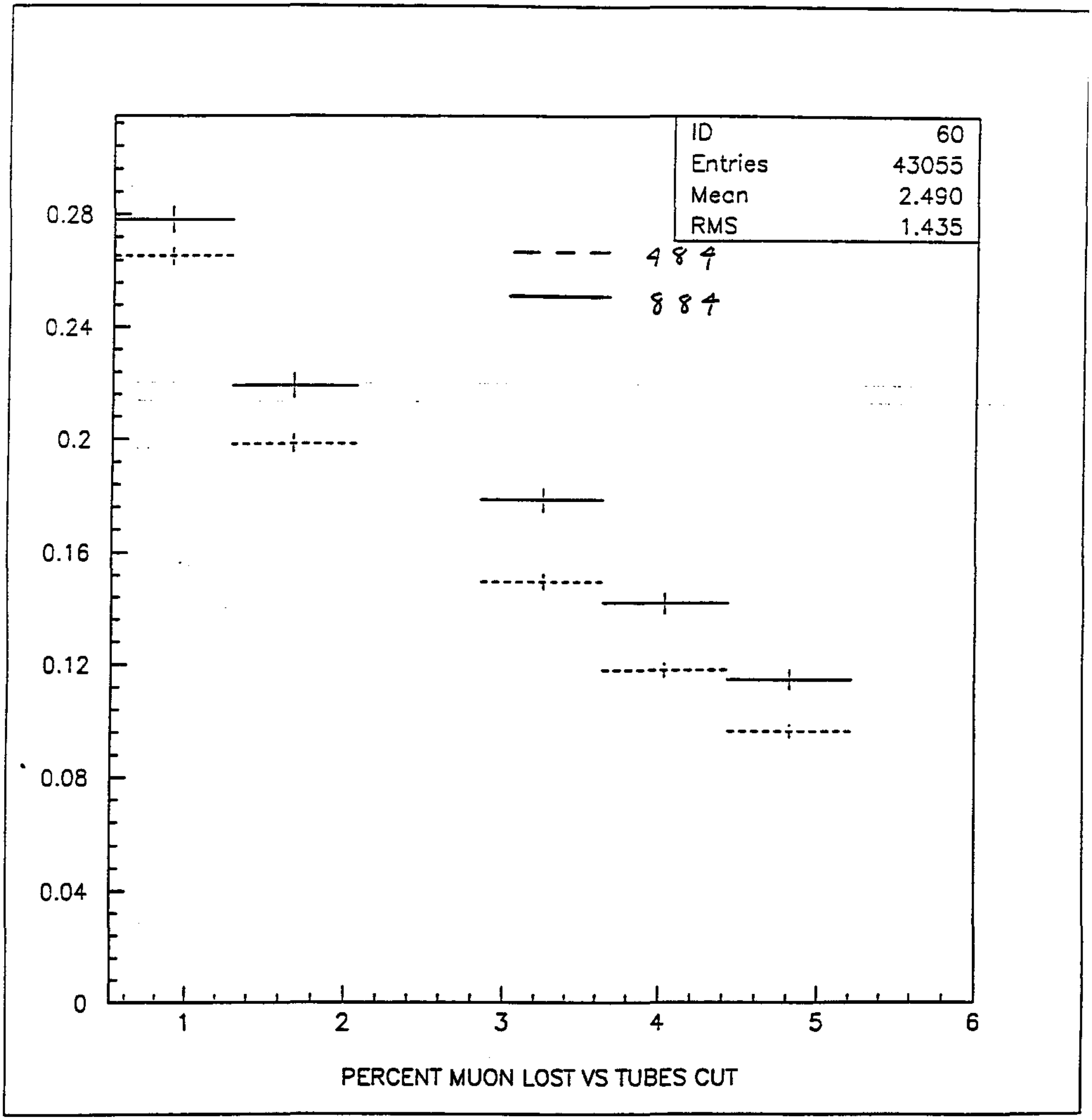
ID 60
Entries 43055
Mean 2.490
RMS 1.435
4 8 4
8 8 4
0.28
0.24
0.2
0.16
0.12
0.08
0.04
0
1
2
3
4
5
6
PERCENT MUON LOST VS TUBES CUT

Energy Lost By μ Not Replaced

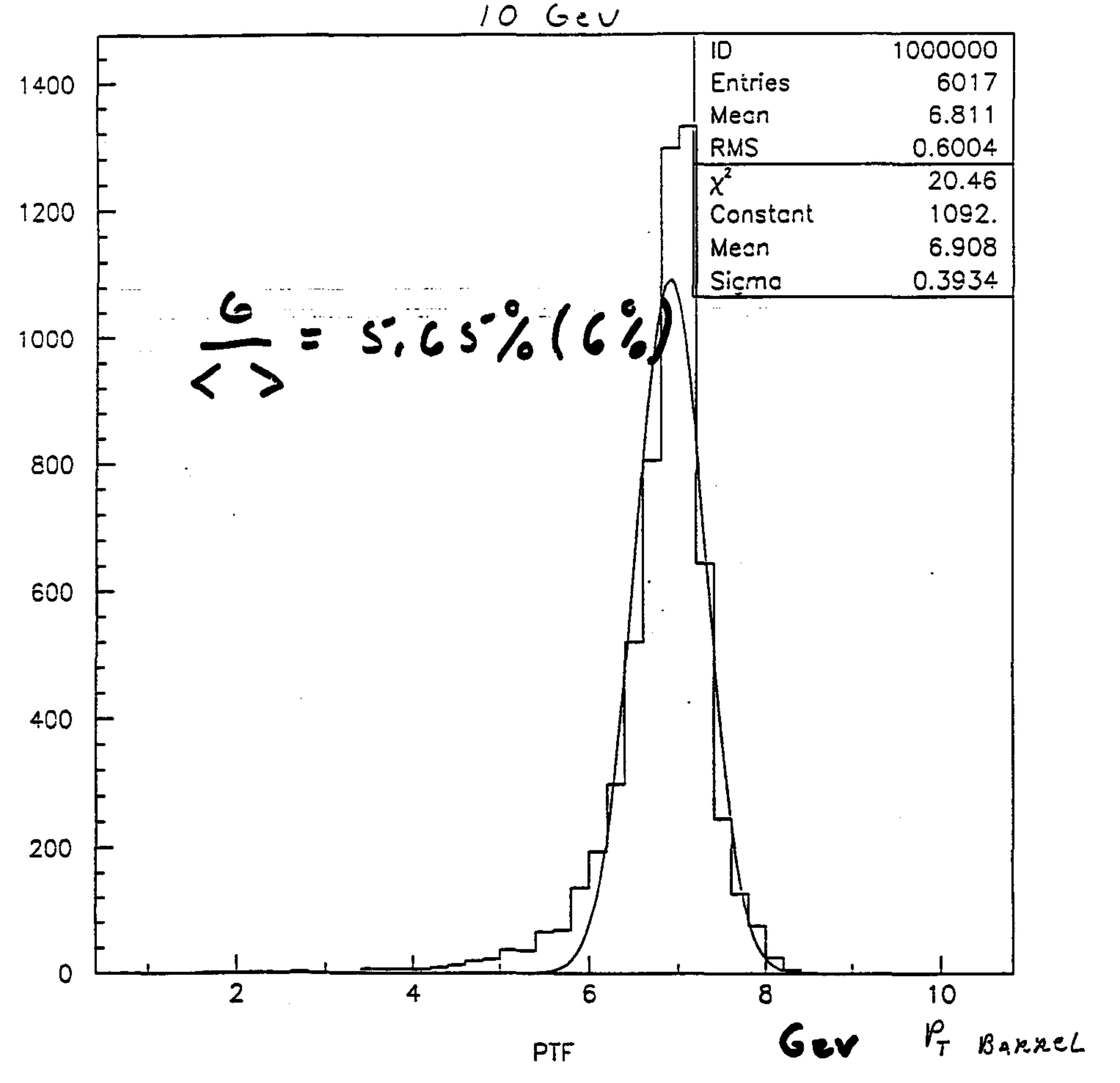

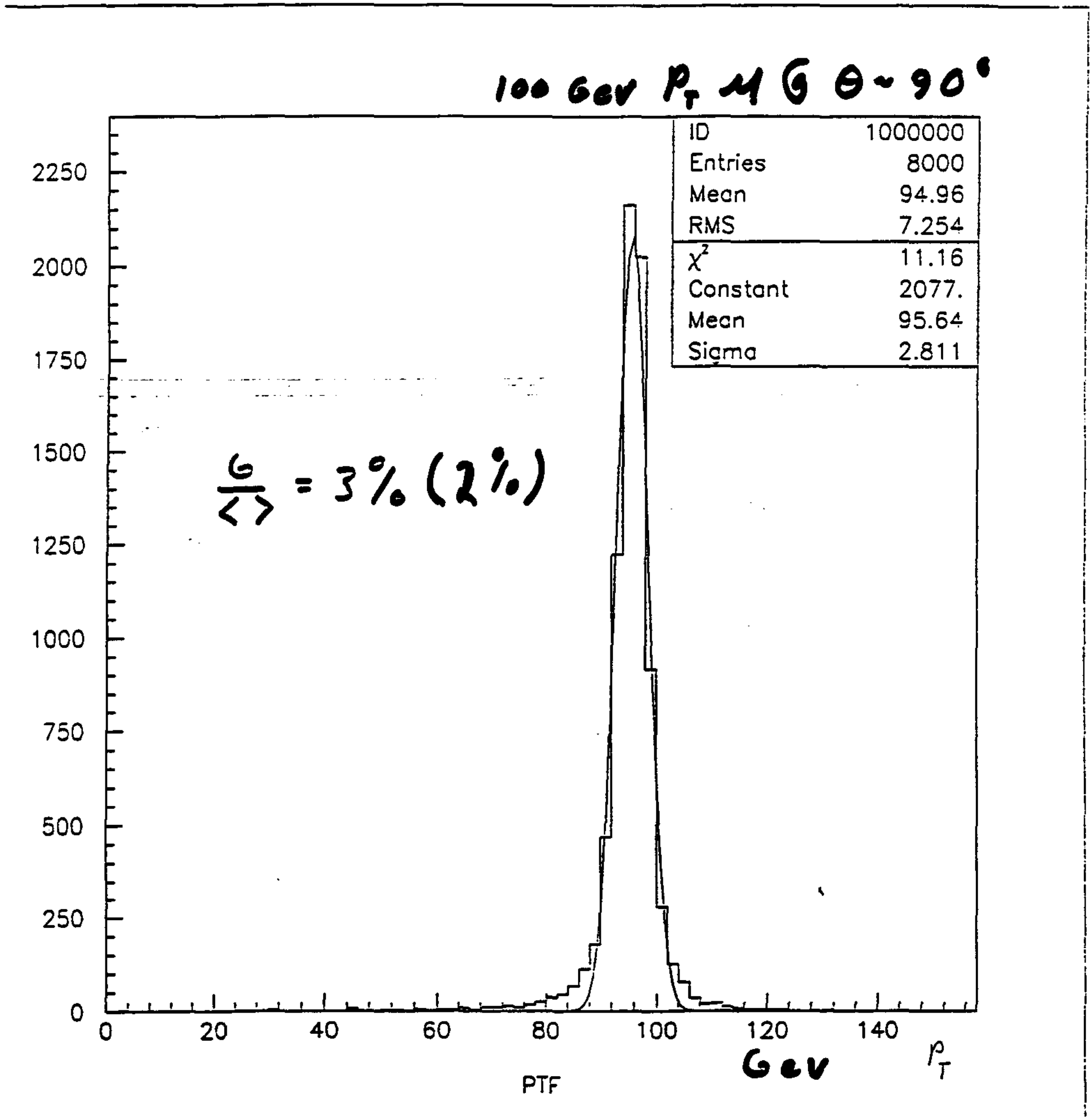
100 GeV P_T μ σ θ ~ 90°
ID 1000000
Entries 8000
Mean 94.96
RMS 7.254
χ^2 11.16
Constant 2077.
Mean 95.64
Sigma 2.811
$\frac{\sigma}{\langle\rangle}$ = 3% (2%)
0
250
500
750
1000
1250
1500
1750
2000
2250
0
20
40
60
80
100
120
140
GeV
p_T
PTF

DINGUS M Res 500 GeV @ 90°

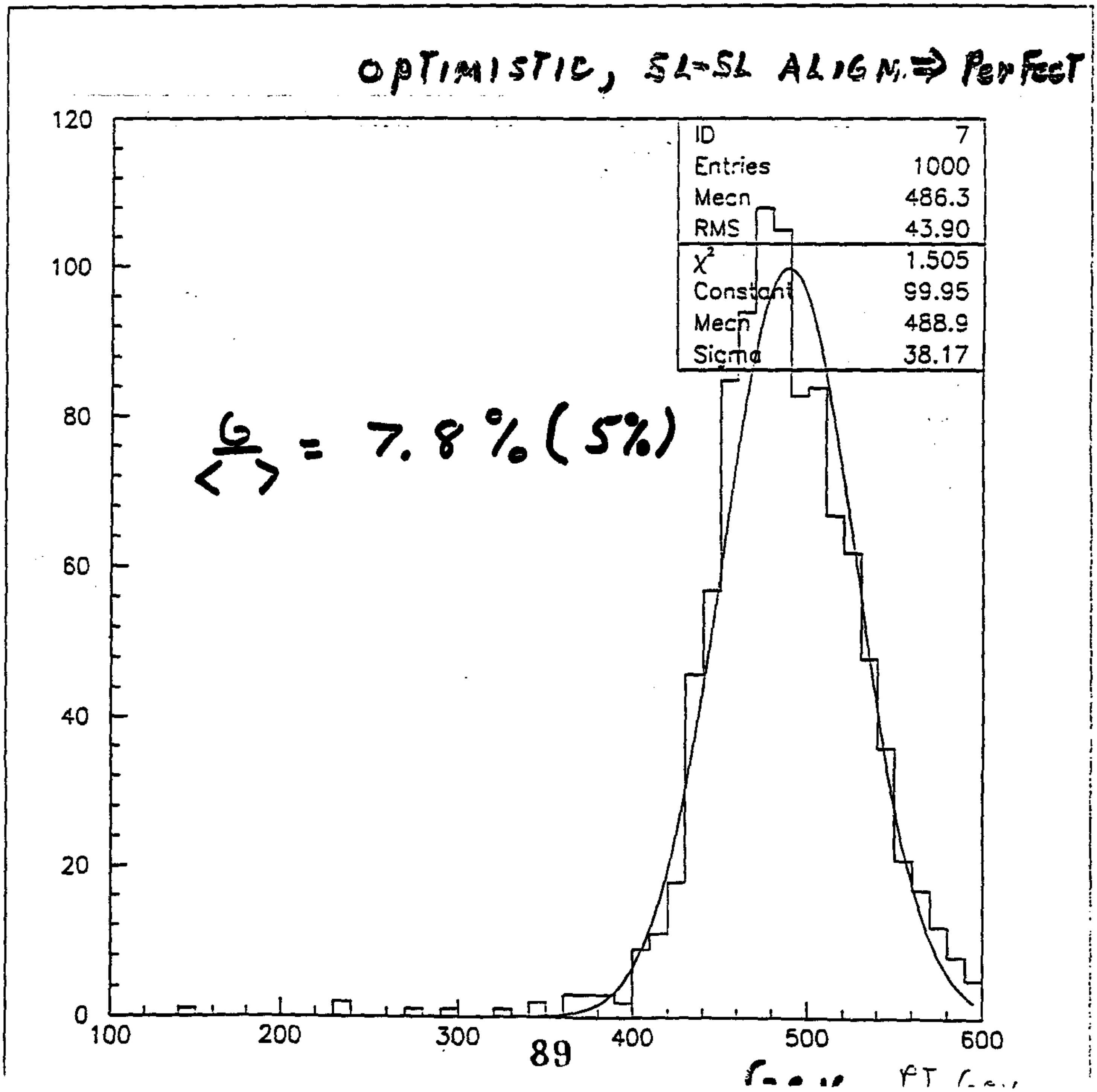

Presentation by:

H. Yamamoto

SDC-92-201

Solenoidal Detector Collaboration

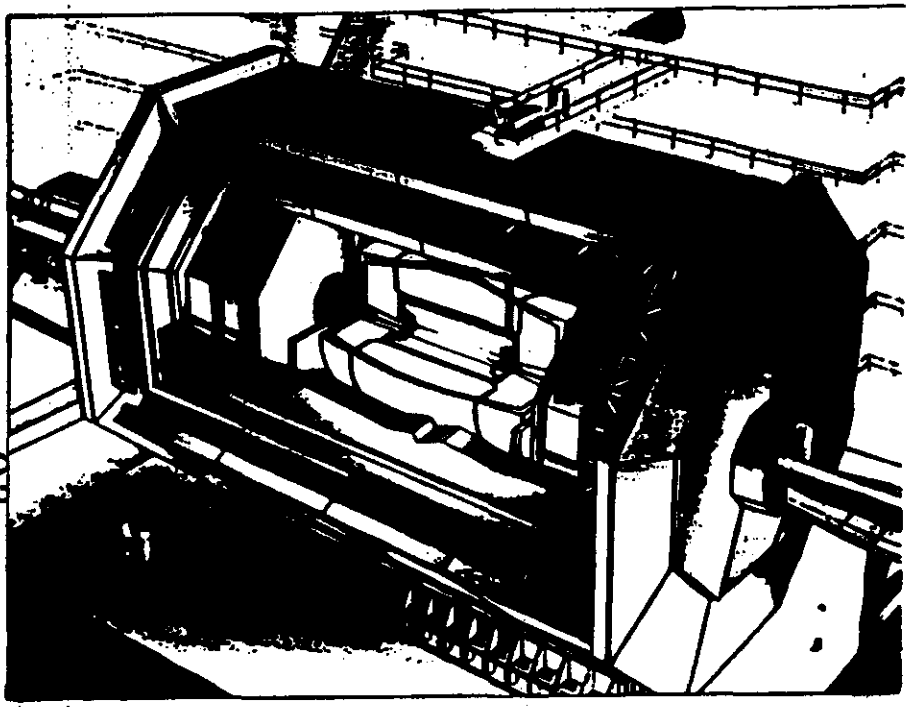

TECHNICAL DESIGN REPORT

1 April 1992

4/24/92

Physics Performance Update

1) Update on $H \to \gamma\gamma$ final state
   - new background calculations

2) Physics during "turn-on" era
   | relevant to staging ... |

3) Staging options and physics performance

$\sigma(\text{[illegible]}) = 5.9 \times 10^{-5}$ mb $= 5.5$ pb

$5.9 \times 10^{4} \cdot \frac{2}{10^{3}}$ [illegible]

$\sigma(\text{[illegible]}) = 2.3 \times 10^{-8} = 23$ pb [illegible]

Table 2-8
Examples of the expected physics performance of the SDC detector described in this Report. The results displayed here assume data samples corresponding to an integrated luminosity of 10 fb^{-1}, or one year at the SSC design luminosity of 10^{33} $cm^{-2}s^{-1}$. Any exceptions are explicitly noted.

Physics Process	Mass Region (GeV)	Physics Signature	#Pa
Associated Higgs Production			
	80 – 150	$W + H,\ t\bar{t} + H \to \ell\gamma\gamma$ 30	8
Direct Higgs Production			
	130 – 180	$H \to ZZ^* \to 4\ell$	5
	180 – 800	$H \to ZZ \to 4\ell$	3
	500 – 800	$H \to ZZ \to 2\ell 2\nu$	6
		$H \to WW/ZZ \to \ell\nu/\ell\ell + 2$ jet	
High Mass Boson Pairs		$Z\gamma \to \ell^+\ell^-\gamma$	
Requires integrated luminosity of at least 50 fb^{-1} for complete studies	1-2 TeV	$W^+Z \to \ell^+\ell^+\ell^-\nu$	
		$W^+W^+ \to \ell^+\ell^+$	
Discovery of t Quark			
	$\lesssim 1$ TeV	$t\bar{t} \to W^+W^- + X \to e^\pm\mu^\mp + X$	8
Mass Measurement of t Quark			
Sequential Dilepton Mode	$\lesssim 500$	$t\bar{t}$, one $t \to Wb$; $W \to e\nu$; $b \to \mu + X$ the other $t \to 3$ Jets	
Lepton + Jets + b-tag Mode	$\lesssim 500$	$t\bar{t}$, one $t \to W + X$; $W \to \ell\nu$ the other $t \to Wb \to b + 2$ Jets	
Non-standard t Decays			
Violation of τ Universality	$M_H \lesssim M_{top} - 15$	$t \to H^\pm b$; $H^\pm \to \tau^\pm\nu$; $\tau^\pm \to \pi^\pm + X$	10
Peak in 2-Jet Mass Distribution	$M_H \lesssim M_{top} - 25$	$t \to H^\pm b$; $H^\pm \to c\bar{s}$	
Gluino and Squark Searches			
Missing-E_t + Jets	300 – 1000	$\tilde{g}\tilde{g} \to E_t^{miss} + 3\text{-}6$ Jets	12
Like-Sign Dileptons	200 – 2000	$\tilde{g}\tilde{g} \to \ell^\pm\ell^\pm + 4$ Jets	
New Z Searches			
Discovery	$\lesssim 4$ TeV	$Z' \to \ell^+\ell^-$	5
Width and Asymmetry	$\lesssim 2$ TeV	$Z' \to \ell^+\ell^-$	
Compositeness			
	$\Lambda \gtrsim 25$ TeV	Inclusive Single Jet Spectrum	

QCD 9

less favorable, due to the large contributions from the $W/Z + jets$ and $t\bar{t}$ processes. Nevertheless, these modes could provide an additional method for studying the very heavy Higgs region, allowing searches to be extended into the TeV region.

Following these studies in the context of the Minimal Standard Model, it is natural to explore what happens in more general models of the symmetry breaking sector. A more complex, but theoretically attractive, model is the minimal supersymmetric version of the Standard Model (MSSM). In this model, there are five Higgs bosons: three neutral (h^0, H^0, A^0), and two charged ($H^\pm$). The theory has two fundamental parameters and the analysis is more complex. It appears that over much of the parameter space, at least one of the neutral Higgs bosons should be visible, either in the SDC detector, or at LEP-II. However, some regions of the parameter space remain inaccessible.

The previous discussion focussed on the W^+W^- and ZZ final states, where the Higgs appears directly as a resonance. It is also important to study other boson pair channels to probe the electroweak theory more thoroughly. In particular, if no Standard Model Higgs is found below 1 TeV in mass, it is almost day towards the end of their last run) become commonplace at the SSC (the SDC detector will be capable of recording $W \to e\nu$ events at a rate of 10 Hz at design luminosity). A second example is the production of the t quark. For $M_{top} = 150$ GeV, Fermilab would produce about 100 events during the next several years, whereas the SSC would produce 10^8 events per SSC year.

The largest interesting cross section at the SSC is that for the production of two jets. One event out of 10^4 (*i.e.*, a rate of 10^4 Hz) has two jets with a dijet mass of greater than 400 GeV. This cross section is 10^7 times larger than that for photon pair production, serving as a reminder that robust photon and lepton identification are essential for SSC physics. Heavy quarks and other colored objects such as gluinos would be produced with large cross sections. Even for a mass of 1 TeV, there are at least 10^4 events produced per year. Heavy new Z bosons are also prolifically produced, with the observable cross section extending out to a mass of 4 TeV. Finally, the Higgs production cross section is very small. At most one event out of 10^9 would contain a Higgs boson, and the branching ratios useful for its detection are also small. For the decays of the Higgs to two photons or to four leptons, the branching ratios are typically 10^{-3}.

In the sections below, we briefly describe the physics capabilities of the proposed SDC detector, and summarize its performance in Table 2-8.

Electroweak symmetry breaking

The single most important physics issue for the SSC is the study of electroweak symmetry breaking. In the context of the Minimal Standard Model, the existence of a fundamental scalar field provides the symmetry breaking mechanism. In this case, a single Higgs boson is the only observable particle associated with the symmetry breaking sector, and its mass is the only unknown parameter. It is imperative that a general-purpose SSC detector be capable of observing such a Higgs boson at any allowable mass in order to either verify its existence, or to rule it out and force consideration of alternate mechanisms.

The search for the Standard Model Higgs divides naturally into three mass regions, each with its associated strategy. For the low mass region ($80 < M_{Higgs} < 130$ GeV), the dominant Higgs decay modes are $H \to b\bar{b}$ and $H \to \tau^+\tau^-$, which are both overwhelmed by backgrounds from the decays of t quarks. The most useful mode in this kinematic region is the rare decay $H \to \gamma\gamma$, which occurs at next-to-leading order through loop diagrams. The Higgs itself is very narrow in this region (the width is less than 100 MeV for Higgs masses below 160 GeV) so that this decay mode provides a very distinctive signature. However, the direct production of the Higgs through gluon fusion suffers from a large background of QCD continuum production of photon pairs. The production rate for a Higgs in association with a W or $t\bar{t}$ pair is suppressed by a factor of 10–20 compared to the gluon-fusion rate, but the presence of an additional high-p_t lepton from the W or t decay provides significant background suppression. A complete analysis of the associated production processes shows that the SDC detector, studying the $\ell\gamma\gamma$ final state, should be capable of discovering a Higgs in the low mass region within a single SSC year (see Fig. 3-11 and Fig. 3-13).

For the intermediate mass region ($130 < M_{Higgs} < 180$ GeV), the branching ratio for $H \to ZZ^*$ becomes significant (the $*$ denotes a virtual particle). This decay mode provides a very distinctive signature of four isolated high-p_t leptons, with little background. The SDC detector, studying this final state, should be able to observe a Higgs anywhere in the indicated mass region after one SSC year (see Fig. 3-18).

For the heavy mass region ($180 < M_{Higgs} < 800$ GeV), the WW and ZZ decay modes dominate. In the lower part of this mass range, discovery via the $H \to ZZ \to 4\ell$ mode appears straightforward (see Fig. 3-22 and Fig. 3-23). As the Higgs mass increases, the cross section for its production decreases, and its width increases dramatically (an 800 GeV Higgs has a width of 270 GeV), making discovery more difficult. We have studied the $H \to ZZ \to 4\ell$ and $H \to ZZ \to 2\ell 2\nu$ decay modes in detail. The latter has six times the event rate of the former, but requires particular scrutiny because of the requirement of observing the missing transverse energy from the neutrinos. The conclusion is that, through a combination of these two final states, a Higgs with a mass of ≤ 800 GeV should be observable within one SSC year (see Fig. 3-25 and Fig. 3-28). Above this mass region, the signal becomes marginal at SSC design luminosity. For this reason the $H \to ZZ \to 2\ell + 2\ jets$ and $H \to WW \to \ell\nu + 2\ jets$ decay modes were also studied (their branching ratios are 20 and 150 times larger than that of the $H \to 4\ell$ mode). The signal to background ratio is much

$H \to \gamma\gamma$ Summary

1) signal slightly smaller

- QED cut $M_{e\gamma} > 40$ GeV
- $t\bar{t}$ weight error

2) total background substantially larger (almost factor 3)

3) further cuts may improve this, but only with further signal loss (e.g. 2nd lepton veto ...)

SDC calorimeter options offer only small improvements → hard to justify cost

$H \to \gamma\gamma$ rapidly becoming a "high luminosity experiment" ...

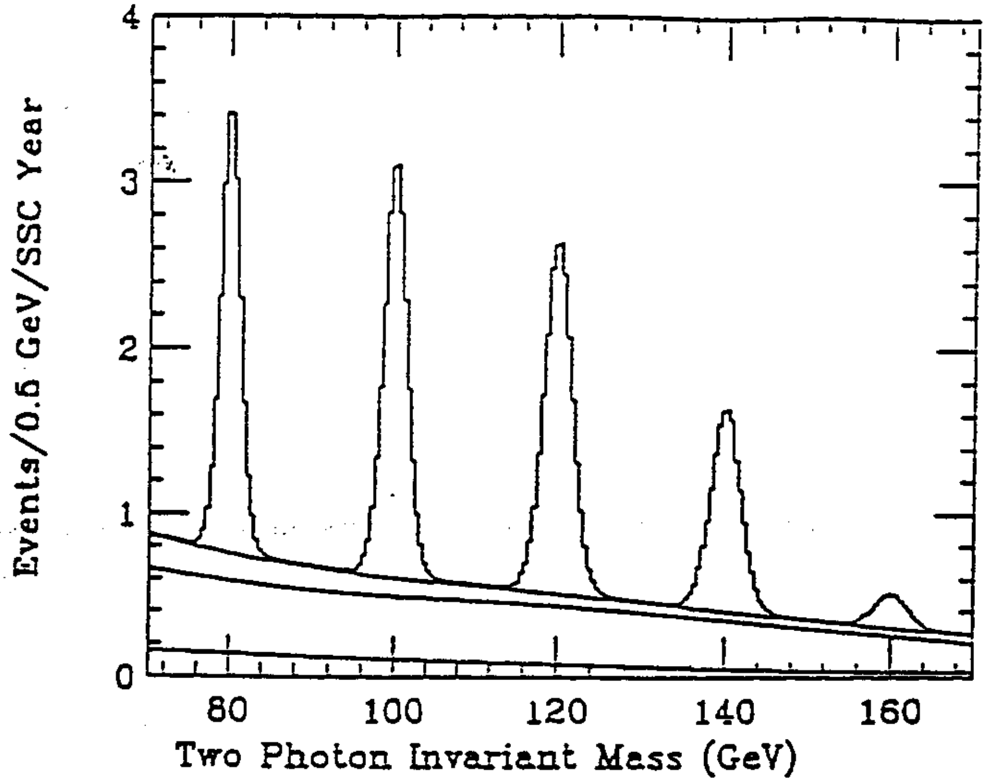

Events/0.5 GeV/SSC Year
0
1
2
3
4
80
100
120
140
160
Two Photon Invariant Mass (GeV)

TDR

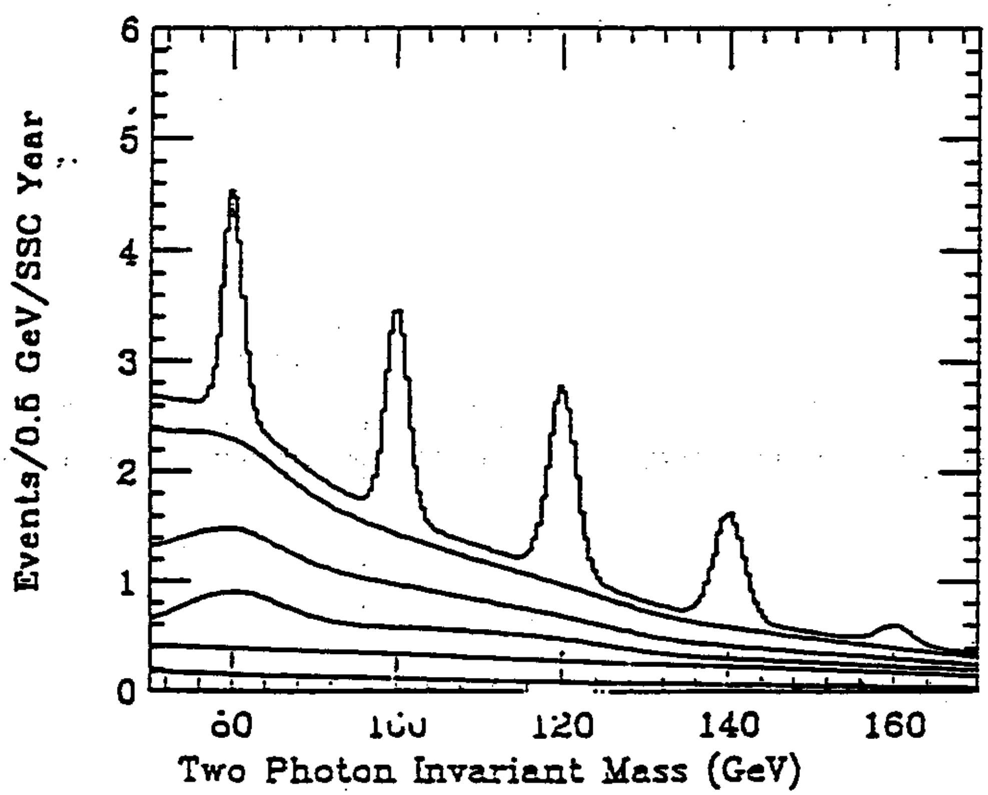

Events/0.5 GeV/SSC Year
0
1
2
3
4
5
6
120
140
160
Two Photon Invariant Mass (GeV)

Now

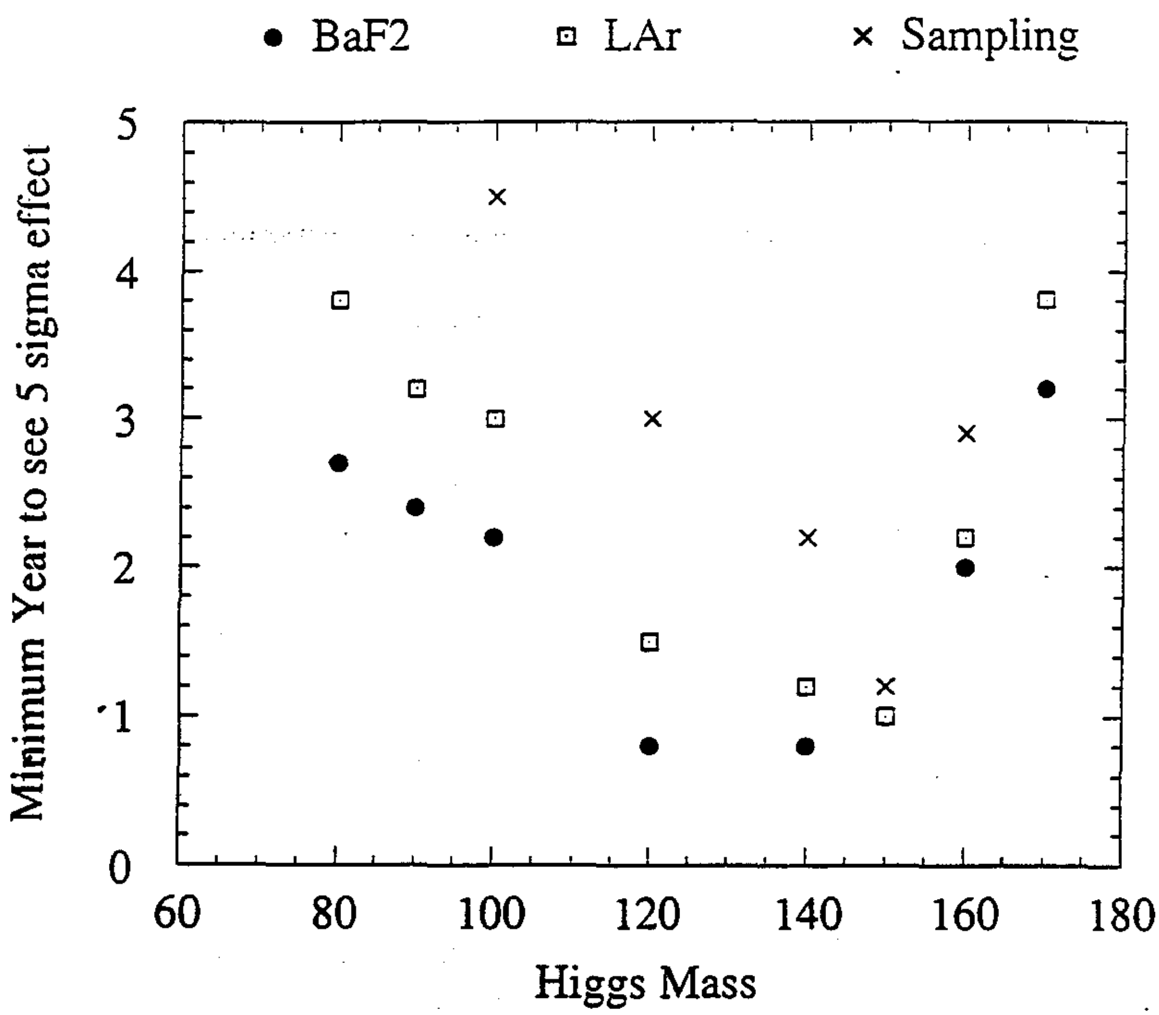

BaF2
LAr
Sampling
Minimum Year to see 5 sigma effect
0
1
2
3
4
5
60
80
100
120
140
160
180
Higgs Mass

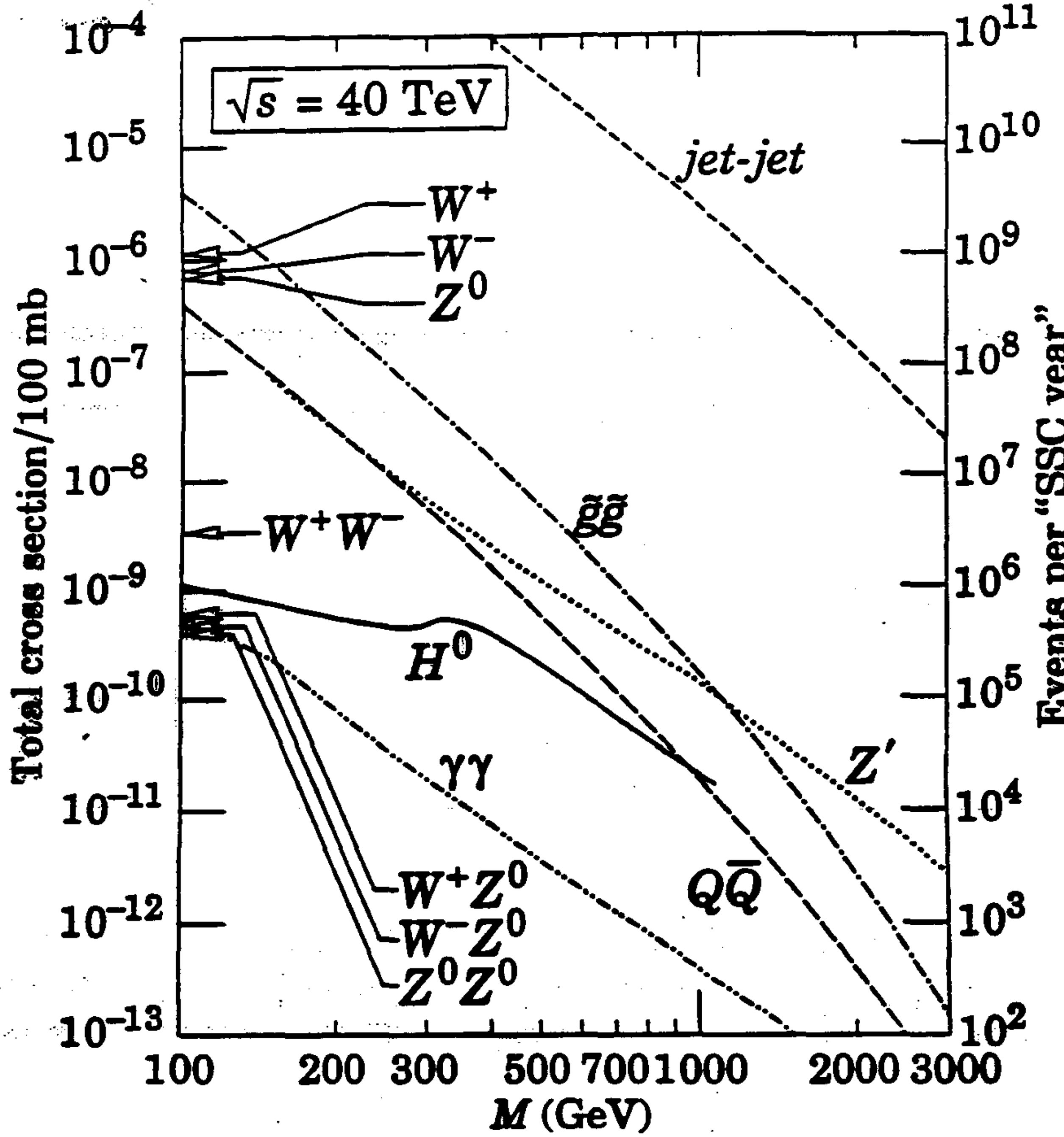

FIG. 2-9. Examples of total cross sections at the SSC. The *jet-jet* and γ-γ cross sections are for wide-angle jet or γ pairs ($|\eta_{jet}|$ and $|\eta_\gamma| < 2.5$) with invariant mass greater than M. For heavy-quark pair (gluino pair) production, the cross section is evaluated at $M = M_Q$ ($M = M_{\tilde{g}}$). The Higgs cross section assumes $M_{top} = 150$ GeV. The left scale is total cross section divided by 100 mb, the approximate total *pp* cross section, and so the numbers are approximate production probabilities per collision. The scale on the right is the number of produced events per year under "standard conditions," defined as operation at $\mathcal{L} = 10^{33}$ cm^{-2}s^{-1} for 10^7 s. These rates must be further dowrated by branching fractions and experimental cuts to obtain measurable rates. References and further discussion are given in Chapter 3.

Table 3-1
A summary of the parameters of the baseline SDC calorimeter which have been assumed in the subsequent analyses. The calorimeter depth is quoted in interaction lengths (λ).

Parameter	Barrel	Endcap	Forward
Coverage	$\lvert\eta\rvert < 1.4$	$1.4 < \lvert\eta\rvert < 3.0$	$3.0 < \lvert\eta\rvert < 6.0$
Radius of front face (m)	2.10		
z position of front face (m)		4.47	12.00
Compartment depth			
EM (+ Coil)	1.1	0.9	
HAD1	4.1	5.1	13.0
HAD2	4.9	6.0	
EM resolution			
a	0.14	0.17	0.50
b	0.01	0.01	0.05
HAD resolution			
a	0.67	0.73	1.00
b	0.06	0.08	0.10
HAD nonlinearity			
α	1.13	1.16	1.16
β	0.31	0.38	0.38

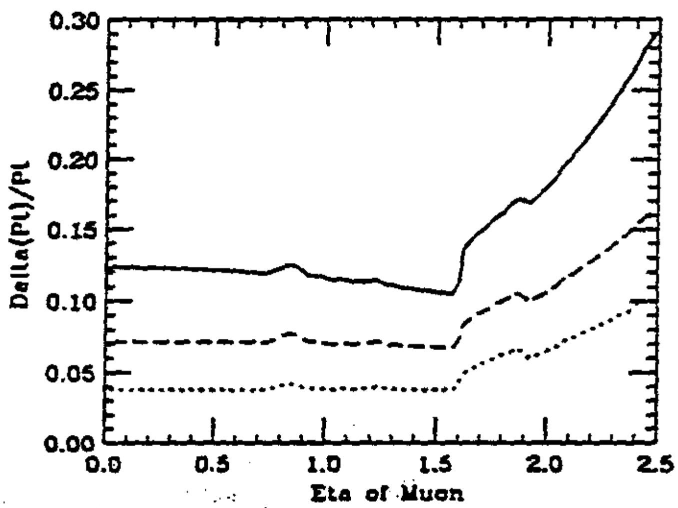

FIG. 3-2. The resolution of the combined baseline tracking and muon system as a function of η for several p_t values. The solid curve is for $p_t = 1000$ GeV, and the dashed (dotted) curves are for $p_t = 250$ (100) GeV.

Lepton and photon identification

We take the global electron and muon efficiencies within the detector acceptance to be 85% for analyses requiring isolated leptons. This can be compared with CDF experience, where a value of $85 \pm 3\%$ is obtained for W and Z electrons, including the effects of triggering and mild isolation cuts[2]. In the case where the analysis requires two such leptons reconstructing to an on-shell Z boson, the lepton identification cuts are relaxed for the second lepton, and the efficiency for the second lepton is taken to be 95%. For electrons, this efficiency includes the effects of track finding and fitting as well as electron identification (*e.g.*, an E/p

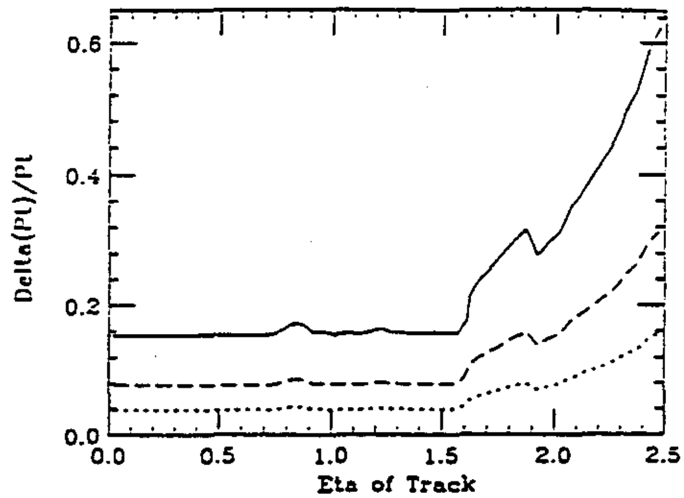

FIG. 3-1. The resolution of the baseline tracking system as a function of η for several p_t values. The solid curve is for $p_t = 1000$ GeV, and the dashed (dotted) is for $p_t = 250$ (100) GeV.

Calorimeter system

The calorimeter is assumed to cover the angular region $|\eta| < 6$ with a basic transverse segmentation that is a multiple of 0.05 in $\Delta\eta$ and $\Delta\phi$. The unit in phi is actually $\Delta\phi = 2\pi/128 \approx 0.049$. In the simulations described in the remainder of this section, the segmentation will be varied within the range of 0.05 to 0.8, but keeping a constant segmentation as a function of eta. The current electromagnetic (EM) calorimeter design has an η-dependent segmentation that increases by a factor of two from a base value of 0.05 at η values of 1.8, 2.6, 4.4, and 5.2. The current hadronic (HAD) calorimeter starts with a segmentation of 0.1 and increases by a factor of two at η values of 2.2, 4.4, and 5.2. The calorimeter is longitudinally segmented into an EM segment (EM) and two hadronic segments (HAD1 and HAD2), with depths given in Table 3-1. Parametrizations of the longitudinal and transverse distributions of energy deposited in individual calorimeter cells have been derived from EGS Monte Carlo simulations for electrons and ZEUS test beam data [1] for hadrons. These parametrizations are subsequently used, in conjunction with the single particle resolutions and nonlinearities, to simulate the response of the calorimeter in the following sections. A uniform magnetic field of 2.0 T is assumed to exist inside the barrel region.

In designing the SDC calorimeter, complex tradeoffs have been made between EM and hadronic single-particle response. High performance EM calorimetry demands fine sampling and large sampling fraction. Maintaining this sampling throughout the hadron calorimeter would be prohibitively expensive. The resulting discrepancy between the sampling in the EM and HAD calorimeters induces a π/e response ratio different from unity. There are other factors which further enhance this nonuniform response (choice of absorber material, ratio of absorber to scintillator thickness, *etc.*). A careful analysis of the physics requirements has been an essential ingredient in optimizing the SDC calorimeter, and the resulting design places greater emphasis on EM than on hadronic calorimetry.

The single particle resolution has been parametrized in terms of a stochastic term (a) and a constant term (b):

$$\frac{\sigma(E)}{E} = \frac{a}{\sqrt{E}} \oplus b \,.$$

The symbol $\oplus$ means that the two terms are added in quadrature. This model can be generalized to the case where the sampling plates in the calorimeter are not projective, assuming that the stochastic term is due to the sampling, and hence varies as the square root of the effective plate thickness. The parametrization for the barrel ($|\eta| < 1.4$) is:

$$\frac{\sigma(E)}{E} = \frac{a}{\sqrt{E_t}} \oplus b$$

Detector simulation

SDC table

Use parametrization

CAL	barrel	: $\Delta E/E = a/\sqrt{E_t} + b$
	Endcap	: $\Delta E/E = a/\sqrt{E_l} + b$
Jet	barrel	: $a = 0.61$, $b = 0.016$

Assume

γ / jet = 5×10^{-4}
e/ jet = $5 \times 10^{-4} / 50$

based on CDF data ???? $R = 0.7$, $E_t = 2$ GeV

FAST 1.5

PYTHIA + PAPAGENO +
ISAJET + HERWIG

Intermediate mass Higgs (80 - 130 GeV)

SDC almost gave up !!!

It is for GEM

We have to do it !!!

It is difficult for them,
and it is difficult for us, too.

=> Two small signals (≤ 100 GeV) or
=> Too large background (≥ 100 GeV)

For both case,
=> Uncertainty of the background
Should be prepared for it

H -> $\gamma + \gamma$
=> QED radiation from quarks
non-zero irreducible background
in jet-jet + jet-γ events
=> Uncertainty of the fragmentation
function

Table 15: Numbers of Signal and Background Events in One SSCY for H($t\bar{t}$/W)$\rightarrow$ $\ell\gamma\gamma$X Searches

	No p_t^{cut}			p_t^{cut} = 40 GeV		
R	0.30	0.45	0.60	0.30	0.45	0.60
Higgs (80 GeV)	28	23	18	21	18	14
Higgs (90 GeV)	30	25	20	24	20	17
Higgs (100 GeV)	30	25	21	25	21	17
Higgs (120 GeV)	24	20	16	22	18	15
Higgs (140 GeV)	17	15	13	15	14	11
Higgs (150 GeV)	10	8	7	9	8	6.5
Higgs (160 GeV)	4	3.4	2.7	3.6	3	2.5
$t\bar{t}\gamma\gamma$	58	48	34	52	44	32
$W\gamma\gamma$	26	25	25	15	15	15
$t\bar{t}$	308	246	185	123	61	61
$Z\gamma\rightarrow e$"γ"γ	93	88	83	49	47	45
$Z\gamma\rightarrow \ell^+\ell^-\gamma\gamma$	206	177	151	122	96	79
$W\gamma\rightarrow \ell\gamma\gamma$	135	108	76	54	43	43

7.2 Significance

Since the statistics of both signal and background is low, Equation 5 can not be used to estimate the significance. We thus estimate the significance by using a convolution of two Poisson probability distributions.

We assume a signal peak with defined width is observed over some background. The expected number of signal events in mass interval of $M_H \pm \sigma_{\gamma\gamma}$ is N_s, and the corresponding number of background events is N_B. The probability of observing certain number of events (n) follows a Poisson statistics:

$$P_n(\lambda) = \frac{\lambda^n e^{-\lambda}}{n!} \tag{14}$$

where λ is the expected value, i.e. N_S for the signal and N_B for the background.

If one observe n events, the probability of these events caused by background

H -> WW/ZZ -> $l + \nu$ / $l + l$ + 2 jets

no serious study, but possiblely interesting points

High pt W/Z -> 2 jet reconstruction

study of W/Z polarization
calorimeter segmentation to reconstruct jet => 0.1x0.1

Forward jet tagging (1 TeV Higgs)

study of gg -> Higgs vs WW/ZZ -> Higgs
ηmax = 5 to have enough jet tagging rate
S / B (W+jets, tt) = 300 / 1500, need improvements

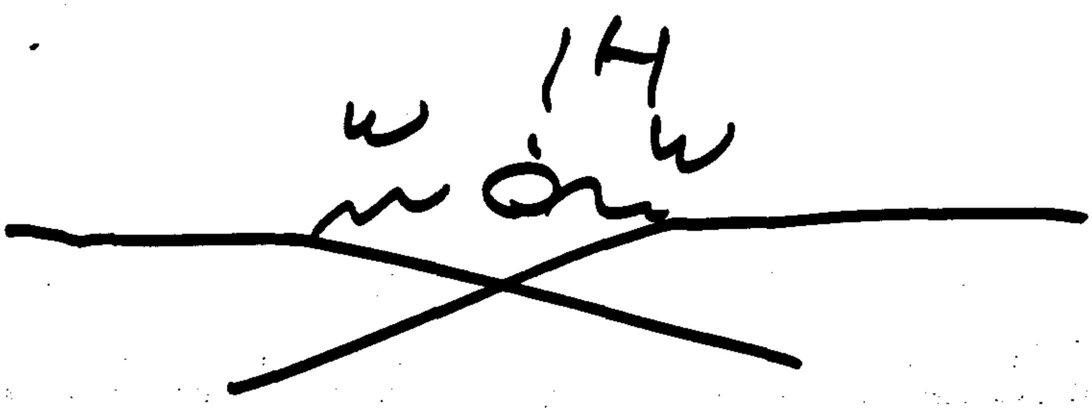

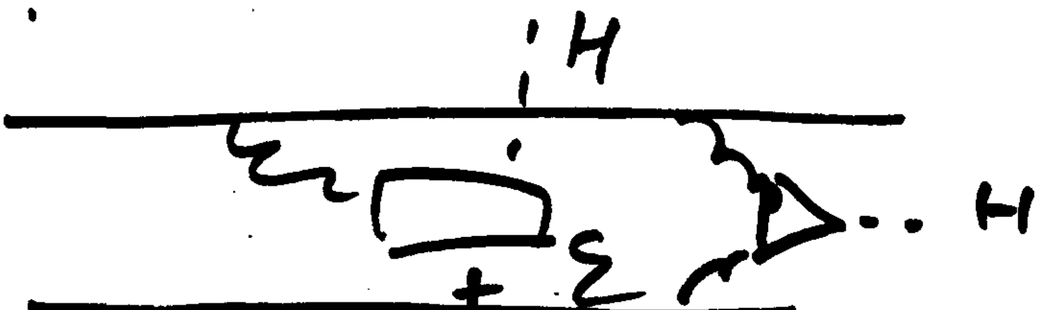

tt H, W H -> l + γ + γ

GEM note table

=> Have to look for all possible backgrouds
=> Detailed MC simulation
generate 10 x 10^6 tt events (tt + "γ"+ "γ")
t t + γ + γ
QED radiation
anybody else ?
=> isolation cut
have to simulate
strong momentum / environ
dependence

Intermediate mass Higgs (130-180)

Careful kinematic study (pt cut, M_{ll} region etc)

Isolation cut to kill bb backgroud

Heavy Higgs (180-600)

H -> ZZ -> 4 charged leptons

piece of cake after pt cut

Heavy Higgs (600-800)

H -> ZZ -> 4 charged leptons

after pt cut on leptons and Zs, very low background
BUT VERY POOR EVENT RATE

H -> $l\,l + \nu\nu$

cross section = 6 x H -> $4l$ s, but
effective significance are the same

Missing E_t

$\eta_{max} = 4$ is OK at 10^{34}

Gauge boson pairs

W + Z -> $l + \nu + l + l$

For quark distribution function calibration
With mass constraint, almost no background

Z + γ -> e + e + γ

Techni-rho 1450 GeV

Narrow resonance
Event rate is low => 10^{34} physics ?
if "γ " / jet = 0.01, S/N = 1
=> need "γ " / jet = 0.001 or better. Doable ?

W+W+

If Higgs is very heavy, scalar sector is strongly interacting

Can we see this ?

raw rate of tt-> Wb Wb -> same sign =
raw rate of tt-> Wb Wb -> opposite sign = 1000 x W+W+
raw rate of W^+W^- = 10-100 x W^+W^+

At 10^{33}, event rate is too small
At 10^{34}, DOES ISOLATION WORKS ???

Top Quark

1. For the background calibration
2. To estimate the tt H production rate
3. Charged Higgs search

Top quark mass

e μ invariant mass - from different top

10^6 / SSCY for 150 GeV top

no background

ΔM = 10-15 GeV

Sequential e μ

isolated electron

non isolated μ (in b jet)

statistical error = 0.5 GeV (150 GeV top) and
0.8 GeV (250 GeV top)

systematic error is dominated by physics input

b fragmentation function

pt spectrum of top quark

2.4 GeV (150) and 3.9 GeV (250)

3 jet mass reconstruction

use b tagging by secondary vertex (30 %)

160K (150) and 40K (250)

W -> two jet mass constrain =>

statistical error = 0.04 GeV

SUSY

Charged Higgs search by top -> H + b

H -> τ + ν vs W -> leptons + ν

isolated e/mu vs isolated hadron from τ

observable if tabβ > 0.5 and

M(h) not too close to m(t)

H -> cs

three jet invariant mass

By requiring 3 jet mass = 120 - 150,

clear peak of two jet mass

observable if tabβ < 1.0 and

M(h) not too close to m(t)

missing Et

non gaussian tails of jet energy reconstruction

angle between missing Pt and nearest jet > 20^{o}

ηmax = 5.0

for jet reconstruction

to require angle between jet and missing pt,

0.2 x 0.2 is required

same sign lepton by gluion pair

2 x 10^6 (180 GeV gluion) and 25 (2 TeV) dileptons / SSCY

+ 4 jets in η < 3

mass of lepton + 2 nearest jets

=> mass resolution 10%

What to do when

1. Tune up time (10**30-32)

2. 10**33 x 1 year

3. 10**33 x 2 - 3 years

4. 10**33 x 3 - 6 years

5. 10**34

extra - staging

gem

γeμ

Presentation by:

T. Skwarnicki

T. Skwarnicki / SMU

FAST MC PROGRAM

History: **Spring** "old FAST1"

Subdetector groups provided parametrization of the subdetector performance in form of subroutines

what and how things should be parametrize was left up to the subgroups

⇓

some important aspects are not parametrized at all

different conventions were chosen by different people

akward to use:

- user organizes code
- user must reconcile different conventions

May "Integrated FAST1"

Interface between user and FAST1 subroutine

- different subdetector programs reconciled as far as possible without re-writting them from scratch
- output information in coherent format

Crude tracking of particles through detector geometry

- pure helix (even in calorimeters)
- no multiple scattering
- cylindrical geometry only
  - thickness of calorimeters parametrized as function of η
  - "mapped" into a cylinder

Decays in flight of stable particles ($\pi^0, K^0_S, K^0_L, \Lambda, \ldots$) a la GEANT

User uses the integrated code by
call fsi_evt
and accessing results in common blocks.

Convenient driving program was provided by Ken MacFarlan with easy to use interfaces to PYTHIA, ISAJET, LUND

<u>Now</u> Irwin Sheer has set-up coherent framew. for <u>all</u> GEM software and has written the new driving program on the generator interfaces

Working right now to move the FASTI code into Sheer's directory structu.
it will be easier to maintain and u
needs to be debugged

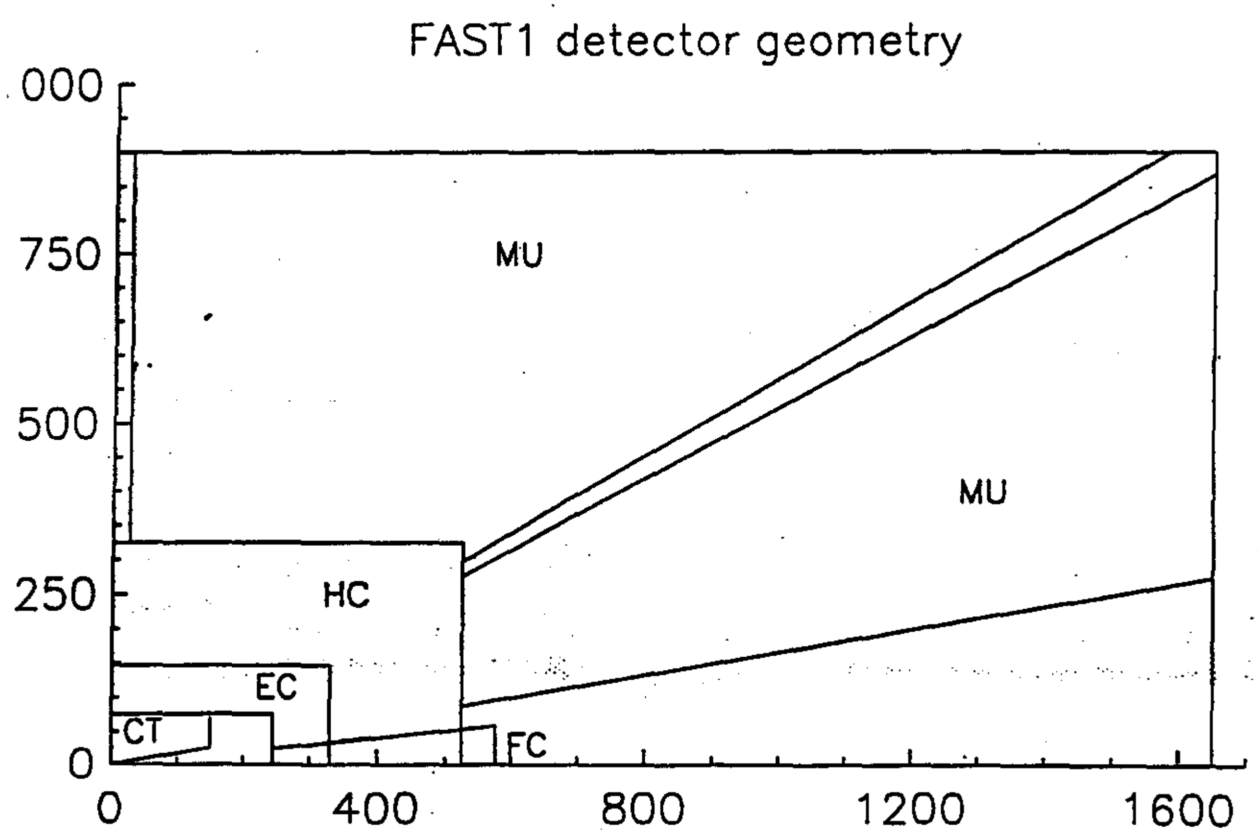
FAST1 detector geometry
000
750
500
250
0
0
400
800
1200
1600
MU
MU
HC
EC
CT
FC

CT   Main contributors: Shawn McKee, Melynda Eric

Every track originating from the IP ($R<0.4$, $|z|<5$ c
is assumed to be "reconstructed"
if $|\eta|<2.5$ and $P>0.1$ GeV

Information provided:
momentum, and track origin resolutions
↓
charge identification
efficiency

Reconstruction efficiency? in jets?

γ-conversions?
parametrization of material vs (η,φ) after silicon tracker and each layer of IPCs has been provided by the CT group ×

Other interactions (preshowering in CT)?
Secondaries from decays in flight?

Pile-up?

True primary vertecies? Right now everything originates from (0,0,0

Should we use other measured entities than "reconstructed track" e.g.
outer tracker stub
IPC layer hits

Multiple scattering?
relevant for: γ/e separation
hadron/e separation by E/p
isolation cuts based on CT

CT FAST1 Radiation Lengths

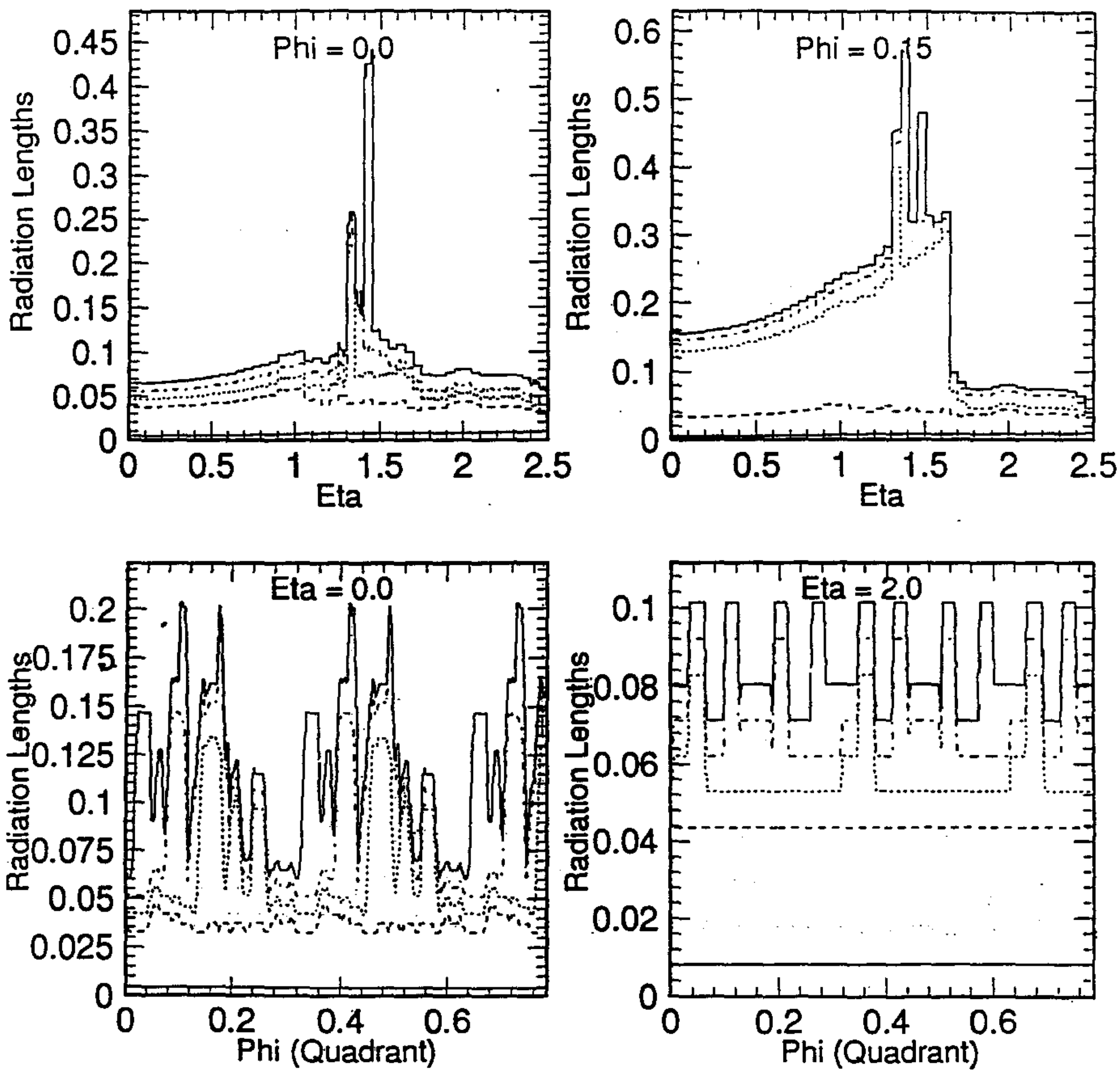

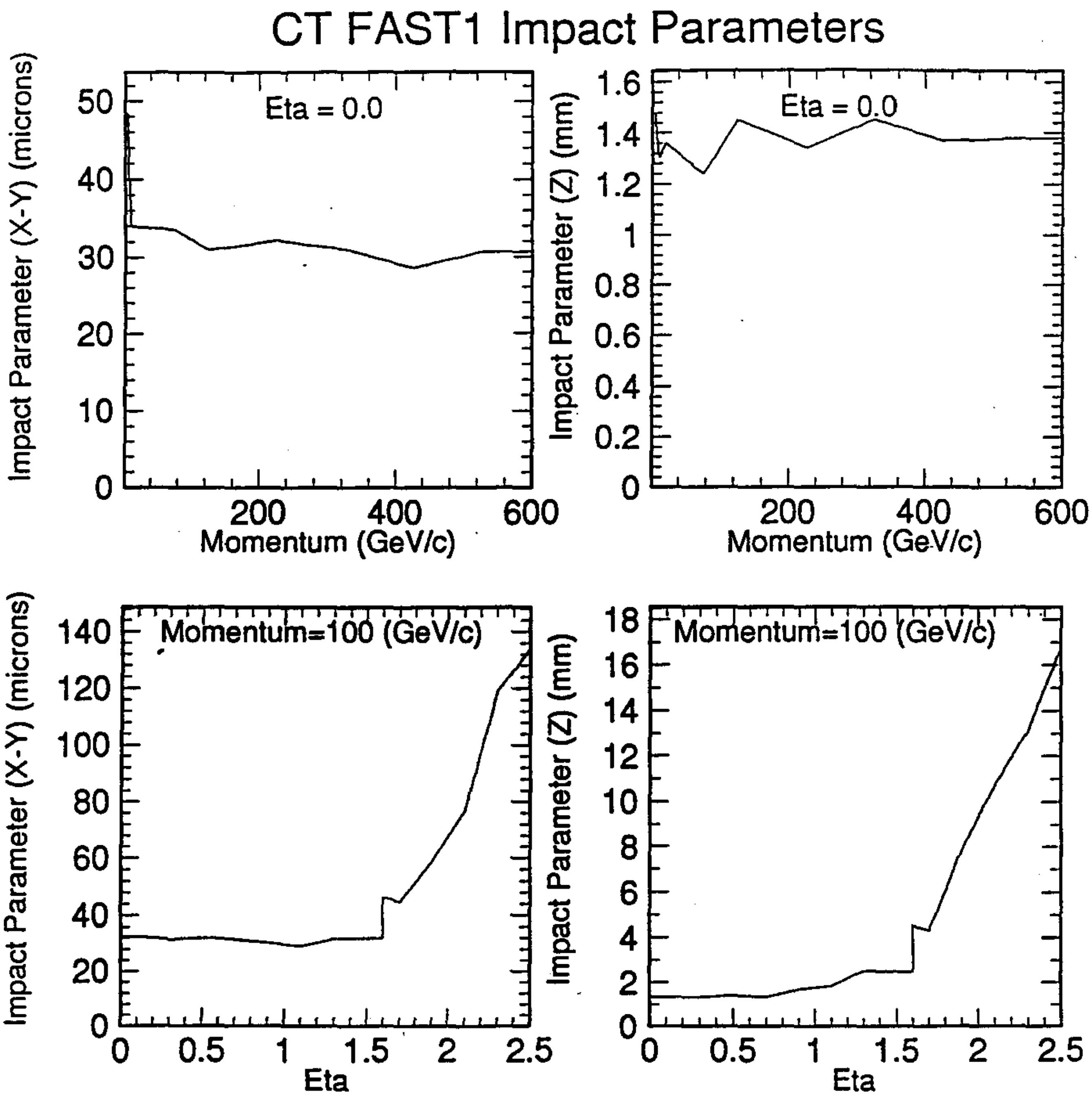
CT FAST1 Impact Parameters
Eta = 0.0
Impact Parameter (X-Y) (microns)
Momentum (GeV/c)
Eta = 0.0
Impact Parameter (Z) (mm)
Momentum (GeV/c)
Momentum=100 (GeV/c)
Impact Parameter (X-Y) (microns)
Eta
Momentum=100 (GeV/c)
Impact Parameter (Z) (mm)
Eta

CT FAST1 Momentum Resolution

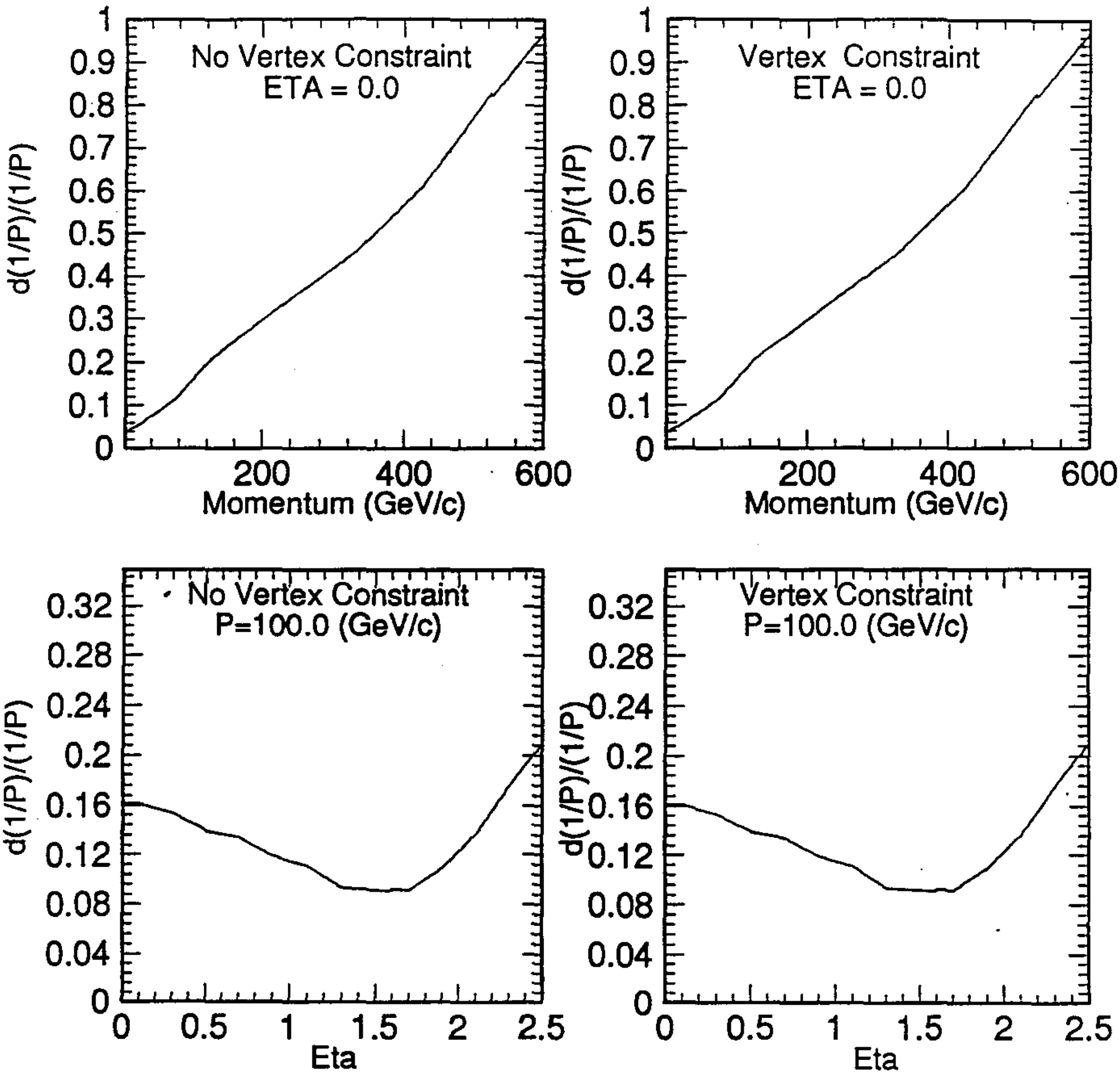

CA = EC, HC   Hong Ma, R. McNeil

EC, HC separate, constant cell sizes in φ, η

cell sizes at large η are unrealistic

no longitudinal segmentation

thickness of calorimeters: LAr Baseline-I[xx]

all volume is active — updated design, different options? → mapping into a cylinder, systematic

cracks? cryostat?

exponential fluctuations in interaction depth for hadronic showers

no depth fluctuations for EM showers (also $\gamma = e$)

no preshowering in CT

longitudinal and transverse shower profiles according to Bock's parametrizations

long. and transv. profiles are not correlated

no fluctuations in shower profiles

shower develop always along straight lines from the detector origin

no true secondaries:

- no shower split-offs (e.g. due to neutrons)
- no leakage to MU (some crude "old" FAST routine exist to do it)
- no backsplash to CT

EM leakage to HC may be wrong

shower center is smeared according to angular resolution before depositing shower energy — this is not done right - should be ...

energy resolution:

EC: η-dependence for LAr

HC: no η-dependence

can be easily rescaled to user specified

$$\frac{a}{\sqrt{E}} \oplus b$$

μ's and hadrons before interaction travel along helix (wrong), change curvature only after whole EC

no multiple scattering (need it for μ's ?)

constant $\frac{dE}{dx}$ for hadrons before interaction

wrong, may matter for tight isolation cuts

$\frac{dE}{dx}$ for μ's parametrized as function of momentum

fraction which goes into bremsstrahlung (deposited as EM shower) done in very crude way

gaussian thermal noise

sophisticated pile-up simulation available

right now valid only for LAr with shaping times 40ns, 100ns

should be tuned to latest design parameters (disk and cpu intensive)

Preradiator ?

FC

M. Schupe

Only total detected energy vector is calculated

no cells, no clusters

Smearing according to Baseline-I design

updated design?

Directional smearing may be overestimated? In the present integrated code

MU

P. Dingus, J.D. Sullivan, R. McNeil

Acceptance gaps in φ, η } according to Baseline-I
Momentum resolution × }

Detection and trigger efficiencies by P. Dingus
most likely not realistic
parametrized as function of $\vec{p}$ at IF

No background tracks from shower leakag
μ bremsstrahlung

(no quite realistic trajectory in CA)

TR

C. Allen

old FASTI routines not integrated yet
should be updated?

CONCLUSIONS

- Number of possible improvements is almost infinite.
- We should define physics goals of FAST simulation and concentrate on improving the most important aspects.
- Much of the work must be done by the subdetector specialists.
- People using FAST MC should well understand its limitations

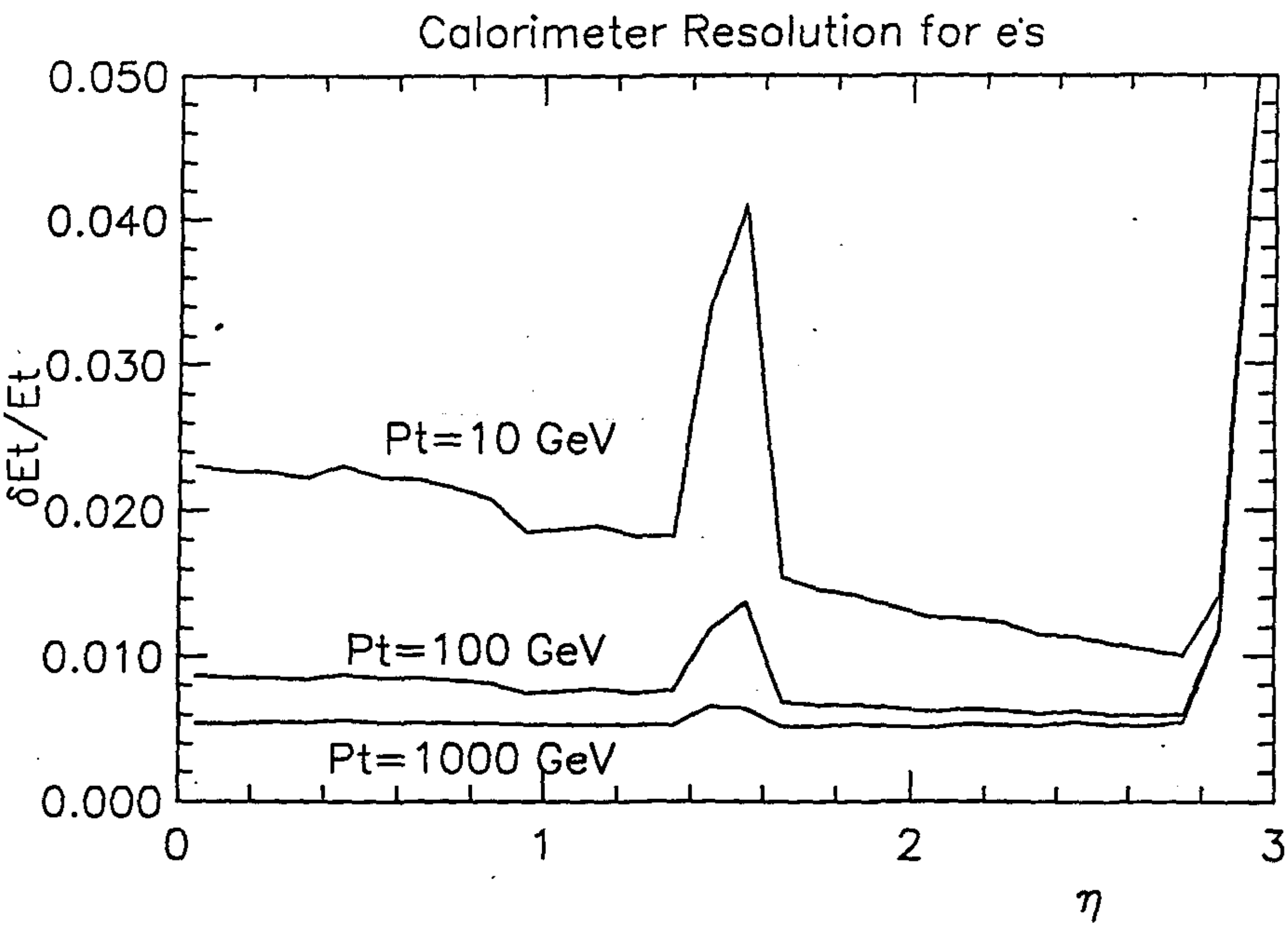
Calorimeter Resolution for e's
0.050
0.040
0.030
0.020
0.010
0.000
δEt/Et
Pt=10 GeV
Pt=100 GeV
Pt=1000 GeV
0
1
2
3
η

Transverse Energy in EC

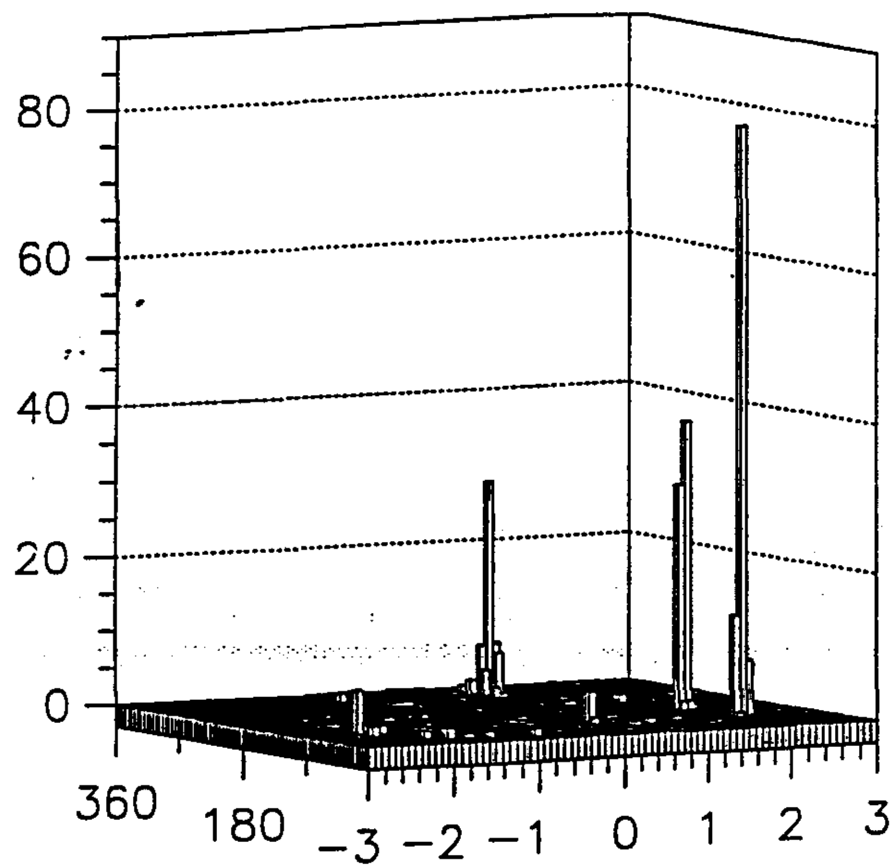

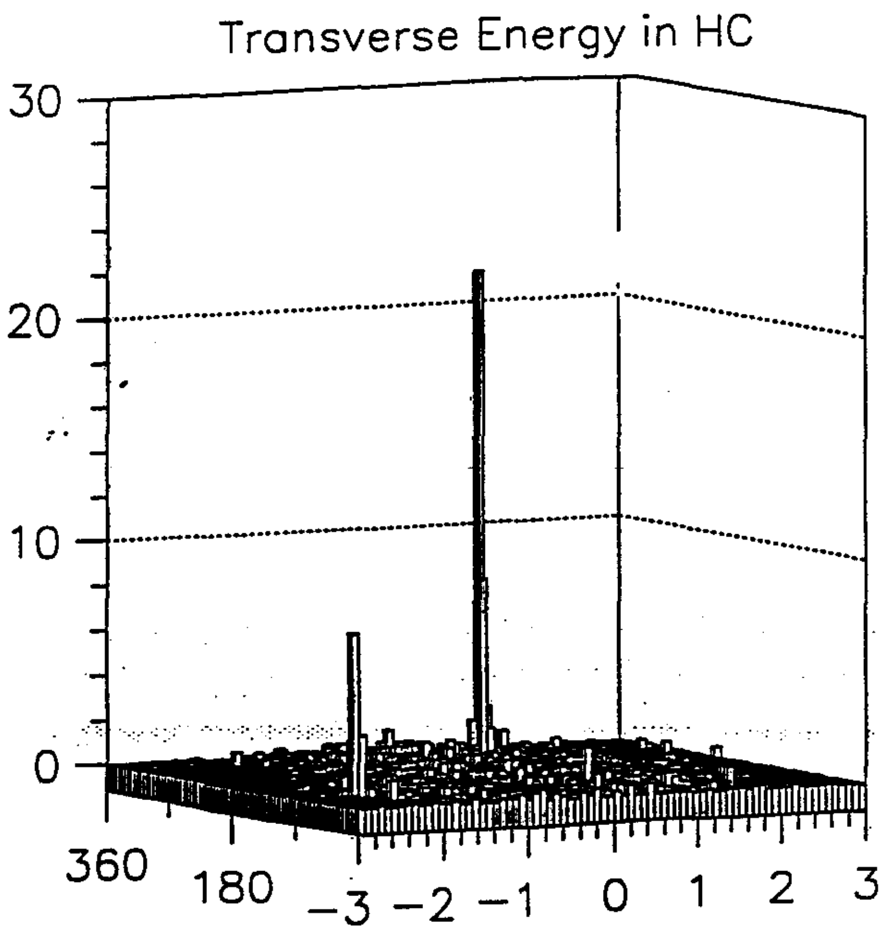

Transverse Energy in HC
30
20
10
0
360
180
−3 −2 −1 0 1 2 3

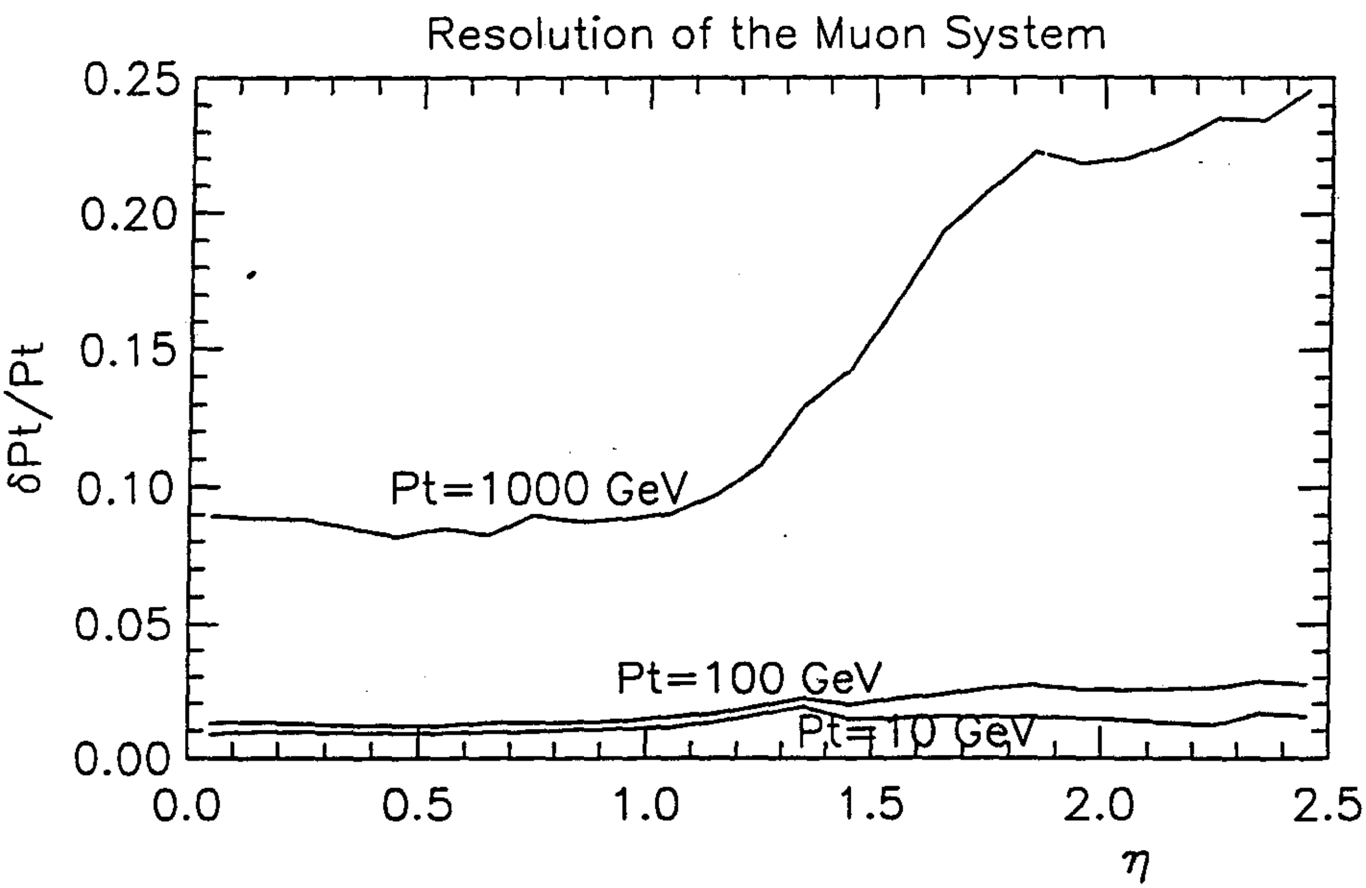

Resolution of the Muon System
0.25
0.20
0.15
0.10
0.05
0.00
δPt/Pt
Pt=1000 GeV
Pt=100 GeV
Pt=10 GeV
0.0
0.5
1.0
1.5
2.0
2.5
η

File: depth.dat

ID	IDB	Symb	Date/Time	Area	Mean	R.M.S.
201	0	−11	000000/0000	3744.	1.437	0.8212
201	0	1	000000/0000	3744.	1.437	0.8212

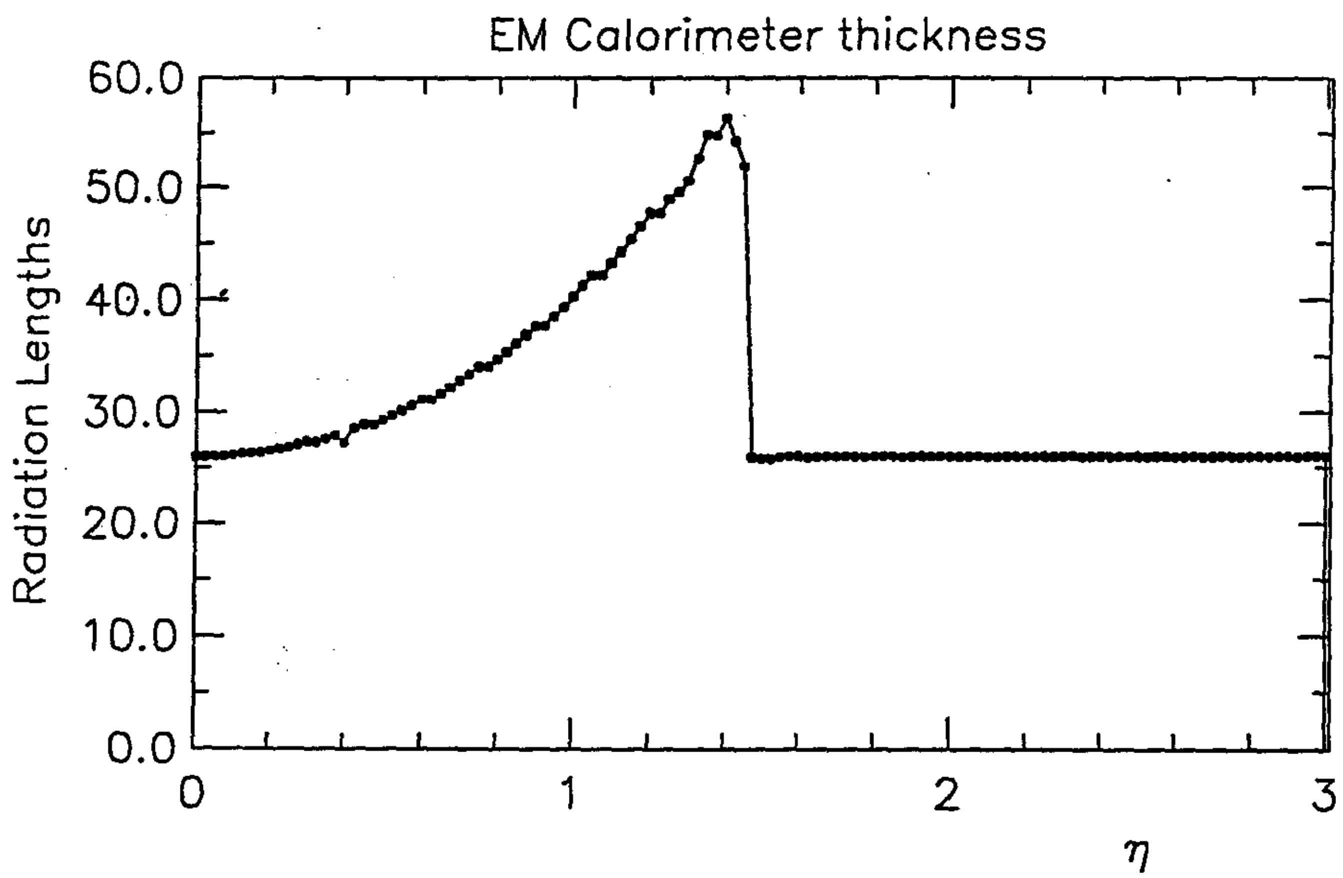

File: depth.dat

ID	IDB	Symb	Date/Time	Area	Mean	R.M.S.
202	0	−11	000000/0000	1502.	1.523	0.8487